DISCONNECTING A ROLE FOR DNA REPAIR IN THE PATHOGENICITY OF THE HUMAN PATHOGEN *CRYPTOCOCCUS NEOFORMANS*

A DISSERTATION IN
Cell Biology and Biophysics
And
Molecular Biology and Biochemistry

Presented to the Faculty of the University
of Missouri-Kansas City in partial fulfillment of
the requirements for the degree

DOCTOR OF PHILOSOPHY

by
Surbhi Verma

M.S., University of Missouri - Kansas City, 2010
B.Sc., University of Delhi, India, 2004

Kansas City, Missouri
2014

DISCONNECTING A ROLE FOR DNA REPAIR IN THE PATHOGENICITY OF THE HUMAN PATHOGEN *CRYPTOCOCCUS NEOFORMANS*

Surbhi Verma, Candidate for the Doctor of Philosophy Degree

University of Missouri - Kansas City, 2014

ABSTRACT

C. neoformans is an opportunistic fungal pathogen causing fatal meningitis and lung infections. Worldwide every year around 625,000 deaths occur due to Cryptococcosis. A basic understanding of *Cryptococcus* virulence mechanisms and survival strategies is required to combat the infections and develop therapies through translational research. Considering the evidence of a role of DNA repair in pathogenesis, I investigated DNA repair strategies adopted by *Cryptococcus* to survive in the environment and to cause successful infection. The repair of UV induced DNA damage was studied for two genes: *UVE1* and *RAD23*, parts of base excision repair and nucleotide excision repair pathways, respectively. My findings suggest that *UVE1* is required to combat UV induced stress. Uve1 is a mitochondrially-localized enzyme that functions to protect the mitochondrial genome from the deleterious effects of UV-induced DNA damage. Another aspect explored was the regulation of *UVE1* by the Bwc1-Bwc2 photoreceptor complex. *UVE1* is a direct downstream target of Bwc1-Bwc2 and is responsible for the UV sensitivity phenotype governed by this complex, without affecting mating or virulence. The regulation of *UVE1*

through the Bwc1-Bwc2 photoreceptor was also extended to two other fungal lineages, ascomycetes and zygomycetes. The second DNA repair gene, *RAD23*, codes for a dual function protein acting in nucleotide excision repair and as an ubiquitin receptor. Those two functions were uncoupled by creating mutant alleles and testing the strains carrying them for their virulence. The DNA repair function of the Rad23 is dispensable for virulence. Hence, specific DNA repair pathways do not necessarily have a major role in the virulence of *Cryptococcus*. However, ancillary functions of a DNA repair protein can contribute to virulence.

The faculty listed below, appointed by the Dean of the School of Graduate Studies, have examined a dissertation titled "Disconnecting a Role for DNA Repair in the Pathogenicity of the Human pathogen *Cryptococcus neoformans*" presented by Surbhi Verma, candidate for the Doctor of Philosophy degree, and certify that in their opinion it is worthy of acceptance.

Supervisory Committee

Alexander Idnurm, PhD., Committee Chair
Division of Cell Biology and Biophysics
University of Missouri-Kansas City

Lawrence A. Dreyfus, PhD.
Division of Cell Biology and Biophysics
University of Missouri-Kansas City

Michael D. Plamann, PhD.
Division of Cell Biology and Biophysics
University of Missouri-Kansas City

Jeffery L. Price, PhD.
Division of Molecular Biology and Biochemistry
University of Missouri-Kansas City

Leonard L. Dobens, PhD.
Division of Molecular Biology and Biochemistry
University of Missouri-Kansas City

CONTENTS

LIST OF ILLUSTRATIONS

Figure Page

LIST OF TABLES

Table Page

LIST OF ABBREVIATIONS

Abf1	Autonomously replicating sequence binding factor 1
AIDS	Acquired immunodeficiency virus
ART	Antiretroviral therapy
BER	Base excision repair
BLAST	Basic Local Alignment Search Tool
bp	Base pairs
CDC	Centers for Disease Control and Prevention
cDNA	Complementry DNA
CNS	Central nervous system
CPD	Cyclobutane pyrimidine dimers
DDR	Direct DNA damage reversal
DNA	Deoxyribonucleic Acid
DTT	Dithiothretiol
ERAD	Endoplasmic reticulum associated degradation
FADH	Flavin adenine dinucleotide
GAL	Galactose
GFP	Green fluorescent protein
GG-NER	Global genome NER
H_2O_2	Hydrogen peroxide
His	Histidine
HIV	Human immuno deficiency virus

hr	Hour
J	Joule
Kb	Kilo base
LM	Long Mitochondrial
LOV	Light, oxygen and voltage
MMS	Methyl methanesulfonate
mRNA	Messenger RNA
MTHF	Methylenetetrahydrofolate
NER	Nucleotide excision repair
nt	Nucleotide
PAGE	Polyacrylamide gel electrophoresis
PAS	Per, Arnt and Sim proteins
PBS	Phosphate buffer saline
PCNA	Proliferating cell nuclear antigen
PCR	Polymerase chain reaction
Pfam	The protein families database
RACE	Rapid amplification of cDNA ends
RFC	Replication factor C
RNA	Ribonucleic Acid
RPA	Replication protein A
SDS	Sodium dodecyl sulfate
SN	Small Nuclear

STM	Signature tagged mutagenesis
T-BOOH	tert-Butyl hydroperoxide
TC-NER	Transcription coupled NER
TFIIH	Transcription factor II H
UBA1	Ubiquitin associated domain I
UBA2	Ubiquitin associated domain II
UBL	Ubiquitin like domain
UVDE	UV damage DNA endonuclease
UV	Ultraviolet
UVE1 (D)	*UVE1* dark form/short form
UVE1 (L)	*UVE1* light form/long form
UVER	UVDE- dependent excision repair
WC-1	White Collar-1
WC-2	White Collar-2
WCC	White collar complex
WT	Wild type
XP	Xeroderma Pigmentosum
YPD	Yeast peptone dextrose
XP	Xeroderma Pigmentosum
YNB	Yeast nitrogen base
YPD	Yeast peptone dextrose

ACKNOWLEDGEMENTS

On the onset I would like to acknowledge and thank my PhD mentor Dr. Alexander Idnurm. Without his guidance and support this research work would not have ever been possible. I thank Alex for his patience, guidance, freedom he gave me in choosing and designing projects, and countless hours he spent trying to shape me as a researcher. Next, I owe my sincere gratitude to my committee members, Dr. Michael Plamann, Dr. Lawrence Dreyfus, Dr. Jeffery Price and Dr. Leonard Dobens. Their comments and ideas refined my scientific outlook and kept me driven. I would like to thank Dr. Michael Ferrari who served briefly on the committee. I learned confocal microscopy from his lab and my research work benefitted from this. A special thanks to Dr. Karen Bame for her guidance on all graduate work related formalities. It would have been very difficult to fulfill all this on time without her advice and guidance.

I would like to thank my present and past lab members. The scientific milieu they created over the course of my PhD is motivating. Denise and Suman, thank you for your help time to time, I missed you both a lot in the lab. Thanks to Silvia and Giuseppe for their cooperation. I would like to thank all my friends in School of Biological Sciences, especially my classmate Jouliana Sadek for her friendship.

I would like to avail this opportunity to thank my grandfather and my grandmother who raised me. I am short of words to thank them for the selfless love they gave and for believing in me. It is their dream that I am cherishing today and the two are my inspiration. I would like to thank my father for believing in my decisions and for his support. I am thankful

to both my parents for giving me confidence and motivation. Here I would like to acknowledge my colleague and my life partner Viplendra for always being there for me. The love and emotional support you have given me is priceless. Thank you, Viplendra, for always being next to me. A special thanks to my mother-in-law and my father-in-law for appreciating my efforts towards research and for their support. I thank my aunt for her encouragement towards education and research. Also I would like to thank my sister, brothers-in-law and sisters-in-law, Pallavi, Priyanka, Shweta, Kamlendra, Rahul and Geeta for giving me a joyful and pleasant atmosphere whenever I visited home. Special thanks to my brother Pankul and to my sister-in-law Reena for their help and support, especially during the start of graduate school.

I cherish the friendship of Divya, Namita and Chaithanya: awesome friends. They are always there for me in time of need no matter when and where. Without them it would have been difficult to live through the hard times. Thank you Prashi and Sudhir, I always felt happy and refreshed in your company; you two are wonderful people.

Finally I would like to thank all funding agencies for their support without which this research would not have been possible. I owe a special thanks to the Women's Council at UMKC for providing financial support, which helped during the research and also enabled me to present my work in national and international conferences.

To my Grandparents

CHAPTER 1

INTRODUCTION

DNA Repair in Photobiology and Virulence of *Cryptococcus neoformans*

The presence of DNA repair mechanisms is proposed to have had a major role in microbial colonization of land more than 400 million years ago, the time when ultraviolet (UV) irradiation was particularly intense. In the environment UV radiations, ionizing radiations and chemical mutagens are one of the primary causes of DNA damage. Such environmental stress affects survival and spread in the environment of all life forms. Alterations in the environment, such as depletion of the ozone layer leads to increased exposure to UV radiation, and introduction of new environmental carcinogens and toxic chemicals due to uncontrolled industrialization, add to this stress. There is need to understand the process of DNA damage and repair in the context of normal genome maintenance, survival in the environment, and the possible role of these processes in infectious disease development.

Conventionally, DNA repair mechanisms are studied in the context of processes such as DNA replication, cell cycle control, meiosis, chromatin remodeling, apoptosis, generating immune receptor diversity, aging and the understanding of diseases like Xeroderma pigmentosum, Cockanye syndrome, Werner syndrome, cancer, and neurodegenerative disorders such as Alzheimer's and Parkinson's disease. However limited attention has been given to the role of DNA repair in the life cycle and virulence of microbial pathogens. There are several examples where DNA repair mechanisms are being used by microorganisms to facilitate their survival and pathogenesis. Processes such as increased mutation rate and

recombination repair has led to the evolution of pathogens such as more pathogenic strains of avian influenza virus (H5N1) (Writing Committee of the Second World Health Organization Consultation on Clinical Aspects of Human Infection with Avian Influenza et al., 2008) and swine flu viral strain (H1N1) (Elderfield et al., 2014; Jackson and Bartek, 2009). Antigenic variation caused by homologous recombination in the surface glycoprotein coat is used as an immune evasion strategy by human pathogen *Trypanosoma brucei* (McCulloch and Barry, 1999). In the human fungal pathogen *Candida albicans* depletion of DNA repair protein Rad52 leads to decreased oxidative stress resistance, decreased resistance to antifungal drug fluconazole and increased white to opaque phenotypic switching which is related to virulence (Alby and Bennett, 2009; Legrand et al., 2007).

Recent evidence in the human pathogenic fungus *Cryptococcus neoformans* suggests that during infection the host mounts a sufficiently strong antimicrobial response to actually damage the DNA of the fungus, as implicated by the discovery of genes involved in DNA repair being also required for full pathogenesis (Liu et al., 2008). There are widespread cases of mortality due to *C. neoformans* infections in immune-compromised individuals in the absence of effective treatment strategies and uncontrolled dissemination in the environment. My research addresses how UV irradiation is sensed and the role to which DNA damage repair genes influence the survival and pathogenesis of *C. neoformans*. The two DNA repair genes chosen for the current study are *UVE1* and *RAD23*, and both are important for the survival of the fungus under UV stress and required for the virulence of the fungus. This study contributes to our understanding about the role of DNA repair in pathogenesis of fungi, and also advances our general understanding of photobiology in the fungal kingdom.

C. neoformans and *C. gattii*

Cryptococcus is a genus with an assemblage of species that all grow as yeasts and belong in the phylum Basidiomycota. Two sister species of *Cryptococcus* cause diseases in humans: *C. neoformans* mainly infects immunocompromised individuals and *C. gattii* is capable of infecting immunocompetent individuals (Heitman, 2011). *C. neoformans* is further divided into varieties, *C. neoformans* var. *grubii* and *C. neoformans* var. *neoformans*. At one point *C. gattii* also had varietal status as *C. neoformans* var. *gattii* until taxonomic revision(Kwon-Chung et al., 2002). Based on the reactivity of monoclonal antibodies to capsular polysaccharides *C. neoformans* was serotyped in the clinic, giving rise to a common serotype classification that is still commonly used. Based on the serotyping, *C. neoformans* var. *grubii* is serotype D and *C. neoformans* var. *neoformans* is serotype A. *C. gattii* is categorized into two serotypes, B and C. Details for these *Cryptococcus* strains and serotypes are listed in **Table 1.**

C. neoformans is an opportunistic pathogen mainly infecting immunocompromised individuals. According to the Centers for Disease Control and Prevention (CDC) the risk factors for developing disease due to *C. neoformans* infection are HIV infection (that can lead to AIDS); immunosuppressive conditions such as organ transplantation conditions; heart, liver or lung disease; diabetes and pregnancy. *C. neoformans* mainly causes lung infections and central nervous system (CNS) infections, and the disease is fatal if untreated. Lung infections have pneumonia-like symptoms with shortness of breath, fever and cough. CNS infections lead to meningitis (inflammation of the membrane that protects the brain and CNS), high fever and even personality changes due to effects on the brain. The worst cases of systemic disease lead to infection of multiple organs and their subsequent failure. According

to an estimate from the CDC in 2009, every year there are around 1 million reported cases of *C. neoformans* meningitis and about 625,000 deaths (Park et al., 2009).

The mortality rate in HIV infected Cryptococcus patients are about 12%, with a recent decline due to increased availability and access to Antiretroviral therapy (ART) in HIV infected *Cryptococcus* patients. A more recent update, from the 9th International Conference for Cryptococcus and Cryptococcossis, is a decline in the annual death number of deaths to around 350,000 due to increased access to ART. However, the situation in sub-Saharan African nations is still alarming. *C. gattii* is an emerging fungal pathogen that is responsible for what has been termed the Vancouver Island outbreak. The outbreak was recognized in 1999 and then spread to mainland Canada and into the northwestern United States. In the U.S. alone there were around 100 cases reported between 2004 and 2011, most of which were from Oregon and Washington (Centers for Disease and Prevention, 2010). Neither *Cryptococcus* species is transmitted from person-to-person, or contracted from an animal reservoir. In the environment *Cryptococcus* is found to be associated with fruits, vegetables, decaying wood and soil samples. The two species have different niches such that *C. gattii* is commonly associated mainly with trees and *C. neoformans* with pigeon guano. These are sometimes termed "opportunistic" pathogens, and the reason why these particular species are part of the small cohort of fungi that are able to cause disease amongst an estimated five million fungal species is an active area of research around the world, especially from the perspective of how the environment may contribute to the ability of these species to cause disease.

The life cycle of *Cryptococcus* can involve different environmental hosts; in soil, in trees, in birds, in animals and in humans. Cells can stay as a yeast form or may show dimorphic transition to hyphal forms during sexual reproduction (Kwon-Chung, 1975). *C. neoformans* undergoes sexual reproduction and a same sex mating (monokaryotic fruiting) process is also characterized under laboratory conditions (Lin et al., 2005; Wickes et al., 1996), both of which lead to the production of a filamentous form **(Fig.1)**.

C. neoformans has a bipolar mating type system, and two alleles of the *MAT* locus (**a** and α**)** encoding interacting homeodomain proteins, confer sex identity to the fungus (Hull et al., 2005; Hull et al., 2002). During sexual reproduction yeast cells of opposite mating type **a** and α fuse to form a hypha with clamp connections for exchange of the nuclei during hyphal progression. The nuclei fuse to form a transient diploid state in the sexual structure called the basidium, in which meiosis occurs to form haploid basidiospores. These basidiospores then undergo rounds of mitosis to form long chains of the sexual spores in a basipetal manner **(Fig. 1)**. During monokaryotic fruiting, endoduplication of the nucleus or the fusion of two nuclei between same sexes occurs (i.e. between **a**/**a** or α/α cells). The fusing nuclei may be genetically different but are essentially of the same sex. After the formation of diploid cells meiosis takes place in the basidium followed by mitosis leading to the formation of recombinant haploid progeny. Monokaryotic fruiting is more prevalent in α mating type cells, which may account for the higher prevalence and virulence of the α matting type in the environment (Wickes et al., 1996).

Table 1: *Cryptococcus* species serotype and strain classification. Strains used in the current study are highlighted in bold.

Species	**Serotype**	**Molecular type**	**MATa strain**	**MATα strain**
C. n. var. *grubii*	A	VNI	**KN99a**	**KN99α**
C. n. var. *grubii*	A	VNII	-	-
C. n. var. *grubii*	A	VNB	Bt63	Bt148
C. n. var. *neoformans*	D	VNIV	**JEC20**, B3501	**JEC21**
C. gattii	B	VGI	E566	WM276
C. gattii	B	VGII	CBS1930	**R265**
C. gatii	C	VGIII	CDC4546	NIH312
C. gattii	C	VGIV	-	Bt26
C. neoformans hybrid	AD	VNIII		
	AD	VNIII		

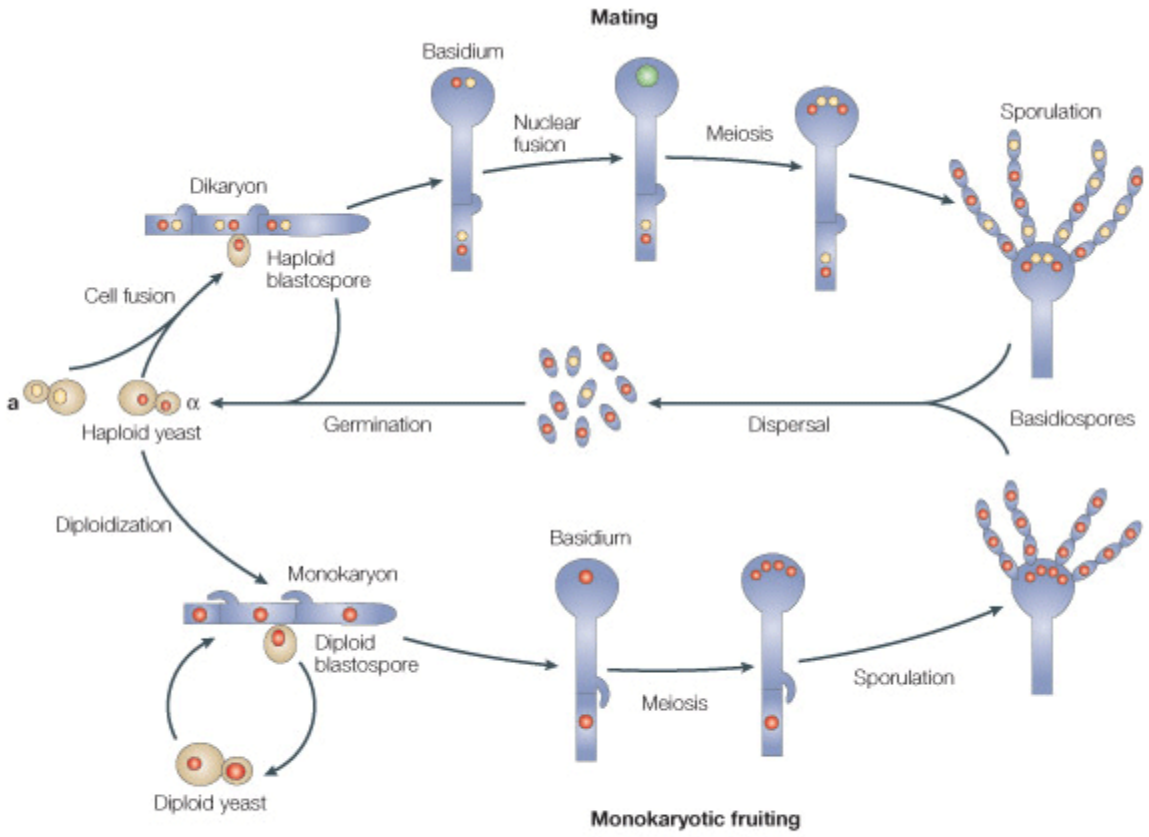

Fig. 1 : Model of the *Cryptococcus neoformans* life cycle. In response to nutrient limitation, **a** and α yeast cells secrete peptide pheromones that trigger cell–cell fusion. Nuclear fusion is delayed, and the resulting dikaryon initiates filamentous growth. The two parental nuclei migrate coordinately in the dikaryotic hyphae, and as each septum forms to separate the cells, one nucleus is transferred to the penultimate hyphal cell through a clamp connection. At the stage of basidium development, the two nuclei fuse and undergo meiosis to produce four meiotic products that undergo mitosis and bud from the surface of the basidium to produce chains of basidiospores. During monokaryotic fruiting, cells of one mating type, for example, α cells, become diploid (α/α) cells, either by endoduplication or by nuclear fusion following

fusion of two cells. The diploid monokaryotic hyphae form rudimentary clamp connections, but these are not fused to the preceding cell. At the stage of basidium development, meiosis occurs and haploid basidiospores are produced in four chains. (Idnurm et al., 2005)

Light Sensing in the Fungi

Many organisms, including species of fungi, are capable of sensing light. Animals have developed photoreceptive sensory organs (i.e. eyes) that use photosensory rhodopsin proteins to detect light. Microorganisms use these same types of photoreceptor proteins, as well as others. Fungi have a suite of photoreceptors capable of sensing wavelengths across the spectrum of the visible to UV light. There are phytochromes for sensing red and far red light, opsins for sensing green light, cryptochromes for sensing blue/UV A light. The most widespread photoreceptor complex is White Collar-1 (*WC-1*) and White Collar-2 (*WC-2*), that senses blue and near UV light (Idnurm et al., 2010). The white collar complex has been well studied in the ascomycete fungus *Neurospora crassa* (Liu et al., 2003), where it provides the light input into the circadian rhythm as well as being an integral component of the clock, pigment production, phototropism and in sexual reproduction (protoperithecia formation) (Crosthwaite et al., 1997; Degli-Innocenti and Russo, 1984). In *N. crassa* WC-1 is a photoreceptor that has three PAS domains (named after the Per, Arnt and Sim proteins). The most N-terminal is called LOV (for light, oxygen and voltage) domain, and this is the domain that binds to a flavin chromophore moiety, which undergoes conformational change on sensing light. Its C-terminus has a GATA-type zinc-finger domain to bind to DNA such that the protein can act as a transcription factor. The second component (WC-2) is more of a dedicated transcription factor protein, which forms a complex with WC-1 (Talora et al., 1999) to execute light dependent responses. It has a sole PAS domain and a zinc finger DNA-binding domain.

C. neoformans is light-sensing model system in the Basidiomycota in which white collar complex components are named Bwc1 and Bwc2. Here Bwc1 acts as a photoreceptor,

having three PAS domains including the LOV domain as in *Neurospora*, but having no zinc finger DNA binding domain which is a feature missing in many Basidiomycota species. Hence Bwc1 can only act as a photoreceptor. Bwc2 has a PAS domain as well as DNA binding zinc-finger domain, which acts as a transcription factor. This complex has three characterized major roles in the biology of *Cryptococcus* (Idnurm and Heitman, 2005; Lu et al., 2005). These are: 1) repression of mating in light, 2) conferring UV resistance to the fungus and 3) in the absence of Bwc1-Bwc2 complex virulence of *C. neoformans* is decreased. In both wild type *C. neoformans* strains (serotype A and D) mating is either reduced or there is no mating at all in the light as compared to the dark. In the dark, both **a** and α parents mate normally and in blue light mating is repressed. In *bwc1*Δ, *bwc2*Δ and *bwc1*Δ *bwc2*Δ double mutant cells the inhibition of mating by light is lost with mating occurring equally well in light and dark. The phenomenon of monokaryotic fruiting is also light regulated in *C. neoformans* (Idnurm and Heitman, 2005; Lu et al., 2005). Wild type cells are more tolerant to UV radiation as compared to *bwc1*Δ, *bwc2*Δ and *bwc1*Δ *bwc2*Δ strains. Similar is the case for virulence of the fungus, in a murine model of infection, wild type cells show higher virulence as compared to the *bwc1*Δ, *bwc2*Δ and *bwc1*Δ *bwc2*Δ strains.

For the three traits controlled by Bwc1-Bwc2, the direct downstream targets that are responsible for the individual phenotypes are still to be discovered. Two light-regulated genes identified in a study of light and dark treated *C. neoformans* cells in a microarray experiment are *CFT1* and *HEM15* (Idnurm and Heitman, 2010). Cft1 is an iron permease that is essential for virulence of *C. neoformans* (Jung et al., 2008). Another gene that is likely to be important for the virulence of *C. neoformans* is *HEM15*, which encodes ferrochetalase

required for the conversion of phototoxic porphyrins to heme (Idnurm and Heitman, 2010). However, only *HEM15* was induced by light at a level to be above the common 2-fold difference used in microarray comparisons. Further, neither of these genes was shown to be direct downstream targets of Bwc1-Bwc2. Lastly, how or through which mediators the presence or absence of a light signal is transduced is unknown.

It is also possible that there are other photo-regulated genes in *C. neoformans* that are yet to be discovered. For instance, the genes *SXI1α* and *MFα1*, encoding a homeodomain transcription factor and a pheromone precursor, respectively, are also categorized as light-regulated, but their regulatory effect is after 24 hours in constant light or dark, which points to them being indirectly regulated through the photoreceptor complex. As far as the UV resistance phenotype is concerned, there is no clear gene implicated, although *HEM15* is a possible candidate gene because of the sensitivity of the deletion strain to white light illumination. On the other hand, *HEM15* is essential for *C. neoformans* survival in vitro yet neither the *BWC1* nor *BWC2* mutant has a growth defect, so the UV sensitivity effect in these knockout strains cannot be solely through impaired *HEM15* regulation. When looking at the major roles that the Bwc1-Bwc2 complex plays in the biology of *C. neoformans* it is important to identify the exact downstream targets responsible for the respective phenotypes as this will contribute to understand the *C. neoformans* photobiology and possibly the control of the fungal virulence. It is also important to establish whether there are links between the phenotypes associated with virulence, protection against UV light, and mating: an obviously common theme would be a role of DNA repair in each of these processes.

DNA repair in virulence

Maintenance of an intact genome requires error-proof DNA repair systems. Impairment in the fidelity of DNA repair is related to aging disorders and cancer in humans, two of the biggest unresolved human health challenges. Hence most of the studies conducted on DNA damage repair are in the context of these non-infectious pathological conditions. Understanding DNA repair is important from the prospective of finding treatment for non-infectious diseases and is equally significant for the understanding of evolution, survival, and microbial pathogenesis. Previous studies have implicated the light-sensing pathway controlled by the Bwc1-Bwc2 proteins as being required for both virulence and protection against DNA damage in the form of ultraviolet light (Idnurm and Heitman, 2005). Moreover other examples exist where pathogenic organisms such as *Trypanosoma brucei*, *Candida albicans* and *C. neoformans* have used DNA repair for avoiding the host defense systems to enable them to cause disease (Alby and Bennett, 2009; Legrand et al., 2007; Liu et al., 2008; McCulloch and Barry, 1999). The two DNA repair genes of interest, *UVE1* and *RAD23*, are the focus of the current study in the context of virulence and photobiology of *C. neoformans* and are introduced below with additional details of DNA repair pathways in general.

Uve1: link between light sensing and DNA repair

Light can be sensed as a danger signal for the presence of deleterious UV radiation. Thus a subset of DNA repair genes is expected to be regulated by components of light sensing pathways. Families of proteins including photolyase and the cryptochromes have been widely studied in the context of light sensing and DNA damage repair. These proteins act as a photoreceptor, a DNA repair enzyme, or both, with functions in light regulated responses (Thompson and Sancar, 2002). Interestingly, the *Cryptococcus* species complex

has no homolog of photolyase in its genome but is still able to sense light and protect its genome from the deleterious effects of UV radiation to the same degree as other fungi. Since *Cryptococcus* has a well characterized photoreceptor complex Bwc1-Bwc2, and one of the downstream effects of the knockout or mutant strains is very high level of sensitivity to UV radiation stress (Idnurm and Heitman, 2005), it is imperative to look for a DNA repair protein responsible for this phenotype of the mutant strains.

In *N. crassa*, an ascomycete fungus with a well characterized white-collar complex, *mus-18* is the DNA repair gene encoding an AP-endonuclease that was shown during these studies to be up-regulated in response to light (Chen et al., 2009). In *Cryptococcus* the homolog of *mus-18* is *UVE1*. The *Neurospora mus-18* deficient mutant has increased UV sensitivity that is rescued by complementation with the wild type copy of the gene. It is also able to rescue the UV sensitivity phenotype of NER mutants, implicating the functional importance of the gene in conferring UV resistance (Yajima et al., 1995). Most of biochemical and molecular characterization studies of Uve1 homologs have been done in the fission yeast *Schizosaccharomyces pombe* where its named UVDE, for UV damage DNA endonuclease, or *uve1*, and it is part of UVER that that executes UVDE-dependent excision repair that is sometimes considered to be completed as part of BER. Purified recombinant *S. pombe* protein expressed in *E. coli* is able to incise UV-induced cyclobutane pyrimidine dimers as well as (6-4) photoproducts and has a role in fixing mismatched nucleotide residues (Kaur et al., 1999; Takao et al., 1996). In *S. pombe* Uve1 localizes to both the nucleus and mitochondria and participates in repairing UV-induced DNA damage for both the genomes, but with no significant role in conferring UV resistance to mitochondrial genome (Yasuhira and Yasui, 2000). The *N. crassa mus-18* is induced in presence of light

and also there is evidence for widespread role of Uve1 in conferring resistance to UV induced DNA damage. Hence there was a possibility of the *UVE1* gene being a downstream target of photoreceptor complex Bwc1-Bwc2 that is required for resistance to UV induced DNA damage in *C. neoformans* and hence might affect its survival in the environment.

Rad23: A dual function protein required for *C. neoformans* virulence

In a large scale study of *C. neoformans* by Liu et al, 1,200 of the 7,000 genes in the genome were deleted and the knockouts tested for three "classical" virulence traits that are growth at 37 degrees, capsule formation and melanization, and competitive survival between mixed populations of strains in a mouse model of disease as a measure of virulence (Liu et al., 2008). In the list of those genes required for virulence were a series of DNA repair genes, including *RAD54* and *RAD23*. Both of these were deleted a second time and tested in the competition model in which both mutants showed a reproducible reduction in growth in the mouse lung relative to control strains. Of these two genes the *RAD23* gene, which is a part of NER, is especially interesting because it is a dual function gene with functions in DNA repair and is a ubiquitin receptor protein involved in the proteosomal degradation pathway (Dantuma et al., 2009). In yeast *S. cerevisiae* and in humans, Rad23 is part of NER and stabilizes another NER protein Rad4 (XPC in humans) (Guzder et al., 1998a). In humans and in yeast Rad4 binds to and recognizes the photolesions for repair (Min and Pavletich, 2007). NER protein Rad23 is also known ubiquitin receptor protein.

Rad23 has four domains - UBL, UBA1, XPC binding domain and UBA2 - with each domain having a specific function (explained later in chapter 5). The functions of the different domains of Rad23 are mostly defined in *S. cerevisiae* (Dantuma et al., 2009). The different roles that Rad23 plays in the cell are related with either DNA repair (NER) or the

proteosome-mediated degradation of unwanted substrate proteins. Rad23 is known to be involved in cell cycle regulation, phosphate metabolism and even regulation of transcription of tumor suppressor p53-dependent genes. Indirectly all these functions may relate to proteosome-mediated degradation or NER.

General overview of DNA repair pathways

DNA repair mechanisms are necessary to combat the DNA damage caused as a result of exposure to environmental mutagens and cellular stresses such as UV radiation, oxidative stress, chemical mutagens and spontaneous mutations. In response to different kinds of DNA damage, different but sometimes overlapping DNA repair mechanisms exist. Major categories of DNA repair pathways are: 1. Direct DNA damage reversal (DDR), 2. Base excision repair (BER), 3. Nucleotide excision repair (NER), 4. Mismatch repair and 5. Recombination repair. DNA repair mechanisms in humans and yeast are similar, having homologous genes and parallels in most of the steps of the repair pathways. Here I will refer mostly to the DNA repair genes/proteins in the ascomycete yeast *Saccharomyces cerevisiae*, with a focus on direct DDR, BER and NER.

1) Direct DNA damage reversal: As the name suggests this type of DNA repair is a single step repair process involving a single enzyme. Two major direct DNA damage reversal genes are DNA photolyase (*PHR1*) and Methyl transferase (*Mgt1*). Phr1 is required for the correction or photoreactivation of the cyclobutane pyrimidine dimers (CPD), and was first identified in fungi as photoreactivation deficient mutants in *S. cerevisiae* (Resnick, 1969). It consists of two non–covalently attached chromophore groups, $FADH^-$ (Flavin adenine dinucleotide) and MTHF (Methylenetetrahydrofolate) (Sancar, 2008). For photoreversal by CPD bound Phr1, a photon is absorbed by MTHF and excitation transferred to $FADH^-$, which

in turn transfers an electron to CPD to go through the structural changes and finally split the ring to restore the proper DNA conformation. Mtg1 mainly prevents AT to GC and GC to AT transitions that occur due to mispairing of O^6-methylguanine with 'T' instead of a 'C' and O^4-Methylthymine with 'G' instead of 'A'. This protein corrects the damage by a suicide reaction that permanently inactivates the enzyme active site by transfer of the methyl residue to S-methylcysteine (Sassanfar and Samson, 1990; Xiao et al., 1991).

2) Nucleotide Excision Repair (NER): is important for correction of mainly UV-induced DNA damage. Defects in the NER pathway leads to increased UV sensitivity in yeast, and in humans leading to Xeroderma Pigmentosum, a predisposition to cancer due to enhanced sensitivity to sunlight (Hoeijmakers, 2001). Unlike direct DNA damage reversal, NER is a multistep process with many enzymatically active complexes formed at different steps. There are two types: Global genome NER (GG-NER) and Transcription coupled NER (TC-NER) **(Fig. 2)**. Major steps in the repair process are lesion recognition, lesion incision, and repair synthesis. Both GG-NER and TC-NER are different at the initiation step until lesion recognition, and thereafter both pathways go through the same steps. In yeast the GG-NER pathway is comprised of, complexes of Rad4-Rad23-Rad33 and Rad7-Rad16 first recognizing the lesion. In the first complex Rad4 recognizes the DNA damage and interacts with Rad23 (Jansen et al., 1998) and Rad33, which are required for the stability of the complex. Rad23 protein is also involved in the ERAD (Endoplasmic reticulum associated degradation) pathway (Medicherla et al., 2004) as discussed later.

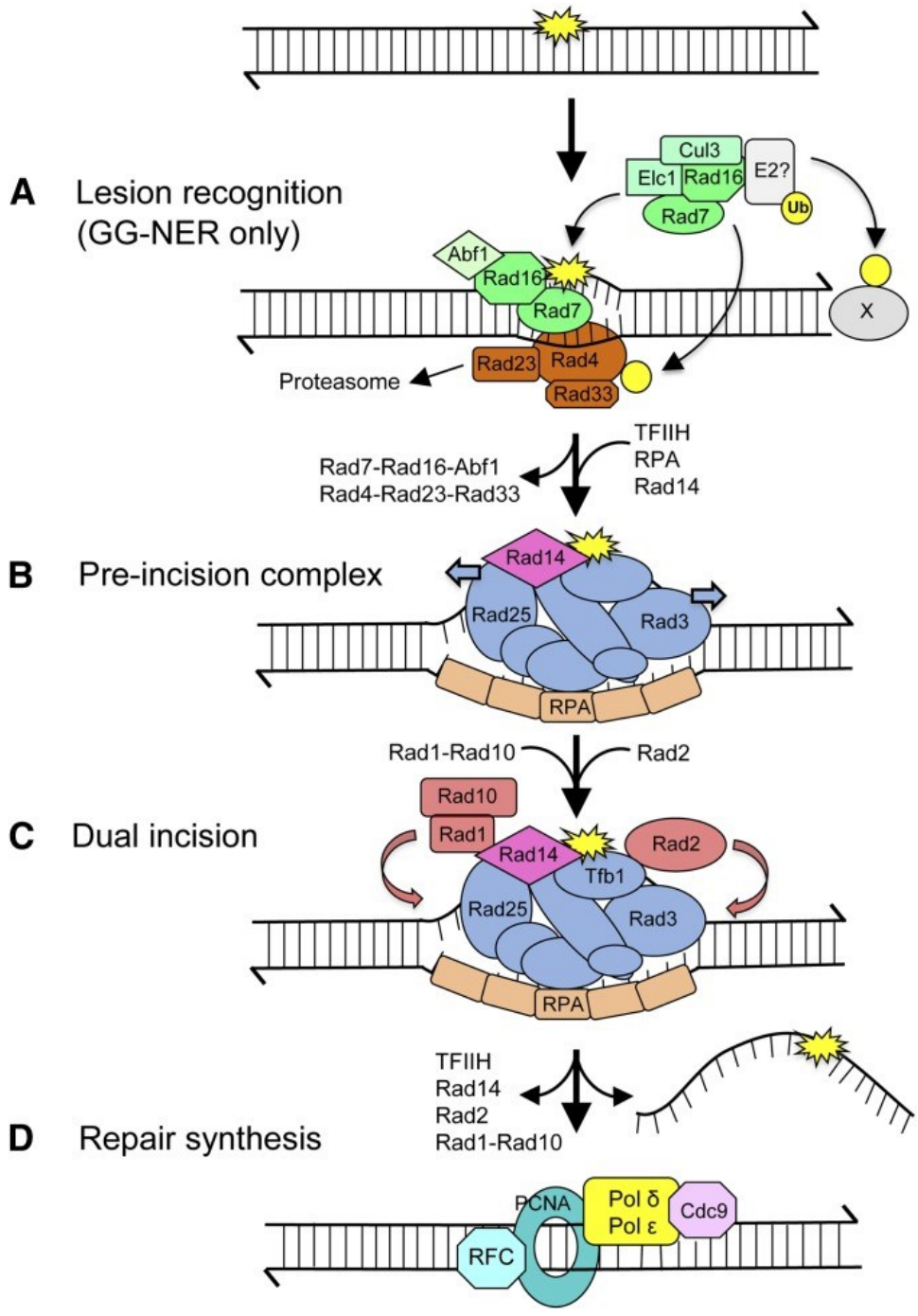

Fig. 2 : The NER pathway. (A) During GG-NER, a helix-distorting lesion (yellow star) is recognized by Rad4-Rad23-Rad33 and Rad7-Rad16 complexes. Rad7-Rad16-Abf1 has chromatin-remodeling activity, whereas Rad7-Rad16-Elc1-Cul3-E2 has ubiquitin (Ub) ligase

activity, which modifies Rad4 and additional factors ("X"). These reactions allow efficient recognition of lesions by Rad4, its proper positioning, and opening of the helix ~10 bp. (B) TFIIH (components are in blue), Rad14, and RPA are recruited to form a pre-incision complex that verifies the lesion and further unwinds DNA. Rad4-Rad23-Rad33 and Rad7-Rad16-Abf1 are released. (C) The structure-specific endonucleases Rad1-Rad10 and Rad2 are positioned to incise 5′ and 3′ of the lesion, respectively. (D) A lesion-containing oligonucleotide (25–30 nt) is released from the duplex, followed by repair synthesis and ligation. (Boiteux and Jinks-Robertson, 2013)

Another Rad7-Rad16 complex binds to the UV-irradiated DNA and in complex with Abf1 (Autonomously replicating sequence binding factor 1) or Elc1-Cul3 has multiple roles during the initiation steps of the DNA repair, which includes conformational changes in DNA, ubiquitination and chromatin remodeling.

Rad16 is involved in H3 acetylation in *S. cerevisiae* in response to UV stress (Teng et al., 2008), and the Rad7-Rad16 in complex with Abf1 cause structural changes in DNA such as superhelical torsions in an ATP dependent manner and to help recruit Rad4 to the damaged DNA (Guzder et al., 1998b; Yu et al., 2004). Rad7-Rad16 Elc1-Cul3 complex leads to the ubiquitination of Rad4 and is required for its stabilization (Ramsey et al., 2004). Further into the repair process TFIIH (transcription factor II H), composed of 10 subunits, is recruited to the DNA damage site. Rad3 and Rad35 subunits of TFIIH complex have ATPase and helicase activity (Feaver et al., 1993; Guzder et al., 1994) with opposite polarity which helps in the process of extending the opening of the damaged DNA site to provide greater accessibility to the repair site. TFIIH engages in interaction with other NER components for the process of efficient DNA repair. Further, Rad14 binds to DNA lesions (Guzder et al., 1993) with RPA which binds to the undamaged strand and is required for the verification of the lesion (Boiteux and Jinks-Robertson, 2013). These sequences of events complete the formation of a pre-initiation complex for the lesion recognition and unwinding of the helix which is followed by the release of Rad4-Rad23-Rad33 and Rad7-Rad16. Two endonucleases with opposite polarity in cleavage - Rad1-Rad10 complex make an incision at 5’ side of the damage about 15-25 nucleotide far from the lesion and Rad2 making an incision on the 3’ side about 2-8 nucleotide away - now joins the complex (Evans et al., 1997). Following the incision step, DNA synthesis and ligation of the nick takes place to

restore the intact undamaged DNA fragment. Rad2 in yeast, with the help of PCNA (Proliferating cell nuclear antigen) and replication factor C (RFC), recruits DNA polymerase δ followed by the release of other factors (Mocquet et al., 2008) and repair synthesis. Finally the nick is sealed by DNA ligase 1.

For TC-NER that is coupled with the active transcription, Rad26 and Rad28 are the two proteins that lead to initiation of the repair process. The absence of the human homologs of both of these proteins (CSB and CSA) results in Cockayne syndrome characterized by sensitivity to UV radiation (Troelstra et al., 1992). Rad26 is attached to the RNA Polymerase II and is an ATPase with chromatin remodeling activity (Hanawalt and Spivak, 2008). At moderate or weak lesions Rad26 promotes the bypass of the lesion by RNA polymerase II; however at strong lesions RNA Pol II is stalled and Rad26 helps in recruiting other NER factors for the repair process. Rad28 has no apparent catalytic activity and is thought to be involved in protein interactions (Bhatia et al., 1996). Another sub-pathway for TC-NER is initiated by Rpb9, which is a subunit of RNA Polymerase II.

3) Base Excision Repair (BER): Excision of damaged DNA bases followed by repair of abasic sites is the task undertaken by BER. It deals mainly with the damage caused due to oxidative stress, alkylation and deamination preventing mispairing and hence mutation accumulation. Major enzymes required for this process are DNA glycosylases, endonucleases or lyases, phosphodiesterases, DNA polymerase and ligases, which act in a sequential way to undertake the repair process. In yeast DNA glycosylases fall mainly in to two categories. The first are monofunctional and act only on the N-glycosidic linkage and release the damaged base (e.g. enzymes Ung1 and Mag1) by acting on the N-glycosidic bond between the altered/damaged base and the sugar moiety. The second are bifunctional enzymes which

can act as N-glycosidases as well as nick phosphodiester bonds to act as lyases on the apurinic or apyrimidic sites (e.g. Ogg1, Ntg1 and Ntg2). All three Ntg1, Ntg2 and Ogg1 have 3' AP lyase activity causing an incision at the 3' side of the AP site via a β elimination reaction (Boiteux et al., 2002; Meadows et al., 2003). Yeast has two AP endonucleases Apn1 and Apn2, which act at the 5' of the AP site to incise the phosphodiester bond. Apn1 is the major AP endonuclease out of the two, taking care of almost 95% of the damage (Popoff et al., 1990). Apn1, Apn2 and another enzyme Tpp1 have 3' phosphodiesterase activity that clears 3' blocked termini such as 3' dRP (Unk et al., 2000; Vance and Wilson, 2001) for efficient progress of DNA polymerase. Based on knowledge from the mammalian homolog Fen1 removal of 5' dRP from the 5' blocked termini is considered to be done by Rad27 in yeast (Hoeijmakers, 2001). Gap formed by the sequential action of the above enzymes in the BER is filled mainly by DNA polymerase ε (Wang et al., 1993) and sealed by the DNA ligase Cdc9 (Tomkinson et al., 1992).

Summary

Study of DNA repair enzymes and their "moonlighting" functions in other cellular pathways has been undertaken in depth to develop an understanding in conventional model organisms. In context of fungi, the existing paradigm is to study important processes in established model systems such as budding and fission yeasts, which have served as the platforms for major scientific discoveries. However, there is need for the development for new model systems as there are some differences between species. For example there are many genes in pathogenic fungi in the genera *Candida* or *Cryptococcus* for which no homologs exist amongst them and/or these well established model systems. DNA repair pathways likely aid in survival of microbial pathogens in the environment (UV stress) and in

infected hosts on experiencing oxidative and free radical stresses, through interactions with macrophages and neutrophils. Also directly or indirectly proper functioning of such pathways may be necessary for their virulence. Such assumptions can be supported by evidence of DNA repair gene functions in the pathogenic fungus *C. albicans* in context of virulence (Chauhan et al., 2005) and also in virulence influencing factors such as phenotypic switching and genome rearrangement (Alby and Bennett, 2009; Mitra et al., 2014).

In this respect *C. neoformans* is an important fungal pathogen that needs to be addressed and developed as a model system for discovering virulence related mechanisms. Such a system is easy to establish because its genome is sequenced for multiple strains, which makes it amenable to basic molecular biology tools, phenotypic analysis of genetic traits is easier as it has a haploid genome, and it can be handled in a BSL2 facility without any danger by healthy individuals. Also with respect to specific pathways such as light sensing, other model fungi such as *S. cerevisiae*, *S. pombe* and *Candida* species are blind fungi because of the absence of the white-collar photoreceptor system. However, to date there is no specific analysis on DNA repair mechanisms in general or in the context of virulence in *C. neoformans*. In conclusion, there is an urgency to move from the conventional model species to address the basic cellular mechanisms of DNA repair in a non-conventional model system such as *Cryptococcus*. Such a strategy in future may help in faster discovery of new antimicrobial targets.

CHAPTER 2

MATERIALS AND METHODS

Strains, culturing methods and transformation protocols

Different fungal strains used in the studies are derived from WT strains of the following species: *C. neoformans*, *C. gattii*, *S. pombe*, *N. crassa*, and *Phycomyces blakesleenaus* (Table 2). All *C. neoformans* and *C. gattii*, *N. crassa*, and *P. blakesleenaus* strains were cultured overnight in liquid YPD (Yeast peptone + 2% dextrose) or YNB (Yeast nitrogen base) media at 30°C in shaking conditions or mentioned otherwise. For *S. pombe*, overnight liquid cultures were grown in YES (Yeast extract with + sucrose supplements) media or otherwise mentioned. For growth on solid media YPD or YNB 2% agar media plates with or without antibiotic or chemical stressors were used for *C. neoformans* and *C. gattii*, *N. crassa*, and *P. blakesleenaus* strains. For *S. pombe* growth YES solid media plates with 2% agar were used. For all *Cryptococcus* crosses V8 pH 5 for serotype A and pH 7 serotype D mating plates or Murashige and Skoog medium plates were used. Basidiospores were manipulated using a Nikon Labophot microscope with a micromanipulation handle attached.

For *E. coli* transformations, chemically competent strains of DH5α or TOP10 were used, and transformations were done by heat shock at 42 °C for 30 seconds. For the *Agrobacterium tumefaciens* transformations strain EHA105 was used, and transformations were done by electroporation with the preset parameters in a Gene Pulser Xcell machine

(Bio-Rad, Hercules, CA). All the strains generated in the study are stored as -80°C stocks by preserving in 30% glycerol.

C. neoformans transformations used either the *A. tumefaciens* co-culture method (Idnurm et al., 2004) or the biolistics delivery with a PDS 1000/He paricle delivery system (Bio-Rad) (Toffaletti et al., 1993). For *S. pombe* transformations, the lithium acetate method was used (Ito et al., 1983).

Plasmid and DNA extractions

E. coli plasmids (Table 3) were extracted using the QIAprep Spin Miniprep Kit (Qiagen Germantown, MD) or the IBI high-speed plasmid mini kit (MIDSCI, St. Louis, MO) Genomic DNA was isolated with a slightly modified CTAB method (Pitkin et al., 1996). Details for primers used in construction of different plasmids or strains are in **Table 5**.

Generation of *UVE1* knockouts and their complementation in *C. neoformans*

Gene knockout cassettes were constructed by fusion of around 1000 bp flanks 5' and 3' of the *UVE1* gene with nourseothricin acetyltransferase (*NAT*) coding sequence for strain JEC21 (var. *neoformans*, serotype D) and neomycin phosphotransferase (*NEO*; confers resistance to G-418) coding sequence for strain KN99α (var. *grubii*, serotype A). To make JEC21 *uve1*Δ, 5' and 3' gene flanks were amplified by primer set AISV030/AISV034 and AISV032/AISV035, respectively, using JEC21 genomic DNA. To make KN99α *uve1*Δ, 5' and 3' gene flanks were amplified by primer set ai830/ai831 and ai832/ai833, respectively, using KN99α genomic DNA. The *NAT* and *NEO* ORFs were amplified by primer set ai290/ai006. Overlap PCR was performed to obtain 5'-*UVE1*-*NAT*-*UVE1*-3' and 5'-*UVE1*-*NEO*-*UVE1*-3' cassettes by mixing equimolar ratio of 5'-*UVE1*, *NAT*, *UVE1*-3' for JEC21 and 5'-*UVE1*, *NEO*, *UVE1*-3' for KN99α. Primers used to perform overlap PCR were

AISV030/AISV032 and ai830/ai833 for JEC21 and KN99α, respectively. About 2 μg of 5'-*UVE1-NAT-UVE1*-3' or 5'-*UVE1-NEO-UVE1*-3' cassette was transformed using biolistic delivery into strains JEC21 and KN99α. Gene replacement was confirmed by PCR and Southern blots for the correct integration of the gene cassette. AISVCN101 and AI191 are the respective *uve1*Δ strains for the JEC21 and KN99α strain backgrounds. For complementation of *UVE1* in serotype A, a wild type copy of *UVE1* was amplified with primers ALID0001 and ALID0002 and cloned into the pCR2.1 TOPO plasmid. The insert was excised with BamHI-XhoI and subcloned into the BamHI-SalI site of pPZP-NATcc. The plasmid was transformed into strain AI191 (*uve1::NEO*) by biolistics, with positive transformants selected for growth on yeast extract-peptone-dextrose (YPD) + nourseothricin (100 μg/ml) plates. Unless otherwise stated, strains were exposed to the laboratory ambient light (400–800 Lux) during experiments.

Northern blot analysis of transcript levels of *UVE1* homologs

Cultures were prepared for *C. neoformans* strains KN99α, AI81 (*bwc1*Δ), JEC21, AI5 (*bwc1*Δ), *C. gattii* (R265), *S. pombe* L972, *N. crassa* wild-type FGSC 4200, *N. crassa* (*wc-1*) FGSC 4398, *P. blakesleeanus* wild-type NRRL1555, and *P. blakesleeanus* (*madA madB*) mutant L51. All strains of each species were plated with equal optical density or numbers of spores in duplicates on 15 cm diameter petri dishes containing YPD, and kept in darkness. For *N. crassa* only, 50 ml liquid cultures were grown in 50 ml YPD medium. Cultures were grown for 23 hours or 47 hours depending on the growth kinetics of the species. On completion of 23 hours or 47 hours, one of the sets was exposed to cool white light (dual Sylvania 4100 K 32W bulbs) of 1600-2600 Lux for 1 hour and the other set left in the dark. On completion of the 24 hour or 48 hour time periods both the light and dark cultures were

scraped in the light or under safe red light (GBX LED safelight, Kodak, Rochester, NY). *N. crassa* cultures were harvested directly from the liquid medium. All cultures were pelleted, frozen using a dry ice-ethanol bath, lyophilized and stored at -80°C.

Total RNA was isolated using Trizol reagent (Invitrogen, Grand Island, NY). To address the low transcript abundance of *UVE1*, total RNA was further purified by polyA mRNA isolation starting with 1 mg total RNA, using the PolyATract Kit (Promega, Madison, WI), except for *P. blakesleeanus* and *C. gattii* where 40 μg of total RNA were used. RNA samples were resolved on 1.4% agarose denaturing formaldehyde gels and blotted on to Zeta Probe membrane (Bio-Rad). Probes for northern analysis were amplified using specific primer sets (Table 4) and radiolabeled with [α-^{32}P] dCTP (PerkinElmer, Waltham, MA) using the RediPrime II labeling kit (Amersham, Pittsburg, PA). The blots were stripped and re-probed with fragments of actin homologs as loading controls. Autoradiograms were scanned, and transcript levels were compared by ImageJ analysis.

Subcellular localization of Uve1

The localization of the two isoforms of Uve1 within the cell was assessed by fusions to green fluorescent protein (eGFP). *C.n.* var. *neoformans* strain JEC21 genomic DNA was used as template to amplify the *UVE1* light (L) isoform using primers AISV001/AISV003 and *UVE1* dark (D) isoforms using primers AISV002/AISV003. The histone 3 promoter for *Cryptococcus* (P_{H3}) and *GFP-NAT* were amplified from the pPZP-GFP-NATcc plasmid using ai255/AISV005 (overlap primer for L) or ai255/AISV006 (overlap primer for D) for P_{H3}, and AISV004/ai256 for *GFP-NAT*. The overlap construct was amplified by mixing equimolar ratios of the three amplicons for the light and dark isoforms using primers M13F and M13R. About 2 μg of gel purified *UVE1* L and D overlap constructs were transformed

into strain AI191 by biolistics. Positives clones were selected by their growth on YPD + 100 μg/ml nourseothricin plates and confirmed by PCR, DNA sequencing, western blotting for eGFP, and fluorescence signal.

Strains AISVCN28 and AISVCN02 were used for localization of the Uve1 light and dark isoforms fused to GFP. Strains were stained with MitoTracker Red CMXRos (Invitrogen) at 3 nM, kept in the dark for 20 min, washed and suspended in phosphate buffered saline (PBS) and used for microscopy. Cells were imaged using Olympus confocal microscopes FLUOVIEW FV10i or FV300.

DNA damage assay

Cultures for *C. neoformans* strains KN99α (WT) and AI191 (*uve1*Δ) were grown overnight in YPD and washed with distilled water. Cells were suspended in phosphate buffered saline to 4 X 10^4 cells/ml. For each strain 150 ml of cells were distributed in 30 ml aliquots for time points 0 min (after stress), 1 hour, 4 hour, 6 hour and control (no stress). For each aliquot the cells were placed in 15 cm petri dishes and exposed to UV light (50 J/m^2) using a UV cross linker. Immediately after the UV stress, cells were transferred to 50 ml falcon tubes and kept on ice. Control and 0 min cells were pelleted and frozen in liquid nitrogen. For 1 hour, 4 hour and 6 hour time points, cells were re-suspended in YPD and incubated at 30°C for these respective times, then centrifuged to pellet and snap frozen. All samples were lyophilized, and DNA was extracted by the CTAB buffer method (Pitkin et al., 1996).

The relative DNA damage to the mitochondrial and nuclear genomes were assessed using a PCR assay based on established methods (Hunter et al., 2010). Concentrations of DNA samples from each treatment were standardized by measuring them by

spectrophotometry and making appropriate dilutions. Primers used for amplification of fragments of the mitochondrial genome were AISV87/AISV91 (giving an 11 Kb fragment). PCR conditions for long mitochondrial PCR were 94°C 4 min, 23 cycles for 98°C 10 sec, 68°C 15 min, and a final extension of 72°C 10 min using Ex Taq (Takara, Kyoto, Japan). For nuclear long amplification (giving an 8 kb fragment) primers were AISV85/AISV95. Conditions for long nuclear PCR were 94°C 4 min, 23 cycles for 94°C 20 sec, 58°C 20 sec, 72°C 6 min and a final extension of 72°C 7 min. Short amplification primers for mitochondrial genome were AISV89/AISV99 and for the nuclear genome AISV85/AISV97 amplifying about 250 bp. PCR conditions for small mitochondrial and nuclear amplicons were 94°C 4 min, 23 cycles for 94°C 20 sec, 55°C 20 sec, 72°C 1 min, and a 72°C 7 min final extension. All PCR amplicons were resolved on agarose gels, and intensities were quantified using ImageJ software. DNA damage was compared by calculating the relative amplification of large PCR fragments of the UV treated samples to that of the respective untreated controls using the method reported (Hunter et al., 2010), and adjusting for differences between nuclear and mitochondrial amplicon sizes.

Virulence assays in wax moth larvae

The *Galleria mellonella* (greater wax moth) assay of the virulence of *C. neoformans* strains followed methods previously described (Mylonakis et al., 2005). Overnight cultures in YPD medium were washed three times with PBS. Cells were suspended in PBS to 2 X 10^7 cells/ml. For each strain 11-12 larvae were injected with 5 µl of the cells, as well as the control PBS. Wax moth were incubated at 37°C and survival monitored daily. To examine the effects of loss of *UVE1*, strains KN99α, AI191 and AI181 were used. The *RAD23* experiments used KN99α, *rad23*Δ, the *rad23*Δ+*RAD23* complementation strain and all the

six domain deletion strains *RAD23* DIΔ, *RAD23* DIIΔ, *RAD23* DIIIΔ, *RAD23* DIVΔ, *RAD23* DIΔ+DIIΔ and *RAD23* DIIΔ+DIVΔ. For the *RAD23* domain deletions, two independently-transformed strains were used as experimental duplicates.

Complementation tests with *C. neoformans UVE1* isoforms in a *S. pombe uve1* knockout strain

An *S. pombe uve1* knockout strain was constructed to serve for the functional analysis of *UVE1* isoforms from *C. neoformans*. For the construction of the gene knockout cassette, genomic DNA from *S. pombe* strain L972 was used to amplify around 320 bp 5'-*uve1* and 300 bp 3'-*uve1* fragments using primer pairs AISV007a/AISV009 and AISV010/AISV011, respectively. The KanMX fragment was amplified using primer set AISV007/AISV008 from plasmid pFA6a-GFP(S65T)-kanMX6. Overlap PCR was performed to generate the gene knockout cassette using primer set AISV007a/AISV011. Around 2 μg of the PCR construct were transformed into *S. pombe* (strain MM72-4A *ura4-D18 h*$^-$) by lithium acetate transformation and cells plated on to YPD + 100 μg/ml G-418. Gene knockouts were confirmed by PCR and Southern blotting. *S. pombe uve1* knockout strain AISVSP1 was selected for *C. neoformans UVE1* complementation studies.

UVE1 cDNA was reverse transcribed from RNA of *C. neoformans* strain JEC20 using Superscript III First strand Synthesis System (Invitrogen), as per company instructions [JEC20 is isogenic to JEC21, with a different *MAT* allele; (Kwon-Chung et al., 1992)]. The synthesized cDNA was amplified by site directed mutagenesis to abolish an NdeI site inconvenient for subcloning while conserving the encoded amino acid residue, and to introduce NdeI and BamHI restriction sites at the start and end of the *UVE1* gene. Primers used for amplification of fragment 1 of the L and D form were AISV014/AISV013 and

AISV015/AISV013, respectively. Primers used for amplification of fragment 2 were AISV012/AISV016. Overlap PCR was performed to amplify full L and D genes from fragment 1 and 2, using primers AISV014/AISV016 for *UVE1* L form and AISV015/AISV016 for *UVE1* D form. The NdeI and BamHI digested cassettes were ligated into the NdeI-BamHI site in the pREP42 vector enabling expression from an *nmt* promoter (Basi et al., 1993). Positive clones were confirmed by sequencing. Plasmids containing *UVE1* L and D isoforms were transformed into *S. pombe* strain AISVSP1 (*ura4-D18 uve1::kanMX*) by the lithium acetate method. Empty vector pREP42 was transformed into strain AISVP1 as a control. Positive *S. pombe* transformants were selected on YNB without uracil and were confirmed by PCR.

C. neoformans* UVE1-GFP localization in *S. pombe

C. neoformans var. *neoformans* Uve1 (L) C-terminal GFP localization in *S. pombe* was done by examining the expression of a fusion of *UVE1* (L) to eGFP as generated by overlap PCR. For PCR of fragment 1, *UVE1* (L) was amplified from pREP42-*UVE1* (L) using primers AISV014/AISV003 and the fragment 2, GFP, was amplified from P_{HXK2}-*RAD23*-*GFP* using primers AISV004/AISV066. Overlap PCR joining fragments 1 and 2 was performed by primer set AISV014/AISV066. The overlap PCR product was cloned in a TA vector (pCR 2.1 TOPO; Invitrogen), and transformed by heat shock into *E. coli* DH5α. Positive clones were selected and sequenced. A plasmid containing the desired Nde1-*UVE1*-GFP-BamHI overlap was digested with NdeI and BamHI. The Nde1-*UVE1*-GFP-BamHI digest was ligated into NdeI and BamHI digested pTN157. Plasmid pTN157-*UVE1*-GFP was transformed into *S. pombe* strain AISVSP1 (genotype *ura4-D18 uve1::kanMX*) by the lithium acetate method. Positive *S. pombe* transformants were selected on minimal medium

without uracil and were confirmed by PCR. Transformants were examined for fluorescence signal and their UV resistant phenotype. Confocal microscopy was performed for strain AISVSP15. For both mitochondrial and nuclear staining, cells were grown in Edinburgh Minimal Medium (EMM; MP Biomedicals, Solon, OH). Mitochondrial staining was performed with MitoTracker Red CMXRos (Invitrogen) at a final concentration of 3 nM in water, kept in the dark for 20 min, washed and suspended in PBS and used for microscopy. Hoechst 33342 was used to stain the nucleus. Cells grown in EMM were washed and suspended in Hoechst (1 μg/ml in water) for 10 min. Cells were washed and suspended in PBS, and microscopy was performed.

UV survival experiments for *S. pombe*

Overnight cultures for strains L972, AISVSP1, AISVSP2, AISVSP3, AISVSP4 and AISVSP15 in YES media were sub-cultured the following day. Strains in exponential phase were dotted on YES medium in ten-fold serial dilutions. One set of plates was exposed to UV light (120 J/m^2) using the UV cross linker, and another plate kept unexposed. Both UV treated and unexposed sets were incubated at 30°C for 2 days. For UV dose response experiments exponentially growing cells for strains at the same optical density were ten-fold serially diluted and equal volumes for all dilutions of the cells were plated on YES media. The control was kept unexposed to UV and others were exposed at UV doses of 60, 120 and 180 J/m^2. All plates were incubated at 30°C for 3 days, and colony forming unit data analyzed for percentage survival.

***UVE1* over-expression in *C. neoformans bwc1* mutants**

The *UVE1* gene was over-expressed in *bwc1* knockout backgrounds to assess if *UVE1* can rescue the UV sensitive phenotype of *bwc1* mutation. A fusion cassette of the JEC21

GAL7 promoter (P_{GAL7}) and *UVE1* gene was made by overlap PCR. The *GAL7* promoter was amplified by primer set AISV025/AISV028 and *UVE1* was amplified using primer set AISV027/AISV026 on JEC21 genomic DNA. The P_{GAL7}-*UVE1* fusion cassette was amplified by mixing *GAL7* promoter and *UVE1* PCRs in equimolar ratios by primer set AISV025/AISV026. The P_{GAL7}-*UVE1* fusion cassette was cloned in a TA vector (pCR 2.1 TOPO; Invitrogen), and transformed by heat shock in *E. coli* Top10 cells. Positive clones were selected and sequenced. A plasmid containing P_{GAL7} -*UVE1* was digested with BamHI and XhoI. The fragment was ligated with pPZP-NEO *Agrobacterium* vector digested with same enzymes, and transformed into Top10 cells. Positive clones were selected by their growth on kanamycin and verified by PCR and restriction digestion. The pPZP-NEO-P_{GAL7}-*UVE1* vector was transformed into *A. tumefaciens*. Selected positive *Agrobacterium* transformants were co-cultured with *C. neoformans* strains AI5 and AI81. Positive transformants were selected for growth on YPD + G-418 + cefotaxime plates. Transformants were cultured overnight in yeast nitrogen base (YNB) medium + 2% galactose or 2% glucose, and 10-fold serial dilutions placed on YPD medium plates. Dotting was performed in duplicate and one set was exposed to UV radiation at 120 J/m^2. Both sets were incubated at 30°C for 2 days.

Cloning and expression of recombinant Bwc2 for Electrophoretic Mobility Shift Assays (EMSA)

JEC21 RNA was reverse transcribed to make cDNA using Superscript III First strand Synthesis System (Invitrogen). A fragment of *BWC2* cDNA was amplified using primers AISV040/AISV041, containing BamHI and EcoRI restriction sites. The amplicon was digested with BamHI and EcoRI, and ligated into the pRSETA vector (Invitrogen) digested

with the same enzymes. Top10 cells were transformed with the ligation product. An error-free clone was identified by sequencing. The plasmid containing *BWC2* was transformed into BL21(DE3)pLysS cells and selected on ampicillin+chloramphenicol SOB medium plates. Protein induction and expression using 1 mM IPTG was performed as described for the pRSET expression system by Invitrogen. The $(Histidine)_6$-tagged Bwc2 protein was semi-purified using Pure Proteome Nickel Magnetic beads (Millipore Corporation, Billerica, MA) as per the manufacturer's instructions.

For EMSA, a 244 bp (P_1) region 5' of the start codon of *UVE1* containing putative Bwc2 binding sites was amplified using primer set AISV019/AISV020. A control nonspecific DNA fragment (NS) of 278 bp was amplified from pRS426 vector using primers ALID1229/ALID1230. About 600 ng of the amplified fragment from *UVE1* promoter region and nonspecific probe was radiolabeled with [γ-^{32}P] dATP (PerkinElmer) using T4 polynucleotide kinase (New England Biolabs, Ipswich, MA). Labeling conditions were 1X T4 polynucleotide buffer, 5 µl 6000 Ci/mmol γ-^{32}P ATP, 10 units T4 polynucleotide kinase in a 50 µl reaction mixture at 37°C for 30 min. The radiolabeled probes were purified using PCR purification columns (Qiagen). The composition of 5X EMSA binding buffer was 20% w/v glycerol, 5 mM $MgCl_2$, 250 mM NaCl, 2.5 mM EDTA pH 8, 10 mM DTT with or without 12 µM $ZnSO_4$ (Holden and Tacon, 2011) (with slight modifications). 20 to 50 µg of purified Bwc2 protein were pre-incubated with 1X EMSA binding buffer for 20 min at room temperature for all reactions. Total reaction mixture of 20 µl consisted of 1X EMSA binding buffer, 20 to 50 µg of purified protein, cold probe (if added), 1 µl of radiolabeled probe and 1X phosphate buffer, followed by 50 min incubation at room temperature. For competition reactions, 600 ng and 900 ng of the cold probes were included in the reaction mixture prior to

addition of radiolabeled probes. At the end of 50 min incubation, samples were transferred to ice followed by addition of EMSA loading dye. Samples were loaded on 6% polyacrylamide Tris-borate-EDTA (TBE) gels (Invitrogen), and run at 130 V for 2 hr in 1X TBE at 4°C. Autoradiography was performed by exposure to Gene Mate Blue ultra autoradiography films.

Generation of *RAD23* knockout

For generation of a *RAD23* knockout the *RAD23*::*NAT* knockout cassette was amplified from the genomic DNA of the *RAD23* knockout strain (Liu et al., 2008) using primer set AISV49 and AISV50. The knockout cassette was transformed by biolistics into KN99a strain background and transformants were selected on YPD+NAT media. The *rad23*Δ strain was confirmed by PCR and Southern blotting. The rationale for recreating this mutant is that the H99 strain used by Liu et al. (2008) has a mating defect, preventing some subsequent experiments.

Generation of *RAD23* full length and domain deletion complementation constructs and strains

To complement the *rad23*Δ strain, full length *RAD23* with its native promoter and terminator was amplified from genomic DNA of *C.n.* var. *grubii* strain KN99α using primers AISV118/AISV119. The amplified PCR product was cloned in the pCR2.1 TOPO-TA vector and transformed into DH5α cells. The plasmids isolated were sequenced to identify one with the correct sequence of *RAD23*. The TA vector with P_{native}-*RAD23*-T and pPZP-NEO were digested with BamHI. The two digestion products were ligated and the resulting product p*PZP*-P_{native}-*RAD23*-T-*NEO* was transformed in *E. coli*. The clones were further verified by PCR of the resulting plasmids and by sequencing. The correct vector p*PZP*-P_{native}-*RAD23*-T-*NEO* was transformed into *Agrobacterium*. The transformed strain containing p*PZP*-P_{native}-

RAD23-T-*NEO* was then co-cultured with the *rad23*Δ *C. neoformans* strain. Fungal transformants were selected for growth on YPD + G-418 + cefotaxime plates and were verified by PCR.

For the generation of Rad23 individual domain deletion constructs the p*PZP*-P_{native}-*RAD23*-T-*NEO* construct, verified by sequencing and its complementation capabilities, was used as a template construct. Primers were designed specific for each type of domain deletion **(Table 3)**. For performing the domain deletions the QuickChange II XL Site-Directed Mutagenesis Kit (Agilent Technologies, Foster City, CA) was used following the suggested protocol. The cycling parameters used were as recommended in the kit, with the extension temperature of 68° C for 15 min for all 18 cycles. After DpnI digestion of the reaction mix for an hour at 37° C, 2 µl of the treated mix was transformed by heat shock in to DH5α cells. The plasmids obtained from the transformants were verified by sequencing, for all four-domain deletions (*RAD23* DIΔ, *RAD23* DIIΔ, *RAD23* DIIIΔ and *RAD23* DIVΔ). Plasmids confirmed by sequencing analysis were then transformed into *A. tumefaciens*. Verified transformants were used for T-DNA transformation into the *rad23*Δ strain to obtain *C. neoformans* strains carrying new alleles of *RAD23*. Transformants were verified by PCR, sequencing and were subjected to phenotypic analysis. For generating the double domain deletion constructs *RAD23* DIΔ+DIIΔ and *RAD23* DIIΔ+DIVΔ, the template constructs used were pPZP-NEO-*RAD23* DIΔ and pPZP-NEO-*RAD23* DIVΔ using the primer set AISV142/AISV143 which is for domain II deletion. The protocol followed was the same as for the single domain deletion strains.

Rad23 subcellular localization

A Rad23-GFP fusion construct was made. *C.n.* var. *grubii* strain KN99α genomic DNA was used as template to amplify the *RAD23* gene using primers AISV165/AISV166 with a NcoI site in both the primers. The p*PZP*-HXK2-GFP-*NAT* vector was also digested with NcoI. The NcoI-digested *RAD23* amplicon and NcoI-digested p*PZP*-GFP-*NAT* vector without the HXK2 insert were ligated and transformed in DH5α. The cloning strategy places a *RAD23-GFP* fusion under control of the constitutive histone H3 promoter when transformed into *C. neoformans* cells. The recombinant p*PZP-RAD23*-GFP-*NAT* construct was sequenced for the *RAD23*-GFP fusion and the correct construct was then transformed by electroporation into *Agrobacterium*. The transformed *Agrobacterium* strain was co-cultured with KN99α. Positive transformants were selected for growth on YPD + NAT + cefotaxime plates. The selected transformed KN99α strains were scanned for green fluorescence. However, localization of the same construct within the *rad23*Δ strain was not possible because it is nourseothricin resistant. *NAT* was switched with *NEO* as a selectable marker in the pPZP- *RAD23*-GFP-NAT construct. For this switch, pPZP-*RAD23*-GFP-NAT was digested with EcoRI to remove the *NAT* construct, and into the EcoRI site was inserted an EcoRI-digested *NEO* insert from plasmid pPZP-NEO11. Ligated pPZP-*RAD23*-GFP-NEO was then transformed into DH5α. The sequenced correct construct was then transformed into *Agrobacterium*. The transformed *Agrobacterium* strain was co-cultured with *rad23*Δ strain. Positive transformants were selected for growth on YPD + G-418 + cefotaxime plates. The mitochondrial and nuclear localization analysis for the Rad23-GFP expressing strains was performed by confocal microscopy, as for the Uve1-GFP expression described above.

For making the domain deletion GFP constructs for *RAD23* DIΔ and *RAD23* DIVΔ the p*PZP-RAD23*-GFP-*NEO* construct was used as the template and the primer combination AISV140/AISV141 and AISV146/AISV147. To generate the domain deletions *RAD23* DIΔ-GFP and *RAD23* DIVΔ-GFP constructs the QuickChange II XL Site–Directed Mutagenesis Kit was used as described above. The two constructs obtained were sequenced, an error-free version confirmed, and were used for *Agrobacterium*-mediated transformation into the *rad23*Δ strain.

Ten-fold serial dilution dotting assays for UV and chemical stress tests for different *C. neoformans* strains

Different *C. neoformans* strains generated for *UVE1* and *RAD23* studies were subjected to different kinds of stress responses for phenotypic observations. Strain were grown overnight in liquid YPD medium at 30° C. Strains were serially diluted to 10 fold each dilution up to 10^{-6} dilution. Serially diluted cultures were spotted on YPD medium plate as control or on the YPD+ stressor. For endoplasmic reticulum stress tunicamycin (0.125 μg/ml) or DTT (10 mM) were used, for DNA damage or oxidative stress *tert*-Butyl-Hydroperoxide (0.3 mM or 0.6mM), H_2O_2 hydrogen peroxide (1 mM), or MMS methyl methanesulfonate (0.025 %) were used. Other chemical stressors used were Paraquat (0.5 mM), and cobalt chloride (60 μM). The UV sensitivities of strains were tested by applying UV (120 J/m^2) in an XL-1500 UV cross linker (Spectronics Corporation, Lincoln, NE). The unstressed control and stress plates were incubated at 30° C for 2 days.

Table 2: Fungal strains used

Strain	Genotype	Parents/Background	Reference
Cryptococcus			
JEC20	Wild type, *MAT***a**		(Kwon-Chung et al., 1992)
JEC21	Wild type, *MAT*α		(Kwon-Chung et al., 1992)
AI5	*bwc1*Δ*::URA5 ura5*, *MAT*α	JEC43	(Idnurm and Heitman, 2005)
AI6	*bwc1*Δ*::URA5 ura5*, *MAT***a**	AI5 X JEC20	(Idnurm and Heitman, 2005)
AI51	*bwc1*Δ*::NEO BWC1*, *MAT*α	AI5	(Idnurm and Heitman, 2005)
AISVCN103	*uve1*Δ*::NAT*	JEC20	This research
AISVCN101	*uve1*Δ*::NAT*	JEC21	This research
KN99**a**	Wild type, *MAT***a**		(Nielsen et al., 2003)
KN99α	Wild type, *MAT*α		(Nielsen et al., 2003)
AI89	*bwc1*Δ*::NAT*	KN99**a**	(Idnurm and Heitman, 2005)
AI81	*bwc1*Δ*::NAT*	KN99α	(Idnurm and Heitman, 2005)
AI191	*uve1*Δ*::NEO*	KN99α	This research
AISVCN52	*uve1*Δ*::NEO*	KN99**a**	This research
AI198	*uve1*Δ*::NEO UVE1-NAT*	AI191	This research
ST239E6	P_{UVE1}*-T-DNA*	KN99α	(Idnurm et al., 2009)
AISVCN28	*uve1*Δ*::NEO UVE1* (L)-GFP	AI191	This research
AISVCN02	*uve1*Δ*::NEO UVE1* (D)-GFP	AI191	This research
VANC.R265	Wild type, *MAT*a		
AISVCN53	*bwc1*Δ*::URA5 ura5* P_{GAL7}*-UVE1-NEO*	AI5	This research
AISVCN66	*bwc1*Δ*::NAT* P_{GAL7}*-UVE1-NEO*	AI81	This research
AI219	*rad1*Δ*::NAT*	KN99α	Unpublished
D320	*rad27*Δ*::NAT*	H99	(Liu et al., 2008)
D893	*rad17*Δ*::NAT*	H99	(Liu et al., 2008)
D1445	*rad50*Δ*::NAT*	H99	(Liu et al., 2008)
D287	*msh201*Δ*::NAT*	H99	(Liu et al., 2008)

Table 2: Fungal strains used continued…

TD397	*rad4*Δ*::NAT*	H99	(Liu et al., 2008)
D1053	*rad53*Δ*::NAT*	H99	(Liu et al., 2008)
D759	*uve1*Δ*::NAT*	H99	(Liu et al., 2008)
D288	*rad23*Δ*::NAT*	H99	(Liu et al., 2008)
D594	*mre11*Δ*::NAT*	H99	(Liu et al., 2008)
D1344	*rad10*Δ*::NAT*	H99	(Liu et al., 2008)
D203	*rad201*Δ*::NAT*	H99	(Liu et al., 2008)
D293	*rad6*Δ*::NAT*	H99	(Liu et al., 2008)
AISVCN120	*rad23*Δ*::NAT*		This research
AISVCN218	*rad23*Δ*::NAT*+*RAD23::NEO*		This research
AISVCN250	*RAD23* DIΔ*::NEO*		This research
AISVCN251	*RAD23* DIIΔ*::NEO*		This research
AISVCN252	*RAD23* DIIIΔ*::NEO*		This research
AISVCN253	*RAD23* DIVΔ*::NEO*		This research
AISVCN254	*RAD23* DI+DIIΔ*::NEO*		This research
AISVCN255	*RAD23* DI+DIVΔ*::NEO*		This research
AISVCN87	*RAD23*-GFP*::NAT*		This research
AISVCN256	*RAD23*-GFP*::NEO*		This research
AISVCN257	*RAD23* DIΔ-GFP*::NEO*		This research
AISVCN258	*RAD23* DIVΔ-GFP*::NEO*		This research
S. pombe			
L972	Wild type		
MM72-4A	*ura4-D18 h*$^{-}$		
AISVSP1	*uve1*Δ::kanMX6	MM72-4A	This research
AISVSP2	*uve1*Δ::kanMX6 *ura4*$^{+}$	AISVSP1	This research
AISVSP3	*uve1*Δ::kanMX6 *C.n. UVE1* (D)-*ura4*$^{+}$	AISVSP1	This research
AISVSP4	*uve1*Δ::kanMX6 *C.n. UVE1* (L)-*ura4*$^{+}$	AISVSP1	This research
AISVSP15	*uve1*Δ::kanMX6 *URA5: C.n. UVE1* (L)-GFP-*ura4*$^{+}$	AISVSP1	This research
P. blakesleeanus			
NRRL1555	Wild type		(Bergman et al., 1973

Table 2: Fungal strains used continued…

L51	*madA madB*	(Lipson et al., 1980)
N. crassa		
FGSC 4200	Wild type	(Kafer and Fraser, 1979)
FGSC 4398	*wc-1*	(Degli-Innocenti and Russo, 1984)

Table 3: Plasmids used in the study

Plasmid Name	**Parent plasmid**	**Comments/Purpose**	**Reference**
pFA6a-GFP[S65T]-kanMX6		*S. pombe UVE1* knockout	
pPZP-GFP-NATcc	pPZP-NATcc	GFP-NAT cassette amplification	(Idnurm et al., 2007)
pPZP-HXK2-GFP-NATcc	pPZP-GFP-NATcc	GFP fusion by subcloning	(Idnurm et al., 2007)
pJAF1		Neomycin amplification	(Fraser et al., 2003)
pRS426		Non-specific probe preparation for EMSA	(Colot et al., 2006)
pREP42		*S. pombe* empty plasmid	(Basi et al., 1993)
pREP42-*UVE1*(L)	pREP42	NdeI and BamHI/*S. pombe UVE1* (L) complementation	This research
pREP42-*UVE1*(D)	pREP42	NdeI and BamHI/*S. pombe UVE1* (D) complementation	This research
pCR 2.1 TOPO-P_{GAL7}-*UVE1*	pCR 2.1 TOPO	TA cloning/*UVE1* overexpression in *bwc1*	This research
pPZP-NEO-P_{GAL7}-*UVE1*	pPZP-NEO	BamHI and XhoI/*UVE1* overexpression in *bwc1*	This research
pRSETA-*Bwc2*	pRSET A	BamHI and EcoRI/Bwc2 expression	This research
pPZP-*UVE1*-NATcc	pPZP-NATcc	BamHI-SalI/*UVE1* complementation in *uve1*	This research
pTN157-*UVE1* (L)-GFP	pTN157	*S. pombe UVE*1 (L)-GFP localization	This research
pPZP-P_{native}-*RAD23*-T-NEO	pPZP-*NEO*	*RAD23* complimentation construct	This research
pPZP-P_{native}-*RAD23* DIΔ-T-NEO	pPZP-P_{native}-*RAD23*-T-NEO	Rad23 domain I deletion construct	This research
pPZP-P_{native}-*RAD23* DIIΔ-T-NEO	pPZP-P_{native}-*RAD23*-T-NEO	Rad23 domain II deletion construct	This research
pPZP-P_{native}-*RAD23* DIIIΔ-T-*NEO*	pPZP-P_{native}-*RAD23*-T-NEO	Rad23 domain III deletion construct	This research
pPZP-P_{native}-*RAD23* DIVΔ-T-NEO	pPZP-P_{native}-*RAD23*-T-NEO	Rad23 domain IV deletion construct	This research
pPZP-P_{native}-*RAD23* DIΔ+DIIΔ-T-NEO	pPZP-P_{native}-*RAD23* DIΔ-T-NEO	Rad23 domain I+II deletion construct	This research
pPZP-P_{native}-*RAD23* DIIΔ+DIV-T-NEO	pPZP-P_{native}-*RAD23* DIVΔ-T-NEO	Rad23 domain I+IV deletion construct	This research
pPZP-*RAD23*-GFP-NAT	pPZP-hxk2-GFP-NAT	Rad23-GFP localization construct with NAT marker	This research
pPZP-*RAD23*-GFP-NEO	pPZP-*RAD23*-GFP-NAT	Rad23-GFP localization construct with NEO marker	This research
pPZP-*RAD23*-DIΔ-GFP-NEO	pPZP-*RAD23*-GFP-NEO	Rad23-DIΔ -GFP localization construct with NEO marker	This research
pPZP-*RAD23*-DIVΔ-GFP-NEO	pPZP-*RAD23*-GFP-NEO	Rad23-DIV -GFP-localization construct with NEO marker	This research

Table 4: Primers used to amplify probes for northern blot analysis

Primer	Sequence 5'-3'	Strain	Gene description	Organism
AISV001	ATGAGGTTCTTGTCGCTC	JEC21	*UVE1*	*C. n.* var. *neoformans*
AISV003	TTCTGCCACCGCTTTTTTCTTCAC	JEC21	*UVE1*	*C. n.* var. *neoformans*
AISV055	ATGCCTCCCCGAAGAAGTG	KN99α	*UVE1*	*C. n.* var. *grubii*
AISV056	CTCTGCCGCCGCTTCTTTC	KN99α	*UVE1*	*C. n.* var. *grubii*
AISV043	GAAGAAGTGCACGTACAG	R265	*UVE1*	*C. gattii*
AISV0044	CTAGGGCATTTCTTTCGT	R265	*UVE1*	*C. gattii*
AISV007a	GCTTAGGCTATTGAAACG	L972	*UVE1*	*S. pombe*
AISV011	CTTCTTTTCTACTACGCC	L972	*UVE1*	*S. pombe*
ALID1415	TAAACTCGATTATACGGTCC	FGSC 4200	*UVE1*	*N. crassa*
ALID1442	GCTTATGTGAGTCCTCCCATATACTAGGAGCTAGCC	FGSC 4200	*UVE1*	*N. crassa*
ALID1412	GCTTAGTACACAAAGATCCG	NRRL1555	*UVE1*	*P. blakesleeanus*
ALID1413	GATACTACTAGCTCATCTGC	NRRL1555	*UVE1*	*P. blakesleeanus*
ai018	ATGGAAGAAGAAGGTACG	JEC21	Actin	*C. n.* var. *neoformans*
ai019	TTAGAAACACTTTCGGTG	JEC21	Actin	*C. n.* var. *neoformans*
ai018	ATGGAAGAAGAAGGTACG	KN99α	Actin	*C. n.* var. *grubii*
ai019	TTAGAAACACTTTCGGTG	KN99α	Actin	*C. n.* var. *grubii*
AISV045	ATGTCTATGGAAGAAGAAG	R265	Actin	*C. gattii*
AISV046	ACCAGACTCGTCGTACTCG	R265	Actin	*C. gattii*
ALID0752	AAGAAATCGCAGCGTTGG	L972	Actin	*S. pombe*
ALID0753	CACTTACGGTAAACGATACC	L972	Actin	*S. pombe*
ai1677	TCTACTGGTTATCATGGG	FGSC 4200	Actin	*N. crassa*
ai1678	AGAAGCACTTGCGGTGCACG	FGSC 4200	Actin	*N. crassa*
ai679	CACACTTTCTACAACGAG	NRRL1555	Actin	*P. blakesleeanus*
ai680	ACATCTGCTGGAAGGTAG	NRRL1555	Actin	*P. blakesleeanus*
AISV69	ACAGTGACGATGTCTTTG	JEC21	*RAD53*	*C. n.* var. *neoformans*
AISV70	AGGCGCATAGATTTTCGG	JEC21	*RAD53*	*C. n.* var. *neoformans*
AISV69	ACAGTGACGATGTCTTTG	KN99α	*RAD53*	*C. n.* var. *grubii*
AISV70	AGGCGCATAGATTTTCGG	KN99α	*RAD53*	*C. n.* var. *grubii*
AISV71	TGACATGCCGCCCAATAC	JEC21	*RAD50*	*C. n.* var. *neoformans*
AISV72	GCGCATTGATATTCTCTTG	JEC21	*RAD50*	*C. n.* var. *neoformans*

Table 4: Primers used to amplify probes for northern blot analysis continued…

AISV71	TGACATGCCGCCCAATAC	KN99α	*RAD50*	*C. n. var. grubii*
AISV72	GCGCATTGATATTCTCTTG	KN99α	*RAD50*	*C. n.* var. *grubii*
AISV73	CAAGCGACAGGAGCCTCA	JEC21	*RAD17*	*C. n.* var. *neoformans*
AISV74	CGTCCACCAAATAATCCTC	JEC21	*RAD17*	*C. n.* var. *neoformans*
AISV73	CAAGCGACAGGAGCCTCA	KN99α	*RAD17*	*C. n.* var. *grubii*
AISV74	CGTCCACCAAATAATCCTC	KN99α	*RAD17*	*C. n.* var. *grubii*
AISV75	ACCCGACTCACAACCAAG	JEC21	*MRE11*	*C. n.* var. *neoformans*
AISV76	CTAATCCTCATCTGATGAC	JEC21	*MRE11*	*C. n.* var. *neoformans*
AISV75	ACCCGACTCACAACCAAG	KN99α	*MRE11*	*C. n.* var. *grubii*
AISV76	CTAATCCTCATCTGATGAC	KN99α	*MRE11*	*C. n.* var. *grubii*
AISV77	ATGACTGAGCAGAACAG	JEC21	*RAD10*	*C. n.* var. *neoformans*
AISV78	CACCTTGTCATCATCCT	JEC21	*RAD10*	*C. n.* var. *neoformans*
AISV77	ATGACTGAGCAGAACAG	KN99α	*RAD10*	*C. n.* var. *grubii*
AISV78	CACCTTGTCATCATCCT	KN99α	*RAD10*	*C. n.* var. *grubii*
AISV81	GCTTGAGATCGATGCTG	JEC21	*RAD6*	*C. n.* var. *neoformans*
AISV82	TCCGCTTCAACCACTTC	JEC21	*RAD6*	*C. n.* var. *neoformans*
AISV81	GCTTGAGATCGATGCTG	KN99α	*RAD6*	*C. n.* var. *grubii*
AISV82	TCCGCTTCAACCACTTC	KN99α	*RAD6*	*C. n.* var. *grubii*
AISV83	GACACATCCCTTATCTTCC	JEC21	*RAD1*	*C. n.* var. *neoformans*
AISV84	GATGTAGAAACTCCCAAGC	JEC21	*RAD1*	*C. n.* var. *neoformans*
SV16RAD27F	ATGGGTATTAAAGGTGAG	JEC21	*RAD27*	*C. n.* var. *neoformans*
SV16RSD27R	CTTCTTATTCTTCTTCTTCG	JEC21	*RAD27*	*C. n.* var. *neoformans*
SV16RAD27F	ATGGGTATTAAAGGTGAG	KN99α	*RAD27*	*C. n.* var. *grubii*
SV16RSD27R	CTTCTTATTCTTCTTCTTCG	KN99α	*RAD27*	*C. n.* var. *grubii*
SV20RAD4F	ATGAGCGCTTCCAGACC	KN99α	*RAD4*	*C. n.* var. *grubii*
SV21RAD4R	AGTCTGATTAATTTTATCTTCC	KN99α	*RAD4*	*C. n.* var. *grubii*
SV24RAD23NcoIF	CATGCCATGGTCAAGATCACTTTC	JEC21	*RAD23* full gene	*C. n.* var. *neoformans*
SV25RAD23NcoIR	CATGCCATGGGTTGATCCTCCTCCATG	JEC21	*RAD23* full gene	*C. n.* var. *neoformans*
AISV134	GATGGTATGGTTGAGATGG	KN99α	*RAD23* missing domain specific	*C. n.* var. *grubii*
AISV135	GGTACCTTCAACAGAAGG	KN99α	*RAD23* missing domain specific	*C. n.* var. *grubii*
Rad23F	GTGGCGATCAGCTCAGC	KN99α	*RAD23* + 3'UTR	*C. n.* var. *grubii*

Table 4: Primers used to amplify probes for northern blot analysis continued…

Rad23R	GATATGCTATTGAAACGAGA	KN99α	*RAD23* + 3'UTR	*C. n.* var. *grubii*

Table 5: Primers used for gene disruption and plasmid construction

Name	Sequence 5'-3'	Strain/Plasmid	Comments
AISV001	ATGAGGTTCTTGTCGCTC	JEC21	*UVE1* (L) GFP localization (F)
AISV002	ATGCATCCAGGTCAGGTG	JEC21	*UVE1* (D) GFP localization (F)
AISV003	TTCTGCCACCGCTTTTTTCTTCAC	JEC21	*UVE1* (L/D) GFP localization (R)
AISV004	GAAAAAAGCGGTGGCAGAAATGGTGAGCAAGGGCGAG	JEC21	*UVE1* overlap primer fused to GFP (F)
AISV005	GAGCGACAAGAACCTCATGGTGATAGATGTGTTGTG	JEC21	*UVE1* (L) start fused to histone promoter
AISV006	CACCTGACCTGGATGCATGGTGATAGATGTGTTGTG	JEC21	*UVE1* (D) start fused to histone promoter
AISV007a	GCTTAGGCTATTGAAACG	L972	*S. pombe UVE1* knockout (F)
AISV007	CGTACGCTGCAGGTCGAC	pFA6a-GFP[S65ST]-kanMX6	KanMX (F)
AISV008	TCGATGAATTCGAGCTCG	pFA6a-GFP[S65ST]-kanMX6	KanMX (R)
AISV009	GTCGACCTGCAGCGTACGTTCGTGTAGACGTAGAAG	pFA6a-GFP[S65ST]-kanMX6/ FY7507	*S. p. UVE1-KanMx* start overlap knockout
AISV010	CGAGCTCGAATTCATCGAACAGAAGCAACATTACTC	pFA6a-GFP[S65ST]-kanMX6/ FY7507	*S. p. UVE1-KanMx* end overlap knockout
AISV011	CTTCTTTTCTACTACGCC	L972	For *S. pombe UVE1* knockout (R)
AISV012	GTGATGATCATCCAcATGGG	cDNA JEC20	Site directed *S. p. UVE1* complement (F)
AISV013	CCCATGTGGATGATCATCAC	cDNA JEC20	Site directed *S. p. UVE1* complement (R)
AISV014	GGAATTCCATATGAGGTTCTTGTCGCTC	cDNA JEC20	*UVE1* (L) + NdeI for *S. p.* complementation(F)
AISV015	GGAATTCCATATGCATCCAGGTCAGTTTAC	cDNA JEC20	*UVE1* (D) + NdeI for *S. p.* complementation(F)
AISV016	CGGGATCCTGGCTATTCTGCCACCGC	cDNA JEC20	*UVE1* (L/D) + BamHI *S. p.* complementation(R)
AISV019	GTAGTCACCAGTCATTCAG	JEC21	EMSA Probe 2 *UVE1* Promoter (F)
AISV020	GAACCTCATGTACTTAATG	JEC21	EMSA Probe 2 *UVE1* Promoter (R)
AISV025	GATCAGGCGCTGGCTGTGAG	JEC21	Promoter *GAL7* (F)
AISV026	AGCGACGTCTTCTTTGCG	JEC21	*UVE1* terminator
AISV027	GCGCTCAATCCCCTCTTGAGAATGAGGTTCTTGTCGCTC	JEC21	Overlap *UVE1-GAL7* F
AISV028	GAGCGACAAGAACCTCATTCTCAAGAGGGGATTGAGCGC	JEC21	Overlap *UVE1-GAL7* JEC21 R
AISV030	CTCCACACACTCGATTC	JEC21	*UVE1* knockout (from B-3501A) (F)
AISV031	CCATCATCCCATCTCCTC	JEC21	Confirmation of *UVE1* knockout (F)
AISV032	GAAGGTGGCTTCATTCG	JEC21	*UVE1* knockout (R)
AISV033	GAGAGACTTCCGCTGGAG	JEC21	Confirmation of *UVE1* knockout (R)
AISV034	GCTTATGTGAGTCCTCCCGACTTTGCTCTAGACTTC	JEC21	*UVE1* knockout overlap with *NAT*

Table 5: Primers used for gene disruption and plasmid construction continued…

AISV035	CTCGTTTCTACATCTCTTCCAATCCCAGCATGCAGAC	JEC21	*UVE1* overlap with *NAT*
AISV040	CGGGATCC AATGGTGCCGCCGAGTTCC	cDNA JEC21	BamHI+ Bwc2, for Bwc2 (F)
AISV041	CGGAATTC AAGTTGAATTTCGTTTTGCCC	cDNA JEC21	EcoRI+ Bwc2, for Bwc2 (R)
ai255	CATTCAGGCTGCGCAACTG	pPZP-GFP-NATcc	GFP-NAT cassette (F)
ai256	CCAATACGCAAACCGCCTC	pPZP-GFP-NATcc	GFP-NAT cassette (R)
ai290	GGGAGGACTCACATAAGC	pJAF1/pPZP-GFP-NATcc	NEO or NAT resistance (F)
ai006	GAAGAGATGTAGAAACGAG	pJAF1/pPZP-GFP-NATcc	NEO or NAT resistance (R)
ALID1229	GTAACGCCAGGGTTTTCCCAGTCACGACG	pRS426	EMSA nonspecific probe (F)
ALID1230	GCGGATAACAATTTCACACAGGAAACAGC	pRS426	EMSA nonspecific probe (R)
ai830	GGGTTGCGTAAGTGCTGG	KN99α	*UVE1* knockout (F)
ai831	GCTTATGTGAGTCCTCCCAGGTAGTCGTGGTTGTCG	KN99α	*UVE1* knockout overlap (F)
ai832	CTCGTTTCTACATCTCTTAGCGACGAAGGAGAAGCC	KN99α	*UVE1* knockout overlap (R)
ai833	GATAGGCAGTTTCGATCC	KN99α	*UVE1* knockout (R)
ALID0001	TCTGATGCTTCTTTGGAAGG	KN99α	*UVE1* complementation (F)
ALID0002	TACCACCTTTTCCTGATGGG	KN99α	*UVE1* complementation (R)
AISV066	CCGGGATCCTTACTTGTACAGCTCGTC	P_{HXK2}-*RAD23*-*GFP*	*C. n. UVE1* (L)-*GFP* in *S. pombe*
AISV85	AGCGCTTGATTCTATGCG	KN99α	Nuclear Long / Short PCR (F)
AISV95	AGTCCTTCTCTTACTCCC	KN99α	Nuclear Long PCR (R)
AISV97	CAATTTCGCTCATGCCGT	KN99α	Nuclear Short PCR (R)
AISV87	CTAAACGGTGACCACCAAC	KN99α	Mitochondria Long PCR (F)
AISV91	GTTCAGGGGTTCGAATCCT	KN99α	Mitochondria Long PCR (R)
AISV89	CATACCAAAACCTGGAATG	KN99α	Mitochondria Short PCR (R)
AISV99	CTCCTGGTATGACACTACA	KN99α	Mitochondria Short PCR (F)
AISV149	CGAAATGAATGATCTAGGTC	D288/ H99	*rad23*Δ
AISV150	CAATTTGGCTGTCGTCCATC	D288/ H99	*rad23*Δ
AISV118	CGGGATCCCTCTGCATGATAATGTCAGCG	KN99α	*rad23*Δ complementation by *RAD23*
AISV119	CGGGATCCCGAAAGTTGGGAAAAGGGAG	KN99α	*rad23*Δ complementation by *RAD23*-
AISV140	ACTGTCCAGAACAAGCCCAAAGCTACCCCTGCG	pPZP-P_{native}-*RAD23*-T-NEO	*RAD23* DIΔ
AISV141	CGCAGGGGTAGCTTTGGGCTTGTTCTGGACAGT	pPZP-P_{native}-*RAD23*-T-NEO	*RAD23* DIΔ
AISV142	CCTGCCTTGCAAGCTGCCGGCAACATTCCTTCTGTT	pPZP-P_{native}-*RAD23*-T-NEO	*RAD23* DIIΔ
AISV143	AACAGAAGGAATGTTGCCGGCAGCTTGCAAGGCAGG	pPZP-P_{native}-*RAD23*-T-NEO	*RAD23* DIIΔ
AISV144	GGTATGCCCGGCGGTATGGGTGGTGGTGGTGAAGGT	pPZP-P_{native}-*RAD23*-T-NEO	*RAD23* DIIIΔ

Table 5: Primers used for gene disruption and plasmid construction continued…

AISV145	ACCTTCACCACCACCACCCATACCGCCGGGCATACC	pPZP-P_{native}-*RAD23*-T-NEO	*RAD23* DIIIΔ
AISV146	GTGAATCTGACACAGGAGCTGTTTGAGAACATGGAG	pPZP-P_{native}-*RAD23*-T-NEO	*RAD23* DIVΔ
AISV147	CTCCATGTTCTCAAACAGCTCCTGTGTCAGATTCAC	pPZP-P_{native}-*RAD23*-T-NEO	*RAD23* DIVΔ
AISV165	CATGCCATGGTCAAGATCACTTTC	KN99α	*RAD23* GFP localization
AISV166	CATGCCATGGGTTGATCCTCCTCCATG	KN99α	*RAD23* GFP localization

CHAPTER 3

UVE1 FUNCTIONS IN MITOCHONDRIAL DNA REPAIR IN *C. NEOFORMANS* POST UV STRESS

Introduction

The major steps of the life cycle of *Cryptococcus* are outside the human or animal host and occur in the environment. There the fungus grows on pigeon guano, tree barks, and soil and hence the fungus is exposed to DNA damaging ultraviolet radiation as a detrimental constituent of sunlight. As the fungus is known to be acquired from the environment in to the host and does not spread human-to-human or animal-to-animal, factors effecting its survival in the environment are important as part of the disease process. The genes coding for the repair enzymes involved in the repair of damage to DNA induced by UV should be vital for the fungus in order to survive in the environment in the presence of UV radiations. Despite the pathogenic potential of the *Cryptococcus* and possible importance of the DNA repair enzymes in its survival, to date there is no study that characterizes DNA repair genes in *Cryptococcus*.

In a T-DNA insertion mutagenesis screen of *C. neoformans* var. *grubii* a UV sensitive mutant strain was identified with the insertion in the promoter of the gene *UVE1* (Idnurm et al., 2009). The *UVE1* homolog is well characterized in *S. pombe* both functionally and biochemically. Based on the role of *UVE1* in *S. pombe* and other microbes, I hypothesize that *UVE1* gene of *Cryptococcus* is required by the fungus to protect its genome under genotoxic

UV stress. In this *UVE1* was characterized functionally in *C. neoformans* and tested for its role in the repair of the nuclear or mitochondrial genomes or both.

***UVE1* is required by *C. neoformans* for survival under UV stress**

The previously isolated T-DNA insertion mutant of *UVE1* was further tested for its phenotype along with the wild type strain under UV stress (**Fig. 3a**). To validate that the UV sensitive phenotype observed for the promoter mutant is because of the absence or aberrant expression of *UVE1* gene product the gene was knocked out in both serotypes of *C. neoformans*, A (AI191) and D (AISVCN101). Also, a *UVE1* complemented strain (AI198) was created in the serotype A *uve1*Δ background to confirm that when the gene is reintroduced into the mutant it can restore the phenotype to the wild type level. The UV stress response phenotype for the serotype A, WT, *uve1*Δ and *UVE1* complemented strain is shown in **Fig. 3a**. All strains grew equally well as ten-fold serially diluted culture on YPD plates. As expected, absence of *UVE1* make the fungus vulnerable to UV stress and growth of the *uve1*Δ strain is compromised in comparison to the wild type. Under the stress condition the complemented strain AI198 is able to rescue the UV sensitivity phenotype and is comparable to WT. Serotype D strains wild type (JEC21) and the *uve1*Δ (AISVCN101) shows the similar pattern of UV sensitivity as serotype A equivalent genotypes (**Fig. 3b**). The *uve1*Δ strain shows extreme sensitivity to UV stress relative to the wild type. These UV sensitivity experiments confirm the role of *UVE1* to overcome the UV stress *C. neoformans* is exposed to, and shows that *UVE1* is indispensible under UV stress conditions for the survival of the fungus.

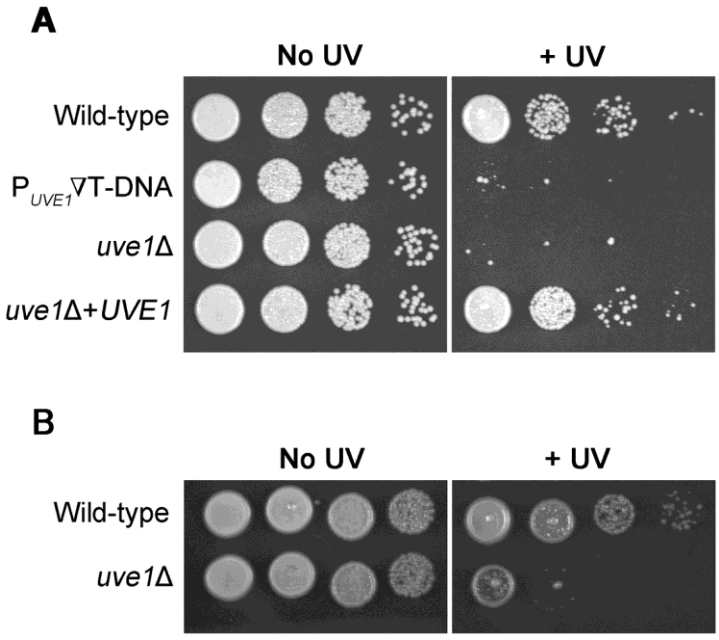

Fig. 3 : *UVE1* of *C. neoformans* confers resistance to UV stress. Ten-fold serial dilutions for different *Cryptococcus* strains grown at 30°C for 2 days. (A) Left panel untreated control and right panel treated with UV dose of 120 J/m^2. Order of *C. neoformans* var. *grubii* strains from top to bottom KN99α, ST239E6, AI191, AI198. (B) Left panel untreated control and right panel treated with UV dose of 120 J/m^2. Order of *C. neoformans* var. *neoformans* strains from top to bottom JEC21, AISVCN101. (Verma and Idnurm, 2013)

In *S. pombe* the role of Uve1 is not restricted to the repair of UV-induced DNA damage, but also implicated in tolerance of other kinds of DNA damage stress tolerance such as oxidative stress and it also has a role in mismatch repair (Avery et al., 1999; Kanno et al., 1999). The above experiments demonstrate that Uve1 is important for the tolerance of UV stress in *C. neoformans*. Looking at the additional roles of Uve1 in *S. pombe* there is a possibility that Uve1 might have additional roles under other kinds of DNA damaging stress especially oxidative stress tolerance, as *C. neoformans* is a human pathogen and hence during infection it can experience heavy oxidative stress. To test the roles of Uve1 under other DNA damaging stress conditions experiments were performed exposing WT, *uve1*Δ and *uve1*Δ +*UVE1* strains to different types of genotoxic stress conditions (**Fig. 4**). Different stress conditions tested are t-butyl hydroperoxide (tBOOH), hydrogen peroxide (H_2O_2) and Paraquat (causes free radical production), to test role of Uve1 under oxidative stress conditions. Methyl methanesulfonate (MMS), an alkylating agent and cause of DNA fragmentation, was also used. Survival under hypoxia-mimetic conditions, by exposing to cobalt chloride stress, was tested. As a control, the strains were also exposed to UV radiation stress. Under all the stress conditions, except for the UV stress, the *uve1*Δ strain behaves similar to the WT and *uve1*Δ+*UVE1* strain. Recently, 429 chemicals were tested on *C. neoformans* deletion strains to examine alterations in growth: none had any effect on the *uve1*Δ strain compare to wild type (Brown et al., 2014). Hence, it appears that *UVE1* in *C. neoformans* is primarily required for UV stress tolerance and has no role in combating oxidative, heavy metal or alkylating agent and many other stresses.

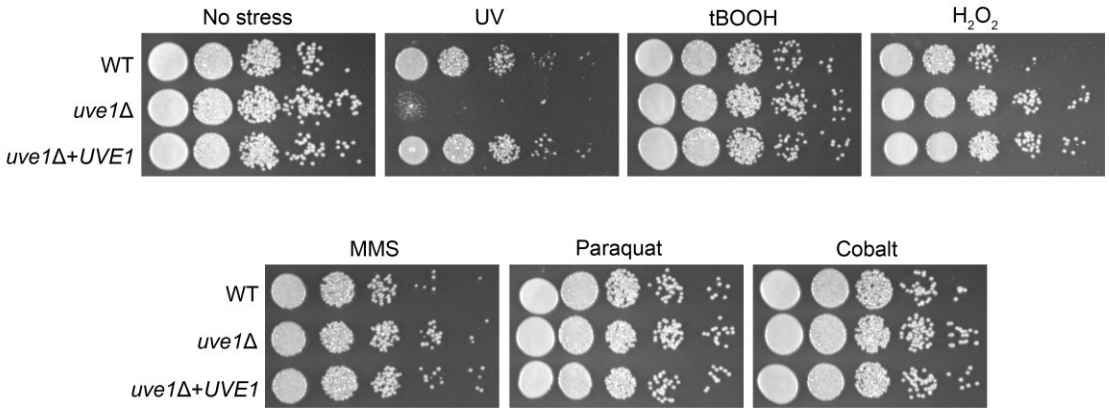

Fig. 4 : Different DNA damage chemicals, UV and heavy metal stress for the WT, *uve1*Δ and *uve1*Δ+*UVE1 C. n*. var. *grubii* strains. The order of the strains from top to bottom for each panel is KN99α (WT), AI191 (*uve1*Δ) and AI198 (*uve1*Δ+*UVE1*). Ten-fold serial dilutions for strains grown on YPD media at 30°C for 2 days. The stresses are UV (120 J/m^2), tBOOH t-butyl hydroperoxide (0.6 mM), H_2O_2 hydrogen peroxide (1 mM), MMS methyl methanesulfonate (0.025 %), Paraquat (0.5 mM), and cobalt chloride (60 μM). (Verma and Idnurm, 2013)

C. neoformans Uve1 is a functional homolog of *S. pombe* Uvde1

In *C. neoformans* var. *neoformans* RACE (rapid amplification of cDNA ends) experiments revealed that there are two transcripts expressed for *UVE1* (**Fig 10).** We named them as *UVE1* (L), the longer form and *UVE1* (D) the shorter form. The shorter form *UVE1* (D) starts in the middle of the *UVE1* (L) and shares the same stop codon. Uve1 is well characterized in *S. pombe* and is required for both nuclear and mitochondrial DNA repair (Yasuhira and Yasui, 2000). To characterize both of these transcripts we decided to their functions with the already characterized Uvde1 of *S. pome*. To perform this characterization, first we constructed a *S. pombe uvde1* knockout strain (AISVSP1), which was tested for its UV sensitivity phenotype. As expected, the *uvde1*Δ strain was extremely sensitive to UV stress. In this *S. pombe uvde1*Δ strain the *C. neoformans* var. *grubii UVE1* (L) and *UVE1* (D) forms were both expressed along with the expression of the empty vector as a control. The strains made were named AISVSP2, AISVSP3 and AISVSP4 for *uvde1*Δ strain expressing empty vector, *UVE1* (L) and *UVE1* (D) forms, respectively. All four strains and the wild type *S. pombe* L972 strain as a control were tested for their survival under UV stress (**Fig. 5a**). Of the two forms of *UVE1* transcripts only the *UVE1* (L) form was able to rescue the UV sensitivity phenotype. The *S. pombe uvde1*Δ strain expressing *UVE1* (D) form showed extreme UV sensitivity phenotype comparable to that of *uvde1*Δ and the *uvde1*Δ strain expressing empty vector. An UV dose response experiment was performed for cells in solution and survival curve was plotted for the strains under UV doses of 60 J/m^2, 120 J/m^2 and 180 J/m^2 (**Fig. 5b**). The results obtained were similar to those from plating on agar media (**Fig. 5a**), emphasizing that only *C. n. UVE1* (L) form is required for UV stress tolerance in *S.*

pombe. Hence the *UVE1* (L) form is functionally similar to *S. pombe UVDE1* whereas the *UVE1* (D) form appears to have no role in protecting the fungus under UV stress.

In *S. pombe* Uvde1 localizes and functions both in the nucleus and mitochondria, but is dispensable for the protection of the mitochondrial genome and is suggested to be a backup repair mechanism (Yasuhira and Yasui, 2000). A *C. neoformans* Uve1 (L)-GFP fusion construct was expressed in *S. pombe uvde1*Δ to check if the Uve1 (L) isoform is functionally similar to *S. pombe* Uvde1 based on it localization to the *S. pombe* nucleus or to mitochondria. The localization pattern and UV sensitivity phenotype of the *C. n.* Uve1 (L)-GFP expressing *S. pombe uvde1*Δ strain (AISVSP15) can test if the *C. n. UVE1* (L) form has a role in repairing the *S. pombe* nuclear or mitochondrial (or both) genomes from UV damage. Confocal microscopy of *C. n.* Uve1 (L)-GFP expressing strains after staining with Hoechst (nuclear stain) and MitoTracker (mitochondrial stain) was performed for the *C. n.* Uve1 (L)-GFP expressing *S. pombe uvde1*Δ strain to study the co-localization pattern (**Fig. 5c and 5d**). The Uve1 (L)-GFP co-localizes with the nuclear stain Hoechst shown in blue (**Fig. 5c**) and is also extra-nuclear. However, the *C. n.* Uve1 (L)-GFP expression does not co-localize with the red MitoTracker stain (**Fig. 5d**). The UV stress experiments for the strain AISVSP15 show it is rescued comparable to the WT *S. pombe* level (**Fig. 5a and 5b**). It can be inferred from these experiments that *C. n.* Uve1 (L) localizes to the nucleus of *S. pombe* and hence has a role in repairing its nuclear genome after UV stress.

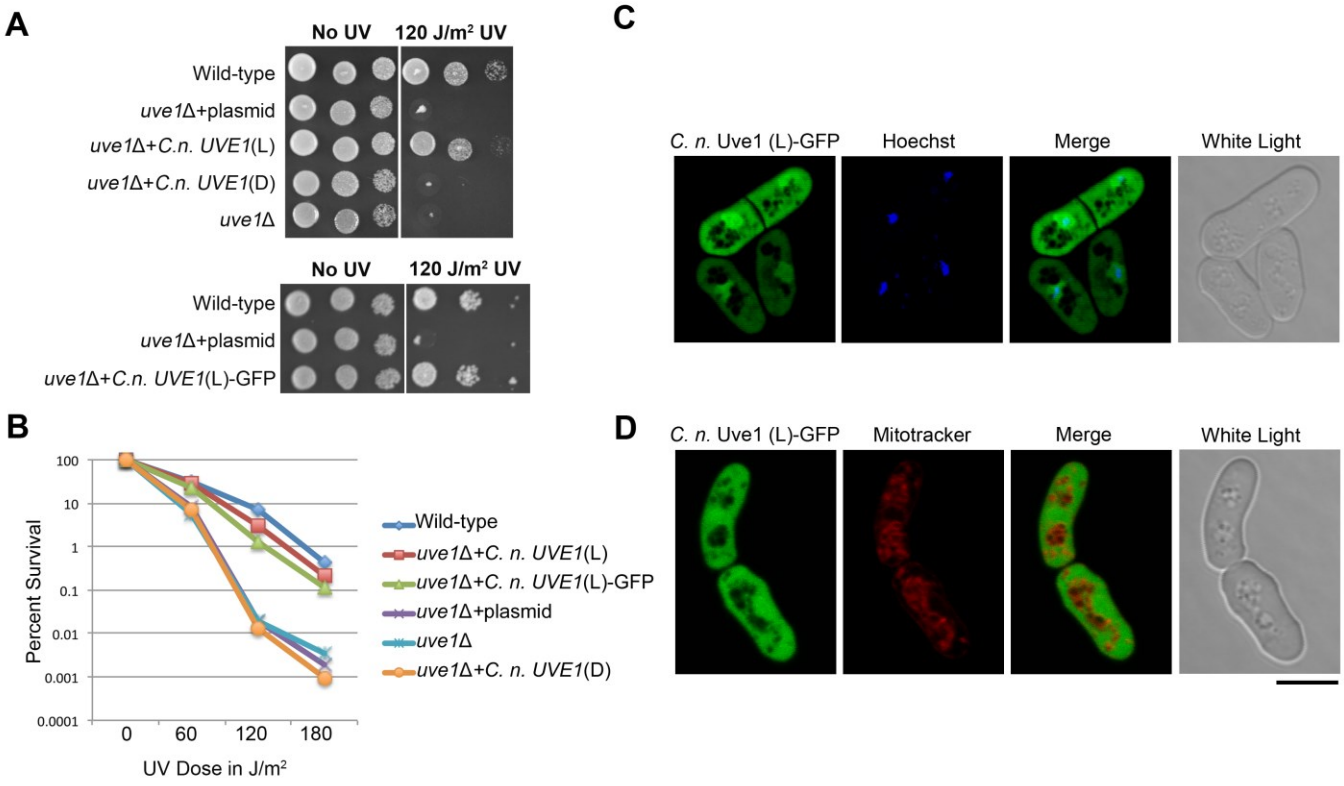

Fig. 5 : *C. neoformans* Uve1 is functionally similar to *S. pombe* UVDE. (A) The *C. neoformans* light (L) and dark (D) isoforms of *UVE1* were expressed in an *uve1* deletion strain of *S. pombe*. (A) Ten-fold serial dilutions for different strains of *S. pombe* grown at 30°C for 2 days. Left panel untreated control and right panel treated with UV dose of 120 J/m^2. The strains used, from top to bottom are L972, AISVSP2, AISVSP4, AISVSP3 and AISVSP1. For the lower portion of the figure strains used are L972, AISVSP2, AISVSP15 (B) Graph of survival of strains L972, AISVSP4, AISVSP15, AISVSP2, AISVSP1 and AISVSP3 in response to UV stress of 0, 60, 120 and 180 J/m^2. (C) Subcellular localization of *C. n.* Uve1 (L)-GFP in strain AISVSP1, left panel 1 GFP only, panel 2 Hoechst only, panel 3 merge of GFP and Hoechst, panel 4 white light only. (D) Subcellular localization of *C. n.*

Uve1 (L)-GFP in strain AISVSP1, left panel 1 GFP only, panel 2 MitoTracker only, panel 3 merge of GFP and MitoTracker, panel 4 white light only. Scale bar = 10 μm. (Verma and Idnurm, 2013)

Uve1 is required for the protection of the mitochondrial genome in *C. neoformans*

Two genomes found in most eukaryotes are in the nucleus and mitochondria. Integrity of the two genomes under stress conditions depends on how efficiently DNA repair systems dedicated to each of the organelles works under genotoxic stress conditions. The results thus far show that Uve1 is a DNA repair gene involved mainly to rescue the growth of *C. neoformans* and *S. pombe* after UV stress. Pressing questions now needed to be answered, such as how exactly Uve1 is involved in conferring protection under the UV stress conditions? Where is Uve1 localized in the cell? Is it involved in the protection of nuclear genome or mitochondrial genome, or both the genomes? Localization and function of Uve1 in *S. pombe* is already known (Yasuhira and Yasui, 2000). The *S. pombe* Uve1 homolog Uvde1 localizes to both the nucleus and mitochondria, hence has a role in repairing both the genomes. In *C. neoformans* the role of Uve1 in repairing the nuclear or mitochondrial genome was not known. In order to begin in this direction I first used MitoProt II - v1.101 software based prediction of the Uve1 localization for both serotype A and serotype D, and the probability of mitochondrial localization was predicted to be 0.988 and 0.880 respectively. Predictions from PSORT II also supported the higher percentage for mitochondrial localization, compared to the nuclear localization. To validate the software prediction, I created GFP fused constructs for both the serotype D isoforms of *UVE1*, *C. n.* Uve1 (L)-GFP and Uve1 (D)-GFP with GFP at the C-terminal end. The constructs were expressed in a serotype A *uve1*Δ strain to study the localization of the two *UVE1* isoforms in the cell and at the same time test for their ability to complement the loss of Uve1 function. The Uve1-GFP expressing strains for the two isoforms were stained with nuclear specific

stains such as DAPI or Hoeschst (the blue staining) or with mitochondrial specific stain MitoTracker (the red staining) to study the co-localization pattern. Both strains *C. n.* Uve1 (L)-GFP and Uve1 (D)-GFP were observed under the confocal microscope. In *C. n.* Uve1 (L)-GFP, the green color for the GFP co-localizes with the MitoTracker giving a yellow color on merging the two individual channels (**Fig. 6a**). However it did not colocalize with the nuclear specific stain Hoechst (**Fig. 7b**). The expression of Uve1 (D)-GFP was cytoplasmic and there was no colocalization with the MitoTracker (**Fig. 6b and 7a**) or DAPI signals. From these experiments it was concluded that *C. n.* Uve1 (L)-GFP is predominantly mitochondrial and Uve1 (D)-GFP is cytoplasmic without localization to mitochondria or nucleus, as it does not have any localization signal. The functionally active Uve1 (L) form localizes to the mitochondria in *C. neoformans*, and hence is predicted to play the role in protecting the mitochondrial genome under stress conditions.

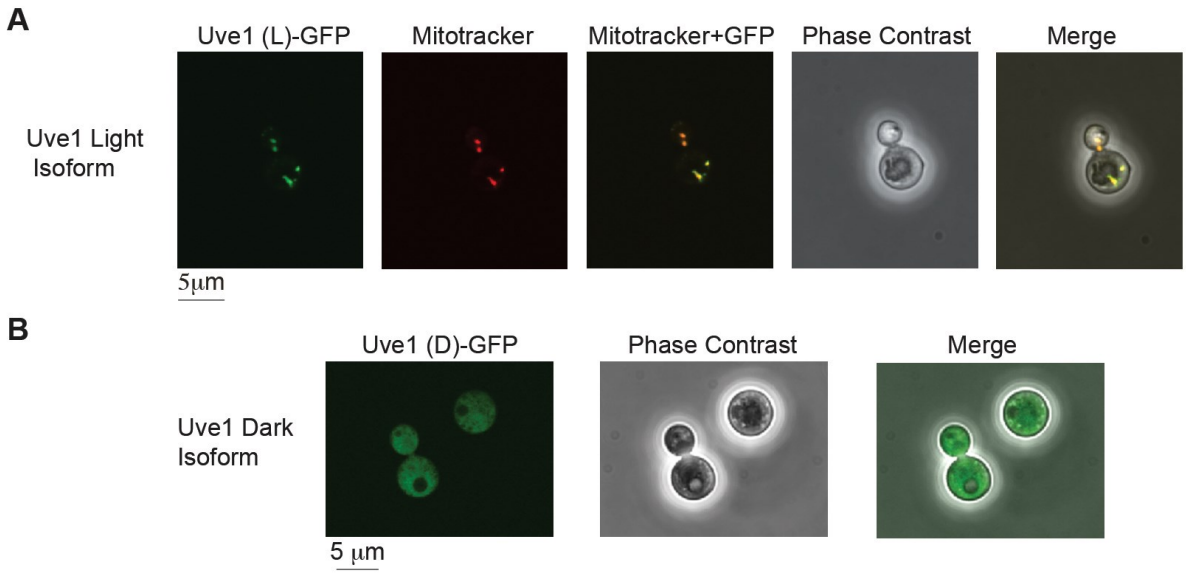

Fig. 6 : Subcellular localization of Uve1 (L)-GFP and Uve1 (D)-GFP from *C. neoformans* var. *neoformans* in the vegetative yeast cells of *C. neoformans* var. *grubii* (A) Uve1 (L)-GFP localization and (B) Uve1 (D)-GFP localization. (Verma and Idnurm, 2013)

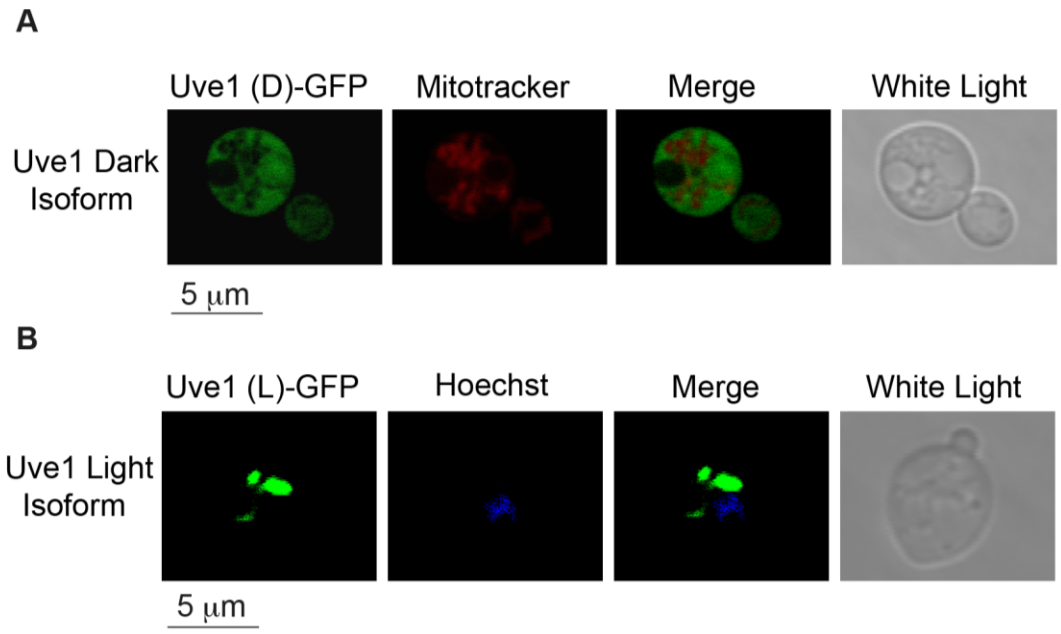

Fig. 7 : Subcellular localization of Uve1 (D)-GFP and Uve1 (L)-GFP from *C. neoformans* var. *neoformans* in *C. neoformans* var. *grubii*. (A) Uve1 (D)-GFP localization compared with MitoTracker, and (B) Uve1 (L)-GFP localization compared with nuclear Hoechst staining. (Verma and Idnurm, 2013)

The Uve1 (L) form localizes to the mitochondria and is functionally active in rescuing the UV stress phenotype. It appears that UV-induced toxicity in the *C. neoformans* *uve1*Δ strains, AI191 and AISVCN101, is largely due to unrepaired UV-induced photoproducts in mtDNA. However there is no direct evidence that Uve1 is involved in the repair of UV photoproducts present in mtDNA. To obtain this evidence, a PCR-based DNA damage assay to access the mitochondrial and nuclear DNA damage in *C. neoformans* wild type and *uve1*Δ strains was designed. The assay is based on the principal that damaged DNA impedes the progression of Taq polymerase on the template DNA in a PCR reaction and hence there is an inverse relationship between the amount of DNA damage and PCR amplification products. For most of the experimental design established methods were followed (Hunter et al., 2010) with one experimental modification to resolve PCR products on agarose gels (to ensure correct amplification) and then quantify them, rather than rely on other fluorescence-based quantification approaches.

A series of pilot experiments suggested using the UV exposure of 50 J/m^2 on both wild type and *uve1*Δ strains would provide a level of damage to the cell without killing those of *uve1*Δ. The repair of the DNA damage in both genomes was then examined. Under the conditions used with the cells suspended in PBS, the viability of the *uve1*Δ mutant with this dose was similar to the wild type. The stressed cells with the dose of 50 J/m^2 for both wild type and *uve1*Δ were then allowed to recover in liquid growth medium and samples were taken for the recovery time points of 0 hr, 1 hr, 4 hr and 6 hr for comparison to the no stress control. The PCR primers were designed to amplify nuclear-specific and mitochondria-specific DNA. The assay is based on the principal that damaged DNA impedes the

progression of Taq polymerase on the template DNA in a PCR reaction. Long amplification primers with product size greater than 8,000 bp were used to assess the amount of DNA damage in both mitochondrial and nuclear genomes. Short product amplification primers with product sizes of about 250 bp were also designed because amplifying over the shorter distances Taq polymerase is less likely to encounter DNA damage and hence has more chances of completing through all the amplification cycles. These shorter products are used to normalize the amount of input DNA and also mitochondrial DNA copy number.

Quantification for the nuclear and mitochondrial genome DNA damage for both WT and *uve1*Δ strains was done for no stress, 0 min, 1 hr, 4 hr and 6 hr time points through densitometric band intensity measurement using imageJ software. For comparing the extent of DNA damage and damage recovery between two strains, relative amplification of stressed DNA samples to that of control no stress samples was calculated for large PCR products for each of the time points. For calculation purposes large amplification products are normalized in comparison to short PCR amplification products to mitigate any background that may be caused from the amount of amplifiable input DNA present or variation due to mitochondrial copy number. Furthermore, throughout the analysis we corrected the proportion of damage to the size of the PCR products; thus, the number of starting lesions is about equal between the nuclear and mitochondrial genome. Finally relative lesion frequency per 10 kb of DNA is calculated by poisson distribution using the formula:

Lesion/amplification = -ln $\mathbf{(A_t/A_0)}$,

Here $\mathbf{A_t}$ is amplification of stressed samples and $\mathbf{A_0}$ is amplification of control sample.

At the 0 hr time-point the mitochondrial and nuclear genomes were heavily and equally damaged, since we observe little amplification of long mitochondrial and long

nuclear PCR products **Fig. 8a and 8c**. The **Fig. 8b and 8d** shows the quantification graphs for the respective gels pictures shown in **Fig. 8a and 8c**. At 1 hr time point there is a delayed recovery in the *uve1*Δ strain for both nuclear and mitochondrial genome. But at 4 hr and 6 hr time points there is delayed recovery only in the mitochondrial genome of *uve1*Δ, and nuclear genomes are almost completely repaired. For WT cells there is comparable amount of DNA damage recovery or repair for both the genomes. These observations support the idea that Uve1 is required for the repair of the mitochondrial genome only and not for the repair of nuclear genome. The data counter to this is the delayed recovery for the *uve1*Δ strains nuclear genome observed at 1 hr time point after stress. This could be due to the retrograde effect of mitochondrial genome damage (Al-Mehdi et al., 2012; Liu and Butow, 2006). A feasible explanation for this curious observation can be that when a mitochondrial genome undergoes stress due to UV radiations, reactive oxygen species can be released and cells' energy state is compromised. Cells tend to go into a "survival" mode and any type of repair process can be stalled until a decent energy state is acquired. The later time points of 4 hr and 6 hr support this where the nuclear genome repair is completed, yet significant lesions can be still observed for the mitochondrial genome.

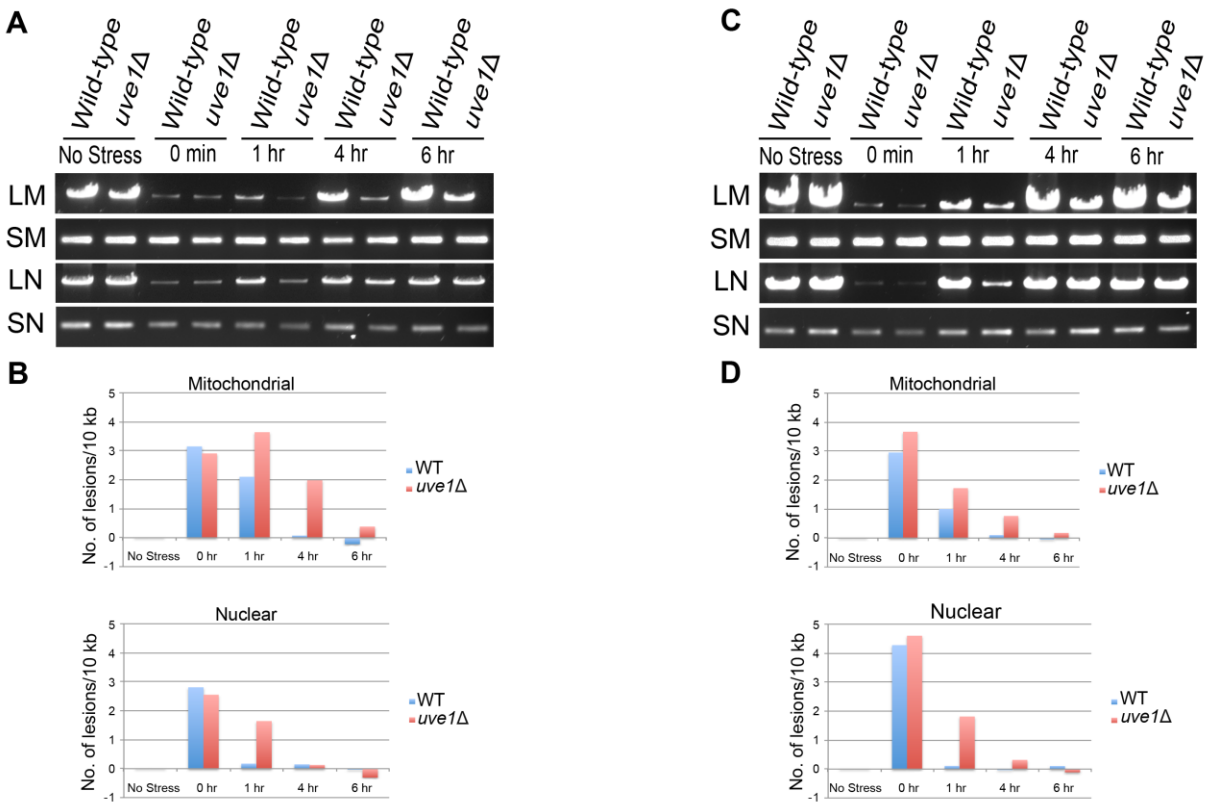

Fig. 8 : Uve1 is required for efficient repair of mitochondrial DNA damage post UV stress. Results from two independent experiments carried out on different days. (A, C) Agarose gels for the PCR amplification of mitochondrial and nuclear DNA on template DNA from undamaged control cells and template DNA from cells exposed to UV stress 50 J/m^2. *C. neoformans* var. *grubii* strains KN99α (WT) and AI191 (*uve1*Δ) PCR amplification pattern for no stress, 0 hour, 1 hour, 4 hour and 6 hour post UV stress recovery. DNA amplification of long mitochondrial (LM) DNA, small mitochondrial (SM) DNA, long nuclear (LN) DNA and short nuclear (SN) DNA. (B, D) Graphical representations of DNA damage experiments in panels A and C, respectively. The Y-axis represents number of lesions/10 kb and Y-axis represents time in hours. (Verma and Idnurm, 2013)

The results obtained from different experiments can be summarized as follows. 1. Uve1 deficient cells are extremely sensitive to UV radiation stress. 2. In *C. neoformans*, Uve1 (L)-GFP localizes to mitochondria, for Uve1-GFP no fluorescence signal is observed in nucleus or any other cell organelle exclusive of mitochondria. 3. Uve1 (D)-GFP is cytoplasmic. 4. The *uve1*Δ strain shows delayed mitochondrial DNA damage repair comparative to the repair in its own nuclear genome and to the mitochondrial and nuclear genome of WT cells. These observations indicate that in *C. neoformans*, Uve1 is a mitochondrial DNA repair enzyme involved in repair of mitochondrial DNA lesions caused by UV stress.

To date Uve1 is the only mitochondrial DNA repair enzyme characterized in *C. neoformans* required to protect its mitochondrial genome from the deleterious effects of UV radiation stress. Indeed it may be one of the few enzymes with a dedicated role in mitochondrial DNA protection identified to date from any organism. Hence this discovery is significant as many of DNA repair enzymes as part of NER or BER pathways are attributed for the maintenance of the nuclear genome, but hardly any knowledge exists for the protection mechanisms existing for the mitochondrial genome. Compared to the nuclear genome, the mitochondrial genome is already under a significant amount of DNA damaging stress due to its proximity to the reactive oxygen species generated during operation of the electron transport chain and oxidative phosphorylation. Exposure to UV radiations present in the environment can add to this stress and can lead to accumulation of deleterious mutations. Discovery of the existing DNA damage repair system enhances our understanding of the basic biology of this pathogenic yeast and also of the mechanisms by which *C. neoformans* is able to survive in the environment.

CHAPTER 4

UVE1 IS REGULATED BY THE WHITE COLLAR COMPLEX

Introduction

The White Collar complex (WCC) is the major blue-light photoreceptor complex common to many fungi. WCC is widely established in its regulation of responses such as phototropism, sporulation, mating, pigmentation, secondary metabolism, circadian rhythm, UV sensitivity and pathogenesis (Idnurm et al., 2010) . In *Neurospora* it regulates sporulation, carotenoid pigment production and circadian responses (Linden et al., 1997a; Linden et al., 1997b); in *Aspergillus* it regulates sexual development, secondary metabolism, hyphal pigmentation and UV resistance (Bayram et al., 2010; Fuller et al., 2013); in plant pathogen *Fusarium oxysporum* WCC has roles in toxin production, pigment production and pathogenesis (Estrada and Avalos, 2008; Ruiz-Roldan et al., 2008). In the human pathogen *C. neoformans* WCC, known as Bwc1-Bwc2, regulates three important light dependent responses, viz mating, UV sensitivity and virulence (Idnurm and Heitman, 2005; Lu et al., 2005). However in many cases the exact mechanism of regulation of these responses or targets for the regulation are still unknown.

A study to identify light regulated genes in *C. neoformans* by microarray experiments identified *HEM15* (encoding ferrochetalase a heme biosynthetic pathway protein) as one of the most highly expressed transcripts. In comparative light and dark expression profiling

experiments *HEM15* was induced two fold (Idnurm and Heitman, 2010). The gene was identified after an hour of light exposure, and further experiments to characterize the gene showed that *HEM15* is an essential gene with effects on the growth of the strain. Another gene that came out to be second most highly expressed under light grown conditions in the same study was *CFT1* (a high affinity iron permease). This gene is required for iron uptake and virulence of *C. neoformans* (Jung et al., 2008). Although *CFT1* is required for virulence, it is not clear how that exactly relates to Bwc1-Bwc2 because no phenotypes related to iron homeostasis have been observed in *bwc1* or *bwc2* mutants (Brown et al., 2014). Hence though both *HEM15* and *CFT1* in *C. neoformans* are somehow regulated through the Bwc1-Bwc2, they do not show any direct physiological response that could be attributed to Bwc1-Bwc2.

To date no direct or indirect target for the Bwc1-Bwc2 has been identified or hypothesized that can explain the UV sensitivity phenotype related to the photoreceptor mutants in *C. neoformans*. The most appropriate candidate genes for the UV sensitivity phenotype are DNA repair genes. Hence I tested *UVE1* encoding the DNA endonuclease that we established as a DNA repair gene in *C. neoformans* required for protection of the fungal mitochondrial genome under UV stress. The following studies explore the possible regulation of *UVE1* by Bwc1-Bwc2 in *Cryptococcus* specifically and also extend the research to two other phylogenetically-distinct branches of fungi, ascomycetes and zygomycetes.

UVE1* is regulated through Bwc1-Bwc2 in *Cryptococcus

The UV sensitivity phenotype of the *uve1*Δ *C. neoformans* strain is shared with that of *bwc1*Δ, *bwc2*Δ, or the *bwc1*Δ *bwc2*Δ double knockout strains. Based on the phenotypic similarity and the fact that Uve1 is a DNA repair enzyme it can be hypothesized that *UVE1* is

regulated through Bwc1-Bwc2 in *C. neoformans*. To experimentally verify the possibility a set of experiments was performed.

Expression in the light and dark for *UVE1* was tested by northern blotting. Experiments were conducted for *C. neoformans* var. *grubii* (serotype A), *C. neoformans* var. *neoformans* (serotype D) and *C. gattii* (serotype B) strains. Strains were cultured overnight under light and dark conditions. For the dark experiments, cultures were constantly kept in 24 hr of dark and for the light experiments after 23 hr of dark growth cultures were shifted for 1 hr in light. The RNA was extracted from the strains and northern blot was performed using *UVE1* full length PCR as to be the probe and actin PCR probe as the normalization control. In JEC21 two transcripts were observed, the bigger transcript was named *UVE1* (L) and the shorter transcript as *UVE1* (D). These names were followed as the longer *UVE1* (L) transcript was expressed more in the light grown conditions and the shorter *UVE1* (D) transcript was expressed more in the dark grown conditions in the WT strain (**Fig. 9**). In the *bwc1*Δ strain expression of the *UVE1* (L) was mitigated and only the smaller transcript *UVE1* (D) was expressed. Induction of *UVE1* (L) in light grown conditions for WT background and absence of induction or expression in *bwc1*Δ background under similar conditions shows that *UVE1* (L) is a *BWC1* regulated transcript. Unlike JEC21, in KN99α and R265 only a single transcript is induced in WT light grown conditions. Negligible induction of *UVE1* is observed in dark grown conditions and in the *bwc1*Δ strain under light or dark grown conditions. Hence in three major serotypes of *Cryptococcus UVE1* is under regulation of photoreceptor Bwc1.

Further characterization of the two transcripts was performed by RACE (**Fig. 10**). The longer light induced transcript *UVE1* (L) is the full length mRNA for the *UVE1*, while

the *UVE1* (D) form 5' end started in the middle of the *UVE1* (L) and both the transcripts share the same 3' end. The two different *UVE1* transcripts observed in JEC21 under light and dark grown conditions have different contributions in terms of UV sensitivity (**Fig. 5a and 5b**). *UVE1* (L) isoform is the major functionally active transcript and *UVE1* (D) seems to have no role in conferring resistance to UV stress. It seems that in the presence of light the *UVE1* (D) form is repressed: this may be due to the increased expression of the *UVE1* (L) form as they might be regulated through the same promoter and *UVE1* (L) is the preferred transcript under the given light conditions. The higher expression of the *UVE1* (D) in dark remains a mystery as no function for this transcript is identified and it is not found in *C. n.* var. *grubii* or *C. gattii*. Very recently in a whole genome RNA-seq analysis of the H99 strain of *C. neoformans* var. *grubii* a large number of miscellaneous RNA were reported, many of which are non coding RNAs with possible roles in gene regulation (Janbon et al., 2014). These RNA species could be spurious non-functional RNA molecules, however there is also evidence suggesting these RNAs have regulatory roles. So, looking at the genome enrichment of such non-coding miscellaneous RNA in H99, which is largely isogenic with KN99 strains, a function of the *UVE1* dark transcript as a regulatory RNA moiety cannot be excluded. However considering the number of other details (such as *UVE1* (D) isoform seems to have no role in conferring resistance to UV stress; localization pattern of the *UVE1* (D) which is neither mitochondrial nor nuclear but cytoplasmic; absence of complete active site; and *UVE1* (D) isoform is exclusive to serotype D and is not expressed in other two important serotypes of *Cryptococcus*) further characterization of this transcript was not pursued.

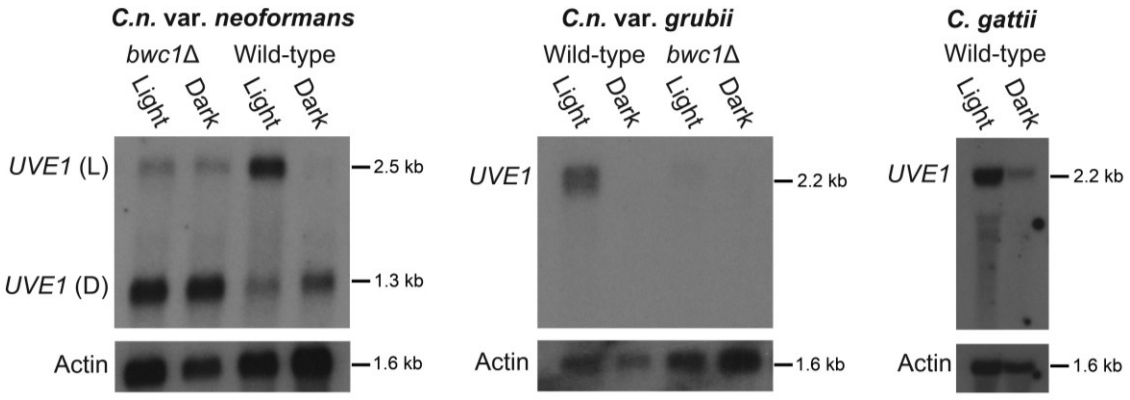

Fig. 9 : *UVE1* is a Bwc1-regulated gene in *Cryptococcus*. Northern blots of *C. n.* var. *neoformans*, *C. n.* var. *grubii* and *C. gattii*. From left to right, panel 1 is for JEC21 (WT) and AI5 (*bwc1*); the upper band is for *UVE1* (L) isoform and the lower band is for *UVE1* (D) isoform. Panel 2 is for KN99α (WT) and AI81 (*bwc1*), panel 3 is for R265 (WT). All experiments were either 23 hr dark + 1 hr light, (Light) or 24 h constant darkness (Dark). Blots were stripped and reprobed with actin as a loading control. (Verma and Idnurm, 2013)

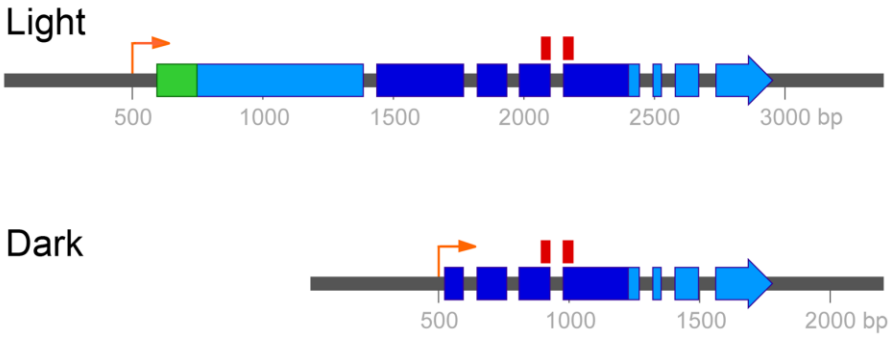

Fig. 10 : Two mRNA isoforms of *UVE1* are produced in *C. neoformans* var. *neoformans*. Boxes indicate coding regions, with the long light-induced isoform encoding a 660 amino acid residue protein and the shorter dark-expressed isoform encoding a 291 amino acid residue protein. Dark blue encompasses the pfam03851 domain that represents the conserved and active site of the endonuclease. The position of the 70mer probe used in the *C. neoformans* microarray, which spans two exons common to both isoforms, is indicated above this region. The green region encodes the predicted mitochondrial localization signal. The orange arrows indicate the start of the *UVE1* light and dark transcripts. Light blue and dark blue is the coding region for the two transcripts. (Verma and Idnurm, 2013)

Since *UVE1* is a light inducible gene under the control of the Bwc1 photoreceptor, wild type strains grown under dark conditions should display a UV-sensitivity level like those of *bwc1*Δ and *uve1*Δ strains, as light as a signal for the *UVE1* induction is absent. To test this hypothesis, WT, *bwc1*Δ and *bwc1*Δ+*BWC1* strains for *C. neoformans* were grown in two different sets under complete darkness. For both the sets, cells were plated as ten fold serial dilution cultures and one set was kept in complete darkness and other set exposed to 1 hour of light. Both the sets were then exposed to UV stress of 60 and 120 J/m^2 and were further incubated in dark for recovery. For the set given an hour of light exposure only *bwc1*Δ showed repressed growth under UV stress in a dose dependent manner, whereas WT and *bwc1*Δ+*BWC1 strains* showed growth comparable to the no stress controls. For the dark grown conditions all three strains WT, *bwc1*Δ and *bwc1*Δ+*BWC1* showed repressed growth under UV stress comparative to light induction condition. However WT under dark grown conditions grew slightly better compared to *bwc1*Δ, this could be that Uve1 expression is induced by the UV lights used to give stress in WT (**Fig. 11**). Hence combining the *UVE1* light and dark expression results, *UVE1* expression in *bwc1*Δ background and the observations from above clearly show that light is the signal that is perceived through the Bwc1 and further channeled to induce *UVE1* expression that in turn can actively confer resistance to UV stress.

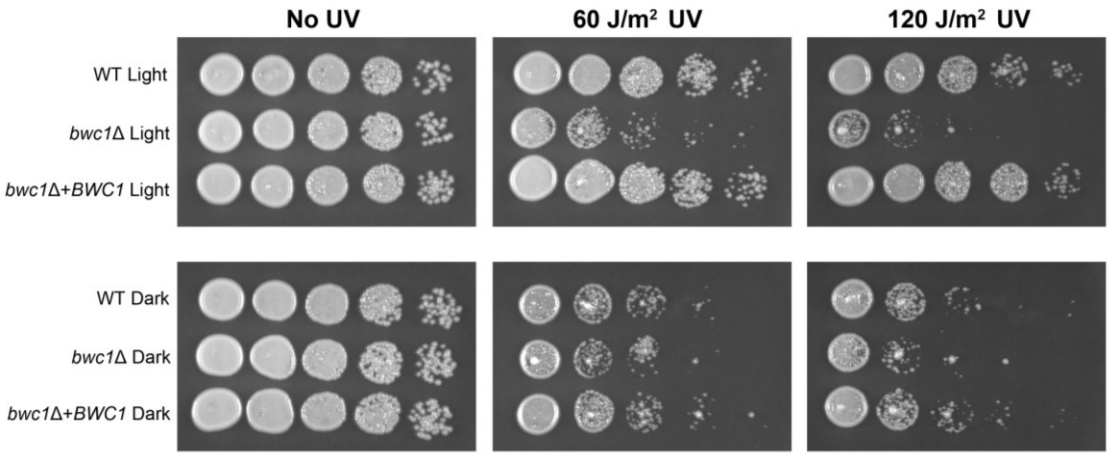

Fig. 11 : Pre-exposure to light increases resistance to UV irradiation. Ten-fold serial dilutions for strains of *C. neoformans* var. *neoformans* grown at 30°C for 2 days after UV stress. Strains used are JEC21 (WT), AI5 (*bwc1*Δ) and AI51 (*bwc1*Δ+*BWC1*). Top three panels are strains grown in dark and given 2 hrs of white light (4,400 Lux) prior to UV stress. Bottom three panels are for the strains kept in constant darkness before UV stress. (Verma and Idnurm, 2013)

To corroborate the light and dark *UVE1* expression results and to gain additional evidence that *UVE1* is under the control of white collar complex further experiments were performed. *UVE1* was expressed under the control of a galactose inducible promoter (from the *GAL7* gene) in *bwc1*Δ strains in both JEC21 and KN99α backgrounds. All strains (WT, *bwc1*Δ and *bwc1*Δ+P_{GAL7}*UVE1*) were grown overnight in 2% galactose and 2% glucose containing media separately. Strains were ten-fold serially diluted and spotted on YPD media plates. One of the sets for serotype D was exposed to UV stress of 120 J/m^2 and other set was kept as control. For the serotype A UV stress of 120 J/m^2 and 60 J/m^2 both were tested. In both the serotypes galactose grown conditions with overexpression of P_{GAL7}*UVE1* rescues the UV sensitivity phenotype of the *bwc1*Δ comparable to the WT level (**Fig. 12 and Fig. 13**). In glucose grown conditions where the expression of the *UVE1* is not induced in the absence of the galactose a minimal improvement in the UV sensitivity is observed in *bwc1*Δ+P_{GAL7}*UVE1*. Its phenotype is comparable to *bwc1*Δ in the absence of any rescue; the approximately 10-fold improvement is likely due to the leakiness in expression from these promoters (Ruff et al., 2009).

***UVE1* is a direct downstream target of Bwc2**

All the experiments performed thus far support a hypothesis that in *C. neoformans* *UVE1* is a light regulated gene through the photoreceptor Bwc1. Further experiments were performed to see if *UVE1* is the direct target of the white collar complex or an indirect target. The promoter of the *UVE1* was scanned for a putative Bwc2 binding site, taking the promoter consensus sequence for the WCC binding sites from *Neurospora crassa* as the reference sequence.

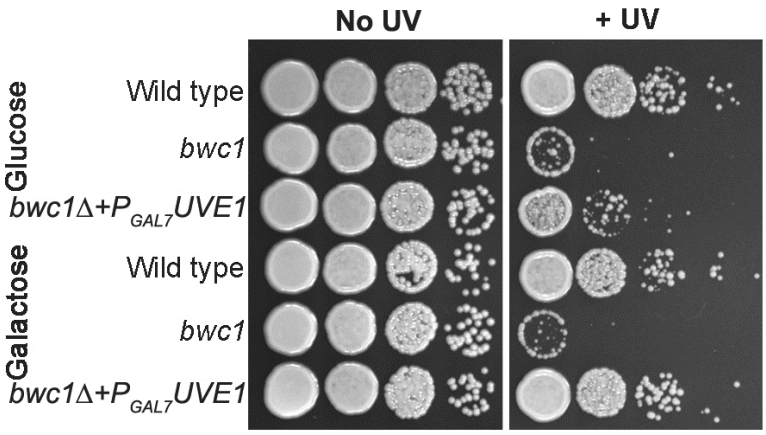

Fig. 12 : *UVE1* overexpression rescues the UV sensitive phenotype of *bwc1*Δ mutants in *C. neoformans*. Ten-fold serial dilutions for different strains of *C. neoformans* var. *neoformans* grown at 30°C for 2 days. Left panel untreated control and right panel treated with UV dose of 120 J/m^2. Top three strains (JEC21, AI5 and AISVCN53) grown overnight in 2% glucose and bottom three strains (JEC21, AI5 and AISVCN53) grown overnight in 2% galactose before inoculating onto YPD plates. (Verma and Idnurm, 2013)

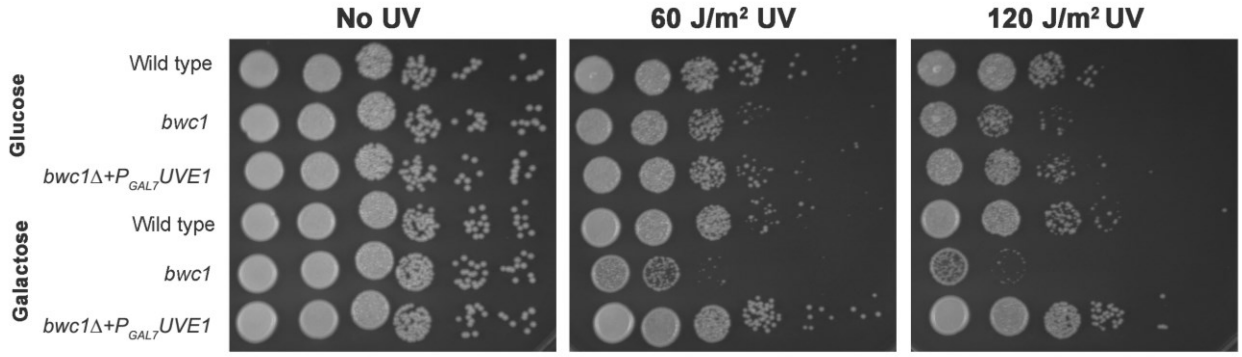

Fig. 13 : *UVE1* overexpression rescues the UV sensitive phenotype of *bwc1*Δ mutants in *C. n.* var. *grubii*. Three strains, KN99α (WT), AI81 (*bwc1*Δ) and AISVCN66 (*bwc1*Δ+P$_{GAL7}$-*UVE1*), were grown overnight in YNB + glucose or YNB + galactose before inoculating onto YPD plates, and grown at 30°C for 2 days. (Verma and Idnurm, 2013)

In *Neurospora* these sites are well characterized (Chen et al., 2009; Froehlich et al., 2002; Lamb et al., 2011). The best match for a Bwc2 binding consensus sequence found in the *C. neoformans UVE1* promoter region is from light regulated element (LRE) in the *frq* gene of *Neurospora*. The *Neurospora* binding consensus sequence is TCGATCCGCTCGATCCCCT and similar sequence was found in the *C. neoformans* promoter as TCGATCTTCATCTCGATCTCCA (the nucleotides common to both sequences are underlined).

To confirm the binding of Bwc2 to the *UVE1* promoter an electrophoretic gel mobility shift assay (EMSA) was performed. *C. neoformans* recombinant his-tagged Bwc2 protein (26 to 383 amino acids) was cloned, expressed and purified for the experiment (**Fig. 14a**). The region of the *UVE1* promoter containing the Bwc2 binding consensus sequence was PCR amplified and was radiolabeled. EMSA was performed with recombinant his-tagged Bwc2 protein and the radiolabeled *UVE1* promoter region (**Fig. 14b**). In the figure the first four wells are loaded with radiolabeled specific *UVE1* promoter region (P_1 *UVE1*) and next six wells are loaded with nonspecific amplified DNA region (P_2 *UVE1*). Well no 1 is just probe, next two wells have purified Bwc2 loaded in increasing concentration, 4^{th} well contains Bwc2 loaded with concentrations same as well two but with zinc added, as Bwc2 is a Zinc finger binding protein. We can clearly observe the shift in well 2, 3 and 4, such that band intensity increases with the increasing concentration of the protein and also with the addition of zinc to the reaction mixture. Lane 5 contains nonspecific probe only, lane 6 and 7 has increasing concentration of Bwc2, and lane 8 and 9 contains Bwc2, radiolabeled P_2 *UVE1* and cold probe P_1 *UVE1* in increasing concentration.

A

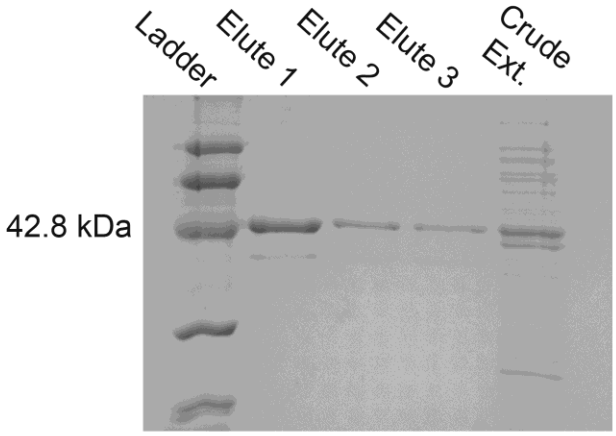
Ladder
Elute 1
Elute 2
Elute 3
Crude Ext.
42.8 kDa

B

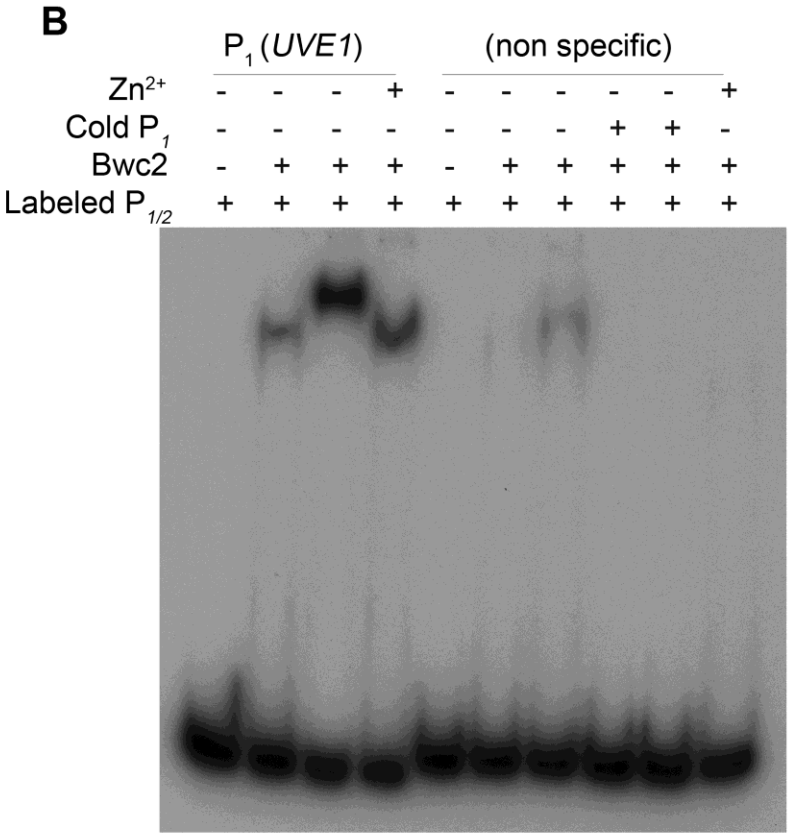
P1 (UVE1)
(non specific)
Zn2+ - - - + - - - - - +
Cold P1 - - - - - - - + + -
Bwc2 - + + + - + + + + +
Labeled P1/2 + + + + + + + + + +

Fig. 14 : Bwc2 binds to the *UVE1* promoter. (A) SDS-PAGE gel for *C. neoformans* recombinant $(His)_6$-Bwc2. Left to right, lane 1 is the low molecular weight Bio-Rad protein ladder, lane 2, 3, 4 are purified recombinant Bwc2 eluted fractions. Lane 5 is crude unpurified protein extract. (B) Gel mobility shift assay for a fragment of the JEC21 *UVE1* promoter with purified Bwc2. Left to right, lane 1 contains just the *UVE1* promoter P_1 (P_{UVE1}), lane 2, 3 and 4 contains P_1 + Bwc2 20 μg, 50 μg and 20 μg + Zn^{2+} respectively. Lane 5 is loaded with the non-specific radiolabeled probe P_2. Lane 6, 7 are P_2 + Bwc2 20 μg and 50 μg. Lane 8, 9 are competition with the increasing amount of specific probe cold P_1 to negate any binding observed in lane 7. Lane 10 is Bwc2 and P_2 with Zn^{2+}. (Verma and Idnurm, 2013)

It can be observed that some residual shift observed in lane 7 can be competed by the lesser concentration of the specific cold probe P_1 *UVE1*. Lane 10 has Bwc2, P_2 *UVE1* and zinc to observe if there is any zinc dependent increase in the binding of the nonspecific probe that was not observed. Binding of Bwc2 to the specific probe P_1 *UVE1* and the other experiments shows that *UVE1* is a direct downstream target of the Bwc1-Bwc2 complex. There is no other direct downstream target of the Bwc1-Bwc2 complex in *C. neoformans* known. White-collar complex in *C. neoformans* regulates three phenotypes, which are UV sensitivity, mating and virulence. The *UVE1* is the target gene of the White-collar complex that is responsible for conferring mitochondrial DNA damage protection by repairing damage post UV stress, hence regulates UV sensitivity. Next was to test if *UVE1* is also responsible for the mating or virulence phenotypes associated with strains with mutations in the Bwc1-Bwc2 complex. In wild type cells mating is repressed in light and in dark cells mate normally. In the mutants of the white-collar complex this repression of the mating is lost under light grown conditions and they produce the dikaryotic mating hyphae equally well as in dark (Idnurm and Heitman, 2005). Mating type **a** and α crosses were set up for wild type X wild type, *uve1*Δ X *uve1*Δ and *bwc1*Δ X *bwc1*Δ in both *C. neoformans* var. *grubii* and *C. neoformans* var. *neoformans* (**Fig. 15a and 15b**). WT and *uve1*Δ crosses showed similar phenotypes in both the backgrounds that is repression of mating under light comparative to dark grown conditions. The *bwc1*Δ X *bwc1*Δ cross show comparable mating under both light and dark grown conditions. The virulence for the *uve1*Δ strain was tested and compared with the wild type and *bwc1*Δ strains in the wax moth larvae (*Galleria mellonella*) model of infection (**Fig. 15c**). The *uve1*Δ strain did not show any defect in virulence and the survival curve for the infected wax moth was comparable to the wild type strain however, the *bwc1*Δ

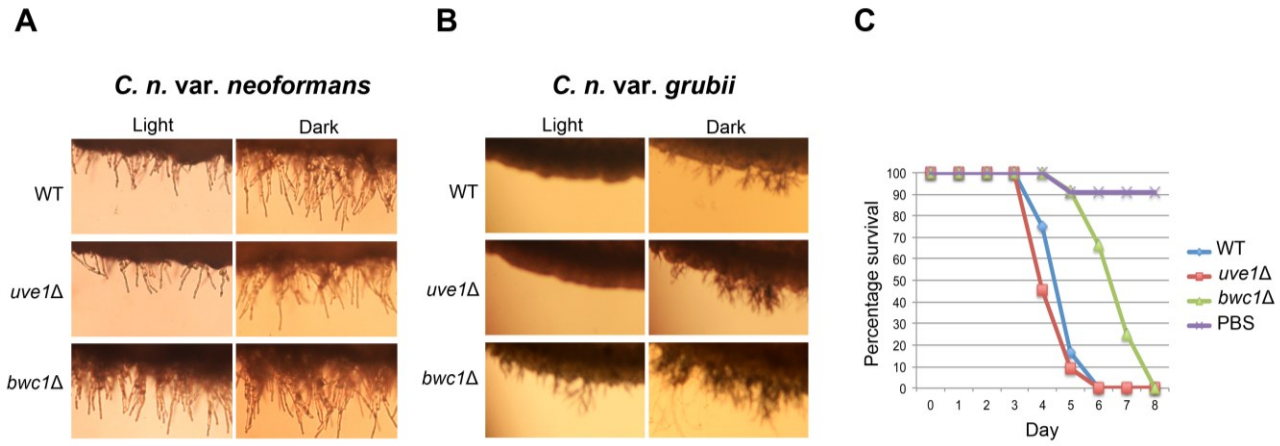

Fig. 15 : The *uve1*Δ strain is unaffected in mating and virulence. (A, B) Crosses were set for *C. n.* var. *neoformans* and *C. n.* var. *grubii* strains. Yeast cells of opposite mating type were mixed on V8 medium and Murashige-Skoog medium, in light grown and dark grown condition for 3 to 4 days and photographed. (A) Mating for *C. n.* var. *neoformans*, top panel JEC21 (WT, *MAT*α) X JEC20 (WT, *MAT***a**), middle panel AISVCN101 (*uve1*Δ, *MAT*α) X AISVCN104 (*uve1*Δ, *MAT***a**) and bottom panel AI5 (*bwc1*Δ, *MAT*α) X AI6 (*bwc1*Δ, *MAT***a**). (B) Mating for *C. n.* var. *grubii*, top panel KN99α X KN99a, middle panel AI191 (*uve1*Δ, *MAT*α) X AISVCN52 (*uve1*Δ, *MAT***a**), and bottom panel AI81 (*bwc1*Δ, *MAT*α) X AI89 (*bwc1*Δ, *MAT***a**). (C) Graph of the percentage survival for wax moth larvae injected with the either PBS or 2 X 10^7 cells/ml of KN99α, AI191 or AI81. (Verma and Idnurm, 2013)

strain was hypo-virulent as expected.

These mating and virulence experiments negate a role of *UVE1* other than UV sensitivity as far as the phenotypes regulated by white-collar complex are concerned. Hence *UVE1* is the dedicated DNA repair gene that is regulated through white-collar complex and confers UV resistance to *C. neoformans*. Other direct downstream targets for the two other phenotypes, mating and virulence, are yet to be discovered.

Uve1 homologs are light regulated through the white-collar complex in other fungi

Light dependent regulation of *UVE1* through Bwc1-Bwc2 in *C. neoformans* suggests of a possibly conserved evolutionarily ancient UV defense pathway. The homologs of *UVE1* are already known to be present in different species of fungi, bacteria and archea. The White-collar complex is widely conserved in different fungal divisions such as basal fungi like the chytrids, Glomeromycotina, Mucoromycotina and what are often considered the "higher" fungal phyla the Ascomycota and Basidiomycota (Idnurm et al., 2010). Looking at the simultaneous presence of both Uve1 and white-collar complex correlates in the fungi, and it can be hypothesized that this type of regulation of an endonuclease through a photoreceptor complex is an evolutionary conserved phenomenon. There are few exceptions such as Saccharomycotina where the complex is absent, and hence these fungi are called blind fungi. In bacteria and archaea, where there is no white-collar complex, LOV domain containing flavin-binding proteins are present and these are the evolutionary precursors of the white-collar complex. An alignment was performed for some of the key fungal, bacterial and archaeal species for the present homologs of Uve1 (**Fig. 16**). The two fungal species other

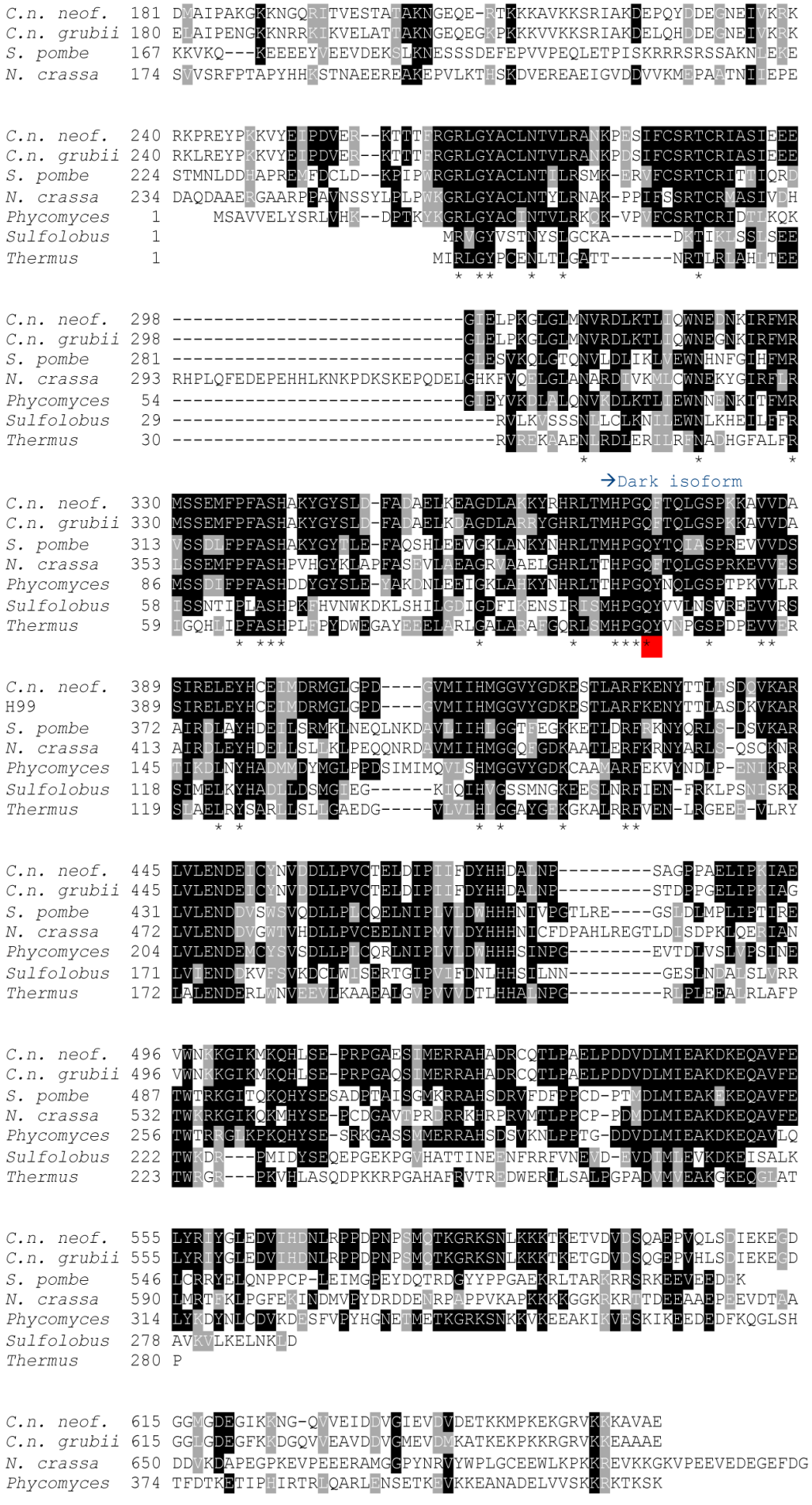
→Dark isoform

Fig. 16 : Alignment of Uve1 homologs from fungi, bacterium *Thermus thermophilus* and Archaea *Sulfolobus acidocaldarius*. Fungal species are *C. neoformans* var. *neoformans* (*C.n. neof.*), *C. neoformans* var. *grubii* (*C.n. grubii)*, *Schizosaccharomyces pombe*, *Neurospora crassa* and *Phycomyces blakesleeanus*. Mitochondrial localization sequences predicted by MitoProt are in green. Residues conserved in all species are marked by an asterisk. The two residues associated with the catalytic active site are highlighted in red. The start of the dark short isoform from var. *neoformans* is indicated by the blue arrow. (Verma and Idnurm, 2013)

than *Cryptococcus* taken in this alignment are *Neurospora crassa* and *Phycomyces blakesleeanus*, representing two major lineages, i. e. phylum Ascomycota and the Mucoromycotina (previously the zygomycetes). It can be seen that residues are conserved, marked by the asterisks that lie near and in the active site region. The two residues Q and Y as highlighted in red belong to the active site of the protein.

To confirm if *UVE1* in other fungal species are also regulated through the white collar complex a set of northern blots was done using light and dark treated RNA samples from respective fungal species using *UVE1* as a probe (**Fig. 17**). In *Neurospora* a light regulated *UVE1* band can be observed in light treated wild type and the same band is absent from wild type dark samples and from *wc-1* mutant light and dark samples. In *Phycomyces* two bands are observed in light treated wild type samples: of these the smaller band is the real *UVE1* transcript. The bigger band is the *UVE1* gene fused with the adjacent 3' gene due to transcriptional read through. No traces of any expression are observed in the wild type dark treated strain or for both light and dark treated *madA madB* strains. The *madA* and *madB* genes are homologs of *wc-1* and *wc-2*. In *S. pombe* a single band of *UVE1* is observed in both light and dark treated samples. This result in *S. pombe* is expected; as this fungus does not have the white-collar photoreceptor complex, hence white light-dependent regulation of transcript levels is missing although the *UVE1* transcript is present.

Since *UVE1* is a DNA repair gene it is probable that there are other DNA repair genes in the genome that are also light regulated and confer protection to UV stress. Hence we screened the 1200 strain knockout set (Liu et al., 2008) for those with a UV sensitivity phenotype and performed northern blots for each gene to see if there is any light dependent regulation (**Fig. 18**). Twelve UV sensitive strains were identified in the collection, including

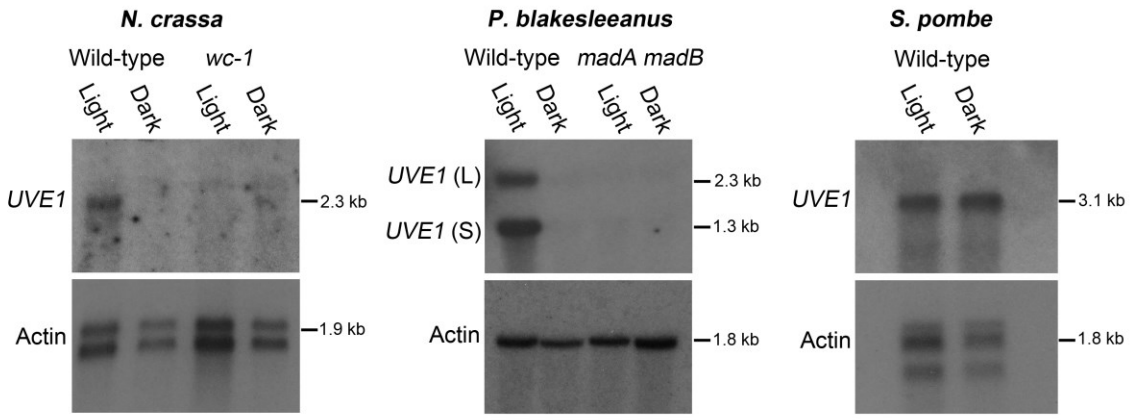

Fig. 17 : Light regulation of *UVE1* through Bwc1 is conserved in fungi. Northern blots for *UVE1* homologs, starting left to right, panel 1 *P. blakesleeanus* [NRRL1555 (WT), L51 (*madA madB*)]; panel 2, *S. pombe* [L972 (WT)] and panel 3, *N. crassa* [FGSC 4200 (WT), FGSC 4398 (*wc-1*)]. All experiments were either 23 hr dark + 1 hr light, (Light) or 24 h constant darkness (Dark). Blots were stripped and reprobed with actin as a loading control. For clarity, the gene name *UVE1* is used to refer to all homologs (*mus-18 N. crassa*; *uveA P. blakesleeanus*; *uve1 S. pombe*). (Verma and Idnurm, 2013)

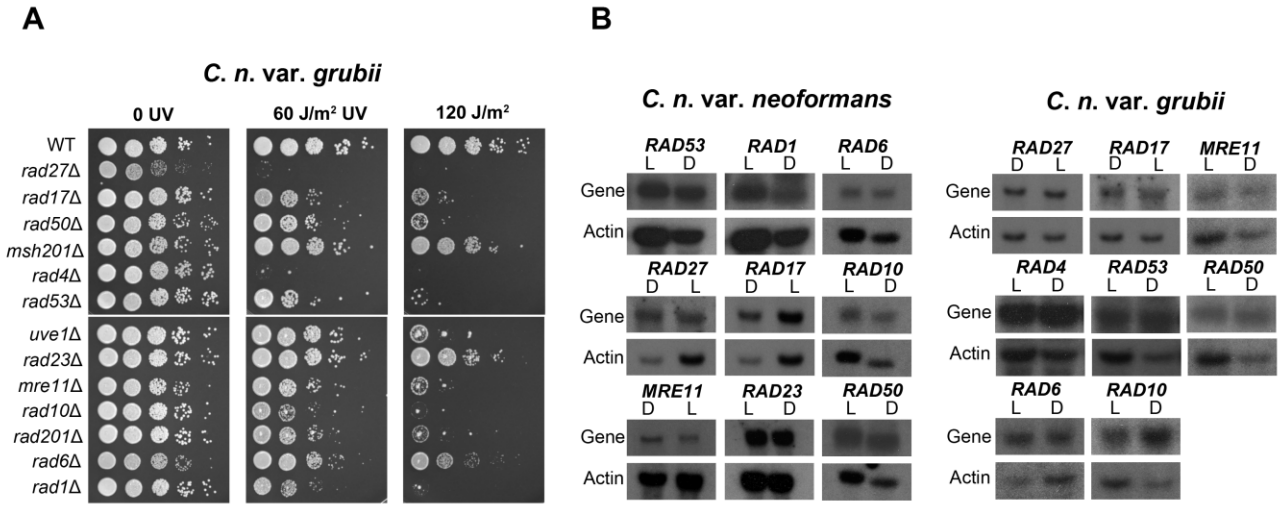

Fig. 18 : UV sensitivity of DNA repair genes and their regulation by light. (A) Ten-fold serial dilutions for *C. neoformans* var. *grubii* strains, untreated or stressed with UV and grown at 30°C for 2 days. Order of *C. neoformans* var. *grubii* strains from top to bottom is KN99α, D320 (*rad27*Δ), D893 (*rad17*Δ), D1445 (*rad50*Δ), D287 (*msh201*Δ), D397 (*rad4*Δ), D1053 (*rad53*Δ), D759 (*uve1*Δ), D288 (*rad23*Δ), D594 (*mre11*Δ), D1344 (*rad10*Δ), D203 (*rad201*Δ), D293 (*rad6*Δ), AI219 (*rad1*Δ). (B) Northern blots for genes implicated in repair of UV damage, in *C. neoformans* var. *neoformans* and *C. neoformans* var. *grubii*. L and D represent light grown and dark grown conditions for the strains. (Verma and Idnurm, 2013)

the *uve1*Δ strain in it. We did not observe any light dependent regulation or splicing in these genes. Hence *UVE1* is the only light regulated DNA repair gene in the *C. neoformans* genome known at present.

Conclusion

For millions of years much of evolution occurred under the influence of sunlight, benefiting from it positively as a source of energy. Along with the positive life-supporting electron enriched radiations sunlight is also composed of UV radiations whose exposure is detrimental to life as UV light can damage the genome. One major question is what protects the genome from the deleterious effects of UV damage and supports continuous existence? Also, does the existence of the white-collar complex have any role to play in conferring resistance to UV stress, as this protein complex is a light-sensing complex, which can sense the presence of the deleterious radiations? Does white collar-complex itself act as a light-sensing DNA repair system, as seen for the photolyase family of DNA repair/light sensing proteins, or does it act through some downstream target gene(s)? The current research on the *UVE1* gene provides the answers to address such questions. Regulation of the DNA repair gene *UVE1* in *C. neoformans* by light has evolved to protect its mitochondrial genome from the deleterious UV radiations. In the absence of this gene the fungus does not survive under UV stress levels that wild type strains are able to combat (**Fig. 1**). Existence of this light-regulated pathway has been also observed in two other major fungal lineages. Moreover a database search shows co-existence of white-collar complex or its ancient precursor flavin binding proteins in bacteria and archea with the *UVE1* gene, perhaps indicative of an ancient photoreceptor DNA repair system. Compiling the results, a model for *UVE1* induction and

regulation in pathogenic model fungus *C. neoformans* can be founded on light dependent regulation of *UVE1* (**Fig. 19**).

When the fungus senses white light it causes activation of the white-collar complex by some conformational changes, which are not known in *Cryptococcus*. Once the complex is activated it translocate to nucleus and the Bwc2 component of the complex that has a zinc finger DNA binding domain binds to the promoter of the *UVE1* gene, activating its transcription. Transcribed mRNA is transported to the cytoplasm to be translated to Uve1 protein. The amino acid sequence bears a mitochondrial localization signal and also the experimental evidence exists for the mitochondrial localization of Uve1. Hence Uve1 is channeled into mitochondria for its final localization where it sits proactively until it senses DNA damage in the form of pyrimidine dimers caused due to UV radiations. On sensing the damage, Uve1 initiates the repair process, which fully restores the intactness of the genome within the first four hours of the damage. Hence *UVE1* is a light-regulated DNA repair gene in the genome of *C. neoformans* that is required for protection of its mitochondrial genome under UV stress.

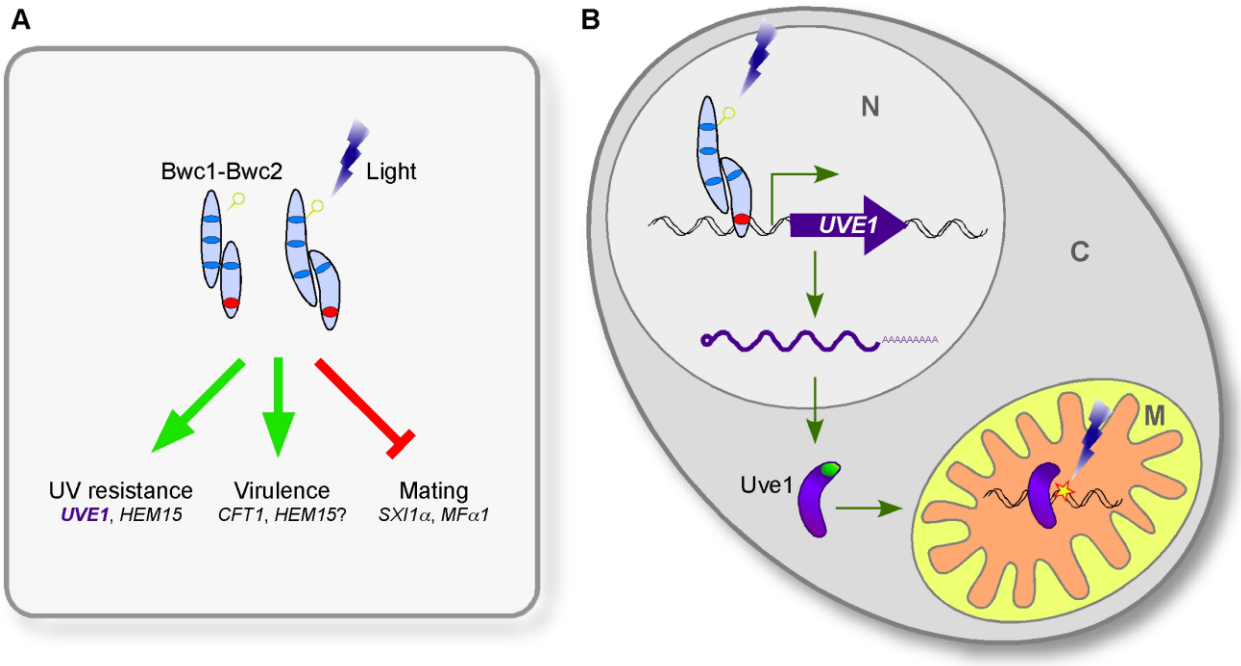

Fig. 19 : The involvement of Uve1 in the photosensory response of *C. neoformans*. (A) Bwc1-Bwc2 influences three aspects of *C. neoformans* biology: mating, UV tolerance, and virulence. Uve1 impacts one of these three. (B) Uve1 endonuclease protects *C. neoformans* under UV radiation stress by protecting its mitochondrial genome. Photoreceptor Bwc1 senses the blue/UV light, undergoes change in its flavin-binding domain, is activated, and forms a complex with Bwc2, a zinc finger transcription factor. Bwc2 with Bwc1 binds the *UVE1* promoter to activate its transcription. Uve1 protein has a mitochondrial localization signal (green), and is transported to mitochondria. In mitochondria, on sensing the UV-induced DNA damage (star) Uve1 binds to damaged DNA and initiates repair by the UVDE DNA damage repair pathway. N nucleus; C cytoplasm; M mitochondria.

CHAPTER 5

UNCOUPLING THE ROLE OF *RAD23* IN DNA REPAIR VERSUS ITS ROLE AS A UBIQUITIN RECEPTOR IN *C. NEOFORMANS* PATHOGENESIS

Introduction

Nucleotide excision repair (NER) is a primary system for the repair of UV-induced DNA damage. NER constitutes multiple enzymes, and defects in any of the genes that encode them results in UV sensitivity in the model ascomycete yeasts *Saccharomyces cerevisiae* and *Schizosaccharomyces pombe* thereby restricting survival under DNA damaging conditions. In humans defects in NER may cause the diseases such as Cockayne syndrome and Xeroderma Pigmentosum (XP), which are a predisposition to cancer due to enhanced sensitivity to sunlight (Hoeijmakers, 2001). NER works on transcribing DNA as TC-NER and in general for the repair of genomic DNA in the form of GG-NER. Repair of genomic DNA is important for the survival at the instance of damage, but also because any mutations in germ cells can be transmitted to progeny and inherited. A defect of NER is a possible determinant to pathogenicity/virulence of pathogenic microbes.

Rad23 is an NER protein with additional roles in cellular process such as protein sorting. The protein has been implicated in the virulence of the human pathogen *C. neoformans* (Liu et al., 2008). In that study, a set of 1200 gene deletion strains was screened for the virulence of each strain. We identified the DNA repair genes from that study, whose mutants showed sensitivity to UV radiation stress **(Fig. 18)**. Comparing the UV screen results and the virulence data from Liu et al, *RAD23* shares those phenotypes. Strains mutated for the gene have reduced signature tagged mutagenesis (STM) scores. The score is calculated such that in a mouse intranasal infection model the ratio of the input cells to the cells

recovered from the mice infected for the strain is measured using a quantitative PCR based assay. The PCR is performed using the primers for the amplification of the signature tag within the insertion cassettes specific for each strain and with another primer being common. The values from the ration of input to recovered were calculated on the $\log_2$ scale as the STM score. The scores of -2.5< to > +2.5 were assigned as the cutoffs for reduced virulence versus increased virulence, after experimental verifications using virulence measurements from studies of individual strains infecting animals (Liu et al., 2008). The two *rad23* mutants had STM scores of -7.6 and -6.7, hence the gene deletion strains were hypo-virulent.

Rad23 warranted further investigation because in addition to its functions as a DNA repair enzyme in NER it is also an ubiquitin receptor protein with roles in protein sorting and the ERAD pathway. Another interesting aspect about *RAD23* is its effects on transcription in yeast: *RAD23* is involved in regulation of almost two-thirds of the UV regulated genes and almost one third of all the yeast genes are mis-regulated in the *rad23* knockout (Wade and Auble, 2010; Wade et al., 2009). Multiple functions of this protein raised the question about the importance of each as they relate to the virulence of *C. neoformans*. Hence, we aimed to uncouple the role of the two different functions of *RAD23*, DNA repair and protein sorting, by creating alleles of the gene impaired in each, and then testing the virulence and other phenotypes of strains carrying them.

Stress phenotypes of Rad23 domain deletion strains

Rad23 has four defined domains in the model fungus *S. cerevisiae* and in humans (Dantuma et al., 2009; Walters et al., 2003). These four domains are UBL, UBA1, Rad4 or XPC binding domain and UBA2 **(Fig 20)**. The N-terminal domain UBL is an ubiquitin-like domain and it binds to the Rpn1 subunit of the 19 S regulatory subunit of the proteosome

(Elsasser et al., 2002). Other proteins that bind to the UBL domain of Rad23 are the ubiquitin chain elongation factor Ufd2 (Kim et al., 2004), peptidyl tRNA hydrolase Pth2 (Ishii et al., 2006) and UBA (Ubiquitin associated domains) (Walters et al., 2003). Interaction of the UBL domain with the UBA domain prevents Rad23 binding to the proteosome as the protein adopts a closed conformation. UBA domains are so called because they are able to bind ubiquitin and polyubiquitin molecules. The central UBA1 domain binds to ubiquitin/polyubiquitin molecules and UBL, and the C-terminal UBA2 domain binds to ubiquitin and UBL domain. The human Rad23 A and B proteins use their UBA2 domains to bind to DNA repair protein 3-methyladenine DNA glycosylase (Miao et al., 2000), and the UBA2 domain of Rad23 A protein binds to human immunodeficiency (HIV) 1 accessory protein Vpr (Withers-Ward et al., 2000). The UBA2 domain is required for the stability of the Rad23 protein in its interaction with the proteosome. The UBA2 domain resists initiation of degradation by the proteosome and hence can efficiently channel a substrate for degradation while preventing its own degradation (Heinen et al., 2011). The third domain of Rad23 is the Rad4-binding domain, also called the XPC-binding domain in humans, and this domain is important for the NER activity of the Rad23 protein. This domain interacts with Rad4 and the peptide N-glycanase protein Png1 (Lee et al., 2005) and primarily contributes to the DNA repair function associated with Rad23.

A

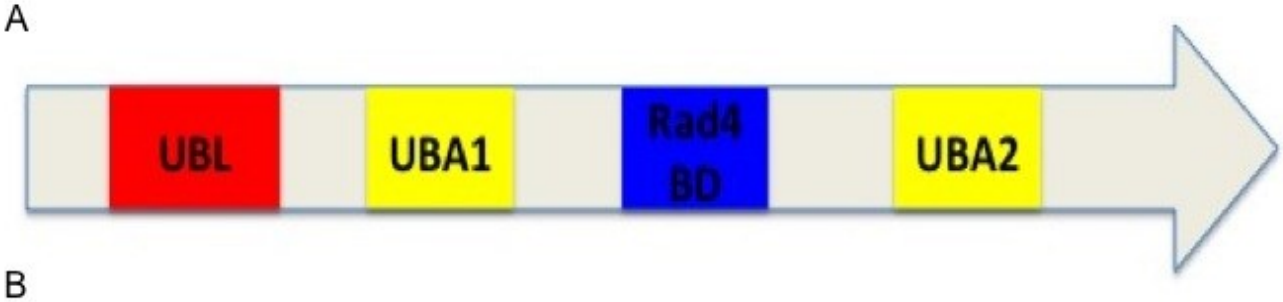

B

MVKITFKTVQNKVADLKKKIQETQTFPVENQKLIYSGKILNDASSVESLKIKEKDFLVVMVSRPKAT
PAATPAAPATPAAPSTPAPAAAASEEASVANPAVPAPSAPSAESAPAPASAPAAEPAQSSAVESGLG
GSFVTGPALQAAIDGMVEMGFERDQVIRALRASFNNPDRAVEYLMSGNIPSVEGTAPAAPAPAA
PSTPSAAAAPAQPAVPSEPAAQPAASAPPASAGGSADNLFAAAEAAMNRDRGVPAAAGAPGLPG
AGAGMPGGMGGGDQLSAIRQMVQQNPAMIQPLLQQIATEHPELAQLIAQNPEALYELLGGGG
GEGDDDDEFGEGPVMRVNLTQEEAAAVERLEALGFDRQTVLQAYMLCDKNEELAANFLFENME
EDQ*

Fig. 20 : Representation of Rad23 domains. A) Diagramatic representation of Rad23 domains. B) Rad23 amino acid sequence from *C. neoformans* strain H99. The color-coding indicates the sequences corresponding to the four domains.

Though these individual domain functions are well studied in *Saccharomyces*, their functions are yet to be established in *C. neoformans*. To uncouple the role of DNA repair versus ubiquitin receptor function of Rad23, in its impact on virulence of *C. neoformans*, we decided on a strategy to delete all four domains one at a time and in combinationatorial double domain deletions. In *Saccharomyces* it is clear that UBA1 and UBA2 single and double deletion does not affect the UV sensitivity phenotype (Bertolaet et al, 2001). Hence we targeted these types of deletions, and with different domain deletions strains it is possible to test the function of individual domains in isolation to the full-length protein in *C. neoformans*.

A knockout of *RAD23* was made in the KN99**a** background and this was used as a parent strain for the introduction of the different *RAD23* alleles as discussed further. A *RAD23* construct was made with its native promoter and terminator, and this construct was used to make subsequent domain deletion constructs by site directed mutagenesis (experimental strategy outlined in **Fig. 21**). The full-length *RAD23* construct was transformed into the *rad23*Δ strain to check that it restored the phenotype back to the wild type level. Three strains, wild type, *rad23*Δ and *rad23*Δ+ *RAD23* were tested for their phenotypes related to UV stress response and in the presence of tunicamycin which disrupts ERAD pathway and hence triggers ER stress, and other chemical stresses **(Fig. 22)**. The wild type and the complemented strain *rad23*Δ+*RAD23* behaved similarly, and the knockout strain *rad23*Δ had increased sensitivity to UV stress and resistance to tunicamycin. No significant differences were observed for Hydrogen peroxide, paraquat stress and for growth at 37 degree Celsius.

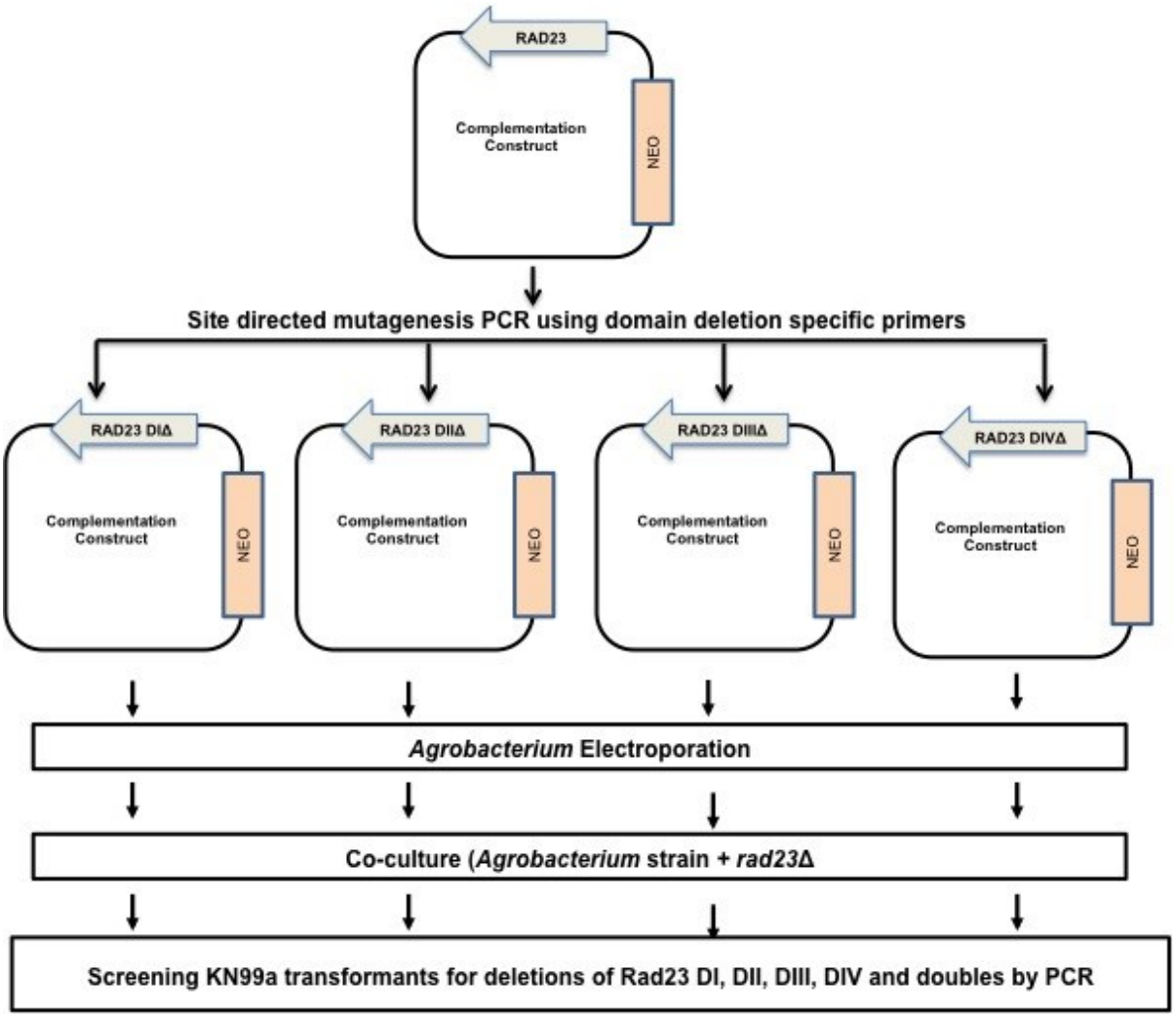

Fig. 21 : Strategy for making Rad23 domain deletion constructs. The backbone complementation construct represented here is p*PZP-RAD23-NEO*. In all the complementation constructs the arrow head represents full length Rad23 domains or the the Rad23 with deleted domains. NEO is for the neomycin selection marker. Arrows represent different steps in the process. Boxes containing the text represent the process at respective steps.

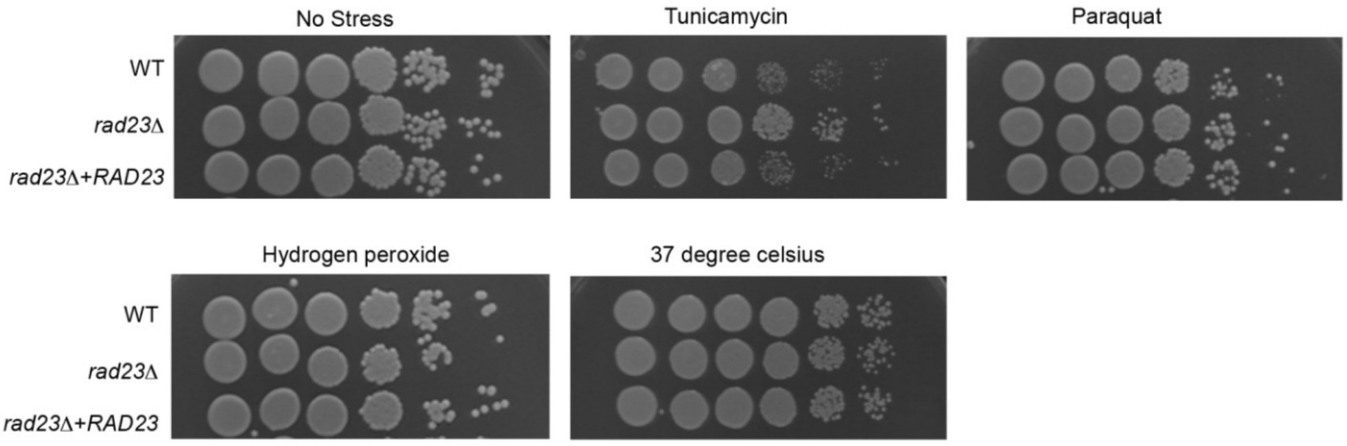

Fig. 22 : Stress responses for Rad23. The WT, *rad23*Δ and *rad23*Δ+*RAD23* strains exposed to chemical, radiation and temperature stress. The stresses are tunicamycin (0.125 μg/ml), hydrogen peroxide (1mM), Paraquat (0.5 mM), and growth at 37 degree celsius.

The plasmid p*PZP-RAD23-NEO* with the full-length *RAD23* (with native promoter and terminator) was the basis used to make DNA molecule constructs with domain deletions **(Fig. 21)**. All constructs were transformed into the *rad23*Δ strain and were tested for the similar phenotypic stress tests, UV, tunicamycin, dithiothritol (DTT) and t-butyl hydroperoxide (T-BOOH) **(Fig. 23)**. The domain III deletion and domain IV deletion strains showed different levels of sensitivity to UV stress, with domain III deletion being more sensitive and comparable to the *rad23*Δ strain. Domain IV deletion strain showed slight UV sensitivity. For tunicamycin stress, again both domain III deletion and domain IV deletion strains showed increased resistance, like *rad23*Δ. The domain IV deletion strain was more resistant compared to the domain III deletion strain a day after the stress. As the domain I and domain II individual domain deletion strains showed a wild type phenotype these domains are not required to combat any of the tested stresses, at least individually. Domain I+II double deletion strain was also tested to see if there is any difference observed in stress tolerance phenotype compared to the individual domain I and domain II deletions. Like the individual domain deletions, no difference in stress tolerance phenotype was observed for the domain I+II double deletion strain, as they behaved comparable to the WT strain. For the DTT and T-BOOH stresses no significant phenotypic difference was observed for any of the domain deletion strains. For DTT stress we expected domain IV and domain III deletions to show some differences in phenotype as we saw for tunicamycin stress since both chemicals triggers UPR. However absence of a phenotype in DTT treated domain III and domain IV deletions suggests a role of Rad23 at different levels in UPR, since DTT and tunicamycin

A

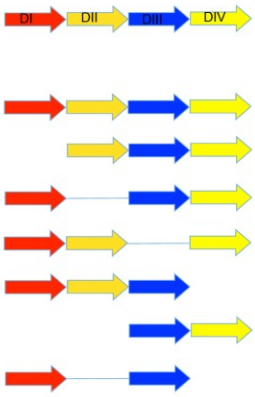

Strain Description	Rad23 missing domain/Function in *S. cervisiae*
KN99α	Full length present
rad23Δ	Full length missing (DNA repair and ERAD)
rad23Δ+Rad23	Full length (DNA repair and ERAD)
rad23Δ+Rad23-domainIΔ	UBL (Ubiquitin like domain)
rad23Δ+Rad23-domainIIΔ	UBA1 (Ubiquitin associated domain 1)
rad23Δ+Rad23-domainIIIΔ	Rad4 binding domain
rad23Δ+Rad23-domainIVΔ	UBA2 (Ubiquitin associated domain 2)
rad23Δ+Rad23-domainIΔ-domainIIΔ	UBL and UBA1
rad23Δ+Rad23-domainIIΔ-domainIVΔ	UBA1 and UBA2

B

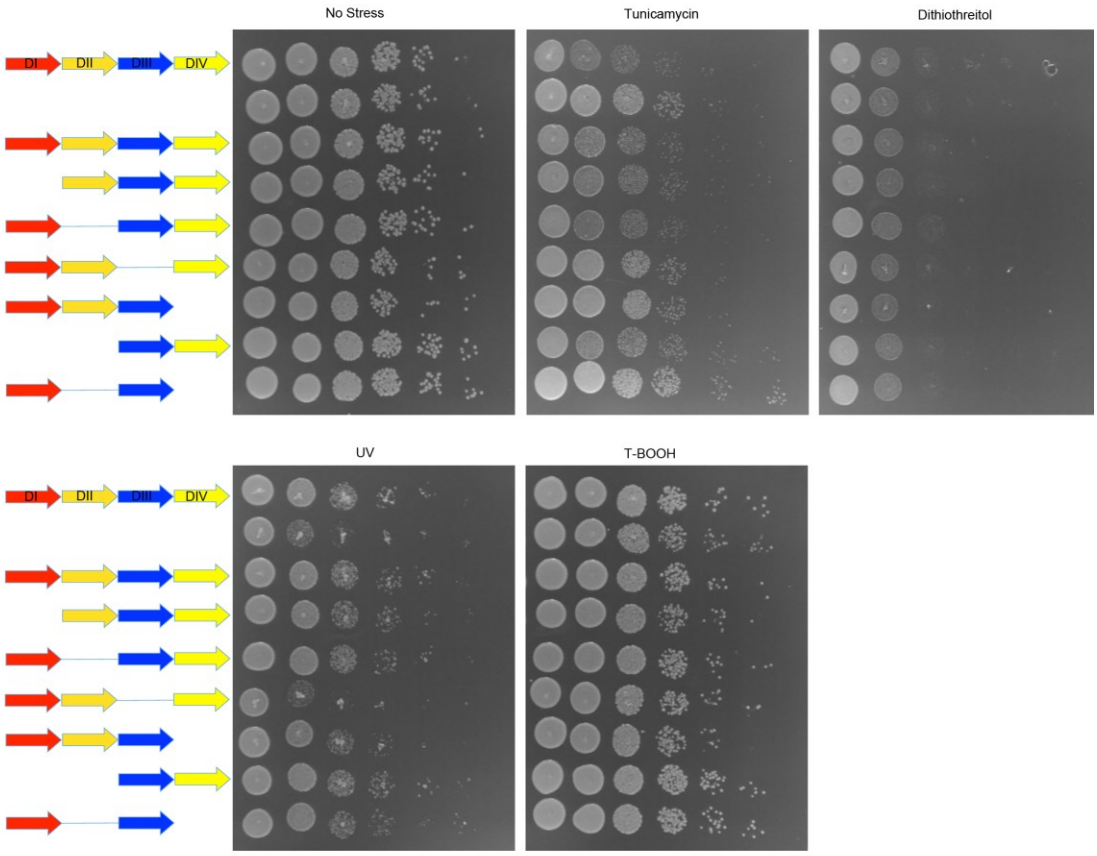

Fig. 23 : Stress responses for Rad23 domain deletions.A) Table explaining the genotype of the strains and the functions of all the deleted domains. Different colored arrows represent

different domains for Rad23. Red (domain I, UBL), dark yellow (domain II, UBA1), dark blue (domain III, Rad4 binding domain) and light yellow (domain IV, UBA2). Lines and missing region represents the deletions for the respective domains at that position. B) *C. neoformans* WT, *rad23*Δ, *rad23Δ+RAD23* complementation strain and all single and double Rad23 domain deletion strains are exposed to tunicamycin (0.125 μg/ml), DTT (10 mM), T-BOOH (0.3 mM) and UV (120 J/m^2).

triggers UPR in different ways. Tunicamycin affects N-linked glycosylation of proteins, and DTT is a strong reducing agent that reduces disulfide bonds.

Since domain II and domain IV are both UBA domains, a strain missing both domain II+IV was generated to see if there is any additive effect in the phenotype. To our surprise, deletions of both these domains combined show some additive effect for the tunicamycin sensitivity phenotype, being slightly more resistant compared to the individual domain IV deletion strain. No additive effect was observed for the UV sensitivity phenotype. These results indicate that when both UBA domains are taken out together there should be total impairment of the ubiquitin receptor function that is not observed for the individual domain II deletion. Moreover, UBA2 (domain IV) is also required for the overall stability of Rad23 as UBA2 efficiently channels a substrate for degradation while preventing its own degradation by the proteasome (Heinen et al., 2011). In *Saccharomyces* it is already shown that domain III binds to Rad4 and Png1. *C. neoformans* has a homolog for Rad4 but no homolog for Png1. An interaction of Rad4, which is a major NER protein, with domain III of Rad23 can explain the UV sensitivity phenotype seen in the strain with the domain III deletion allele. However as no homolog of Png1 exists, it is difficult to account for the tunicamycin resistance phenotype observed for the domain III deletion strain with the current knowledge and data available. Domain IV, UBA2 in *Saccharomyces*, interacts with ubiquitin and the UBL domain. In humans the UBA2 domains of the Rad23 A and B proteins bind to DNA repair protein 3-methyladenine DNA glycosylase (Miao et al., 2000) and human Rad23 A protein's UBA2 domain binds to human immunodeficiency (HIV) 1 accessory protein Vpr (Withers-Ward et al., 2000), but no homologs for these proteins exist in *Cryptococcus* as assessed by BLASTp analysis of the *C. neoformans* genome sequences.

Hence it is difficult to explain the slight UV sensitivity phenotype observed for the domain IV deletion strain based on the protein interaction possibilities with DNA repair protein. However another explanation that can account for the phenotype is that it is a secondary consequence of altering Rad23 protein stability. Interaction with ubiquitin and UBL domains explain the observed role in the ER stress response, through tunicamycin triggering the unfolded protein response.

Role of individual Rad23 domains in virulence of *C. neoformans*

The domain deletion strains were analyzed for their virulence using the wax moth (*Galleria mellonella*) model of infection. For this experiment, two independent transformants carrying the *RAD23* constructs were used, due to concerns about position effects from the T-DNA inserting into the genome accidentally in genes that would be required for virulence. **Fig. 24** shows the percentage survival curves for larvae infected with wild type, *rad23*Δ, *rad23*Δ+*RAD23* and individual and combinational domain deletion strains. The survival data show least percentage survival for the Rad23 complemented strain *rad23*Δ+*RAD23*, wild type and domain III deletion strain where almost 90 percent of the wax moth are dead by day 6 to day 7. Also the percentage survival is less for the wax moth infected with domain I deletion, domain II deletion, domain II+I deletion and also domain II+IV strain which shows only 20 to 25 percent survival by day 7. For the domain IV deletion strain the survival percentage is maximum with almost 60 % at seven days post-inoculation and close to 90 % at six days post-inoculation, similar to the domain II+IV deletion strains. However for the domain II+IV deletion strain towards day 7 there is a sudden fall in wax moth survival but then tapers and the remaining infected wax moth strains

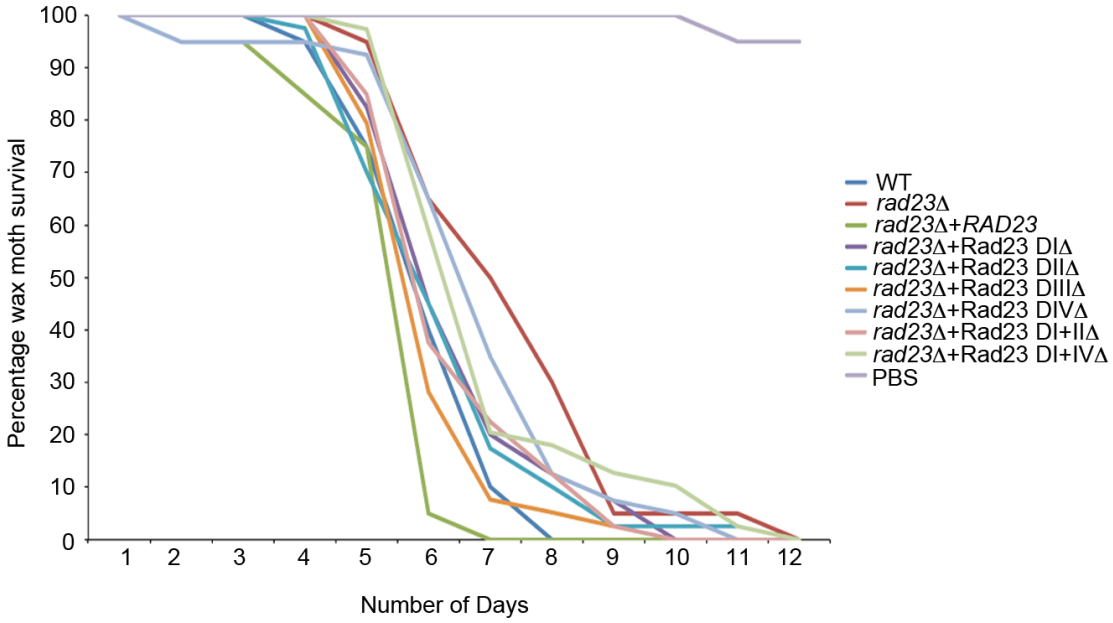

Fig. 24 : Wax moth virulence assay for Rad23. The graph represents the percentage survival for wax moth larvae injected with the either PBS or 2 X 10^7 cells/ml of *C. neoformans*, WT (KN99**a**), *rad23*Δ, *rad23Δ+RAD23* strain and all domain deletion strains and control PBS. X-axis represents percentage survival and Y-axis represents number of days after inoculation.

are alive until day 11 to 12, which is comparable to the *rad23*Δ and the domain IV deletion strains. However interpreting these results is complicated due to enhanced survival rates observed for some of the domain II strain infected wax moth that did not show the earlier days survival trend as for the *rad23*Δ, domain IV deletion and domain II+IV deletions strains.

Several important observations come from the wax moth virulence experiments. The first is that domain IV of Rad23 is the most important domain required for virulence of *C. neoformans*. The second is that domain III deletion does not affect the virulence potential of *C. neoformans* yet does the UV sensitivity phenotype. Domain III is clearly implicated in Rad4 dependent NER pathway in other eukaryotes, and hence this data indicates that Rad23's role in NER does not impact the virulence aspect of the *C. neoformans* homolog. The findings in the insect model could be further verified in mice intranasal infection studies. These mice studies are further advocated, as the wax moth model can be hard to interpret due to phenomenon like molting and the short time scales involved. Moreover, virulence testing in the mouse model is of better relevance to human disease.

Organelle localization of Rad23

Rad23 is a DNA repair protein and an ubiquitin receptor whose localization could be in the nucleus, mitochondria, or cytoplasmic. Using the PSORT II online software, the prediction for the localization pattern of Rad23 is 47.8 % nuclear, 26.1 % mitochondrial, 13 % cytoplasmic and the rest from vesicle secretory system and vacuolar. To determine the subcellular localization of Rad23, I made a GFP fused construct for Rad23 with GFP at the C-terminal end. The Rad23-GFP expressing strain was crossed to laboratory made strains that express either a Hem15-mCherry or H2b-mCherry construct. Hem15 is a

mitochondrially-targeted protein and H2b is the nuclear-specific histone 2b protein, and hence Hem15-mCherry or H2b-mCherry are localized in mitochondria and nucleus respectively. The strains with Rad23-GFP and Hem15-mCherry or Rad23-GFP and H2b-mCherry were examined by fluorescence microscopy. Rad23-GFP clearly co-localized with H2b-mCherry, giving a yellow signal, and hence Rad23 is nuclear (**Fig. 25**). We observed Rad23-GFP expression outside the nucleus. Next, microscopy for Rad23-GFP and Hem15-mCherry expressing strain was done and we observed negligible co-localization, as we could see red and green expression individually exclusive of each other with no yellow fluorescence signal (**Fig. 25**). Hence it can be concluded that Rad23 is primarily nuclear and cytoplasmic.

The virulence experiments indicated that Rad23 domain III deletion, which is most important for the DNA repair function of Rad23, has no role to play in the virulence of *C. neoformans*. Domain IV stood out with a role in virulence. Rad23 domain IV acts as an ubiquitin receptor. This is a UBA2 domain that is the second ubiquitin-binding domain in the protein after UBA1. Yeast domain IV binds to ubiquitin molecules and UBL that is domain I of Rad23. Interaction of domain IV with the UBL domain is important for the proteasome binding function of Rad23. If there is interaction between UBL and UBA domains Rad23 will be in closed confirmation and its interaction with proteasome will be hampered. Also domain IV channels substrates to the proteasome but at the same time prevents its own degradation by the proteasome.

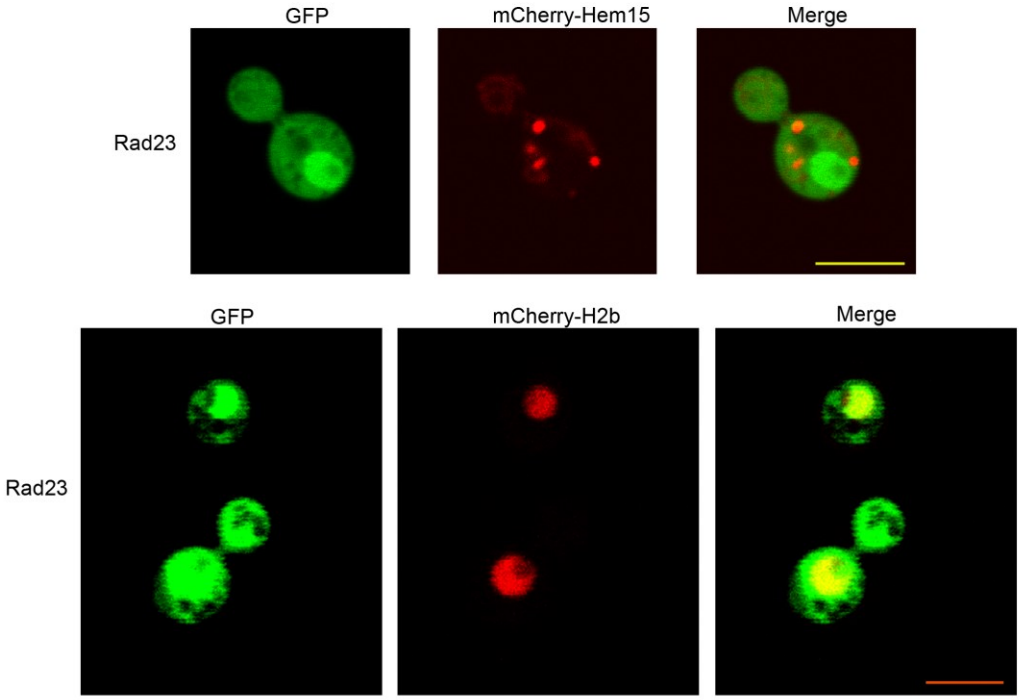

Fig. 25 : Organelle localization of Rad23. Rad23-GFP localization in the *C. neoformans* strains expressing mCherry-Hem15 (mitochondrial) and mCherry-H2b (nuclear). Top panel tests mitochondrial localiation and bottom panel tests nuclear localization. Scale bars represent 10 μm.

We examined the localization of the Rad23 in the absence of either domain IV or domain I. These GFP expression experiments would shed light on the overall stability of the protein in the absence of these domains. The Rad23-DIΔ-GFP and Rad23-DIVΔ-GFP expression was performed in the *rad23*Δ strain background. Microscopy was performed and it seems that Rad23-DIVΔ-GFP expression **(Fig. 26)** was equally good as that of full-length Rad23-GFP strain. The Rad23-DIΔ-GFP fluorescence level was not as high as for the full length Rad23-GFP strain and only few cells were green, but nevertheless the signal was sufficient to access subcellular localization. The most important information from these experiments was that due to the domain deletion the protein was not impaired such that it might have triggered degradation, although this is with a caveat that a constitutive promoter drives the GFP fusion constructs. The virulence defect observed for the Rad23 domain IV deletion strain was not because of destabilization of the protein in the absence of the degradation resistance signal but because of the some other reason. Different reasons could be its ubiquitin receptor function, which in turn can affect the turnover of the other proteins. Also it is possible that the Rad23 degradation by the proteasome is affected but not observed under normal conditions (normal GFP expression), but when given stress, such as during growth in a mammal or insect, Rad23's turnover is affected. Another study gives one more possibility and suggests the role of lack of proteosome initiation region in escape of Rad23 degradation (Fishbain et al., 2011). These proteosome initiation regions are defined as unstructured loops or sequences, which can trigger degradation. The group showed that even in the absence of UBA2 domain, which according to previous reports is required for Rad23 stability, Rad23 could be protected from degradation on addition of a structured domain such as DHFR (dihydrofolate reductase).

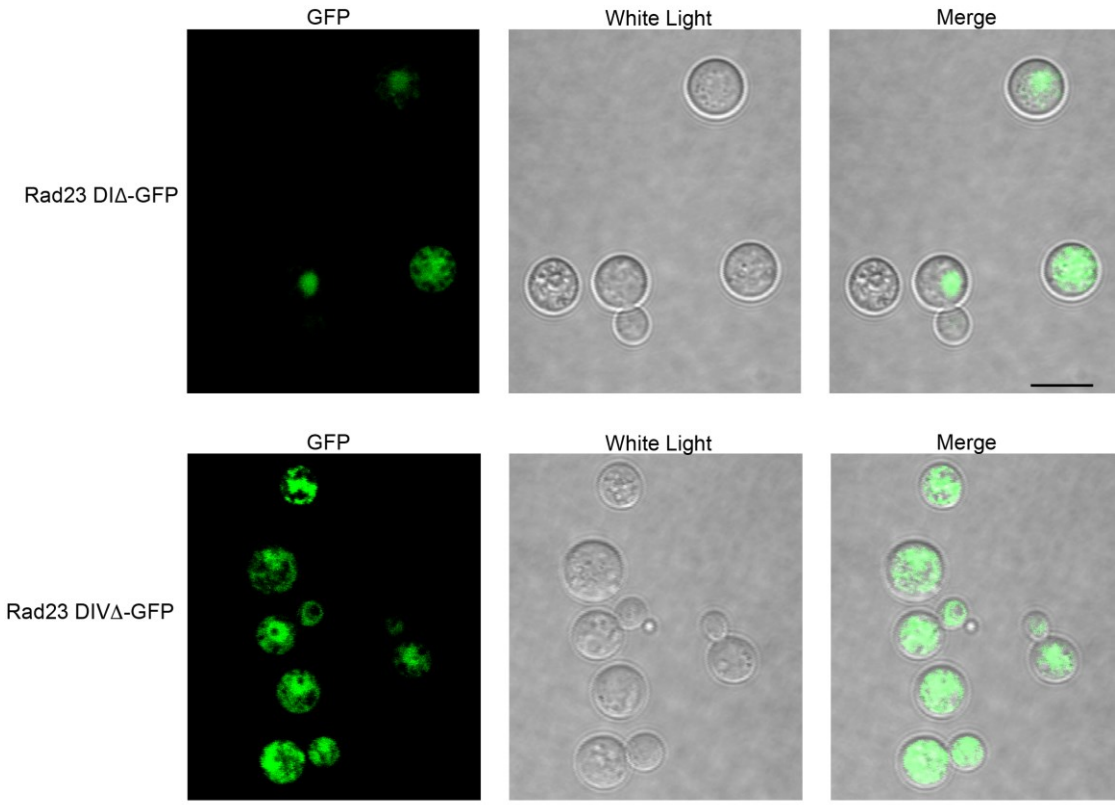

Fig. 26 : Expression of GFP fused Rad23 domain deletion constructs. The top panel shows expression for Rad23-DIΔ-GFP and bottom panel shows expression of Rad23-DIVΔ-GFP. Scale bar represents 10 μm.

This study suggests that it is possible that tagging the domain IV truncated Rad23 with GFP at its C-terminal end might cover the unstructured region exposed due to domain IV deletion. This may also be one of the reasons that this fusion construct of Rad23-GFP escapes degradation as it could have been for just Rad23 domain IV. If so, the scenario for the virulence defect we observe in the Rad23 domain IV deletion strains might be due to instability of Rad23 and hence lack of its ubiquitin adaptor functions. However Rad23-DIVΔ-GFP strain had a similar phenotype as of Rad23-DIVΔ strain, suggesting that the virulence defect observed is because of the missing UBA2 domain function and is not due to an issue with Rad23 protein stability.

***RAD23* is not a light regulated gene**

Like Uve1, Rad23 is a DNA repair enzyme and also shows sensitivity to UV radiation stress. This raised the question about the possible regulation of *RAD23* by light as occurs for the *UVE1*. Hence northern blot for the *RAD23* transcript, along with other DNA repair genes, was performed from RNA samples obtained for the light and dark grown cultures of *C. neoformans* (**Fig. 18**). No light regulation was observed for *RAD23*, as under light or dark grown conditions the *RAD23* transcript levels were equal.

However for *RAD23* RNA there is an interesting story regarding a miscellaneous band in northern blots and the odd splicing which I will describe briefly. First, while performing the *RAD23* northern when using a probe that extends into the 3' UTR of *RAD23* in the strain JEC21 we observed two bands. One band is approximately the size of the *RAD23* transcript and the other band is small (around 300 nt). Using the full length probe which covers the whole gene start to stop we got one transcript only, which is comparable to the size of the full length *RAD23* transcript. Second, when trying to clone the full length

RAD23 transcript we never obtained a full transcript clone after direct amplification from the cDNA. There was always a region from the middle of the gene, in which the whole or the partial domain II was missing. This was observed in multiple cloning attempts and finally we had to take a strategy where we combined sequences from two partial *RAD23* clones, one from the 5' portion of the gene and another from the 3' portion of the gene using a linker sequence in the primer, to cover the whole transcript. This missing domain II mystery added to our two band problem in the northern blots of *RAD23* and made us think that the small band observed in the northern blots may be due to the signal given by the missing part of the *RAD23* transcript. Careful examination of the probes used for the northern blot and looking at the *RAD23* transcripts in the reannotated version of strain H99 at the Broad H99 resolved the problem. We observed that in the 3' UTR of *RAD23* there is a small transcript of 311 bp CNAG_12112T0, which is in the reverse orientation. Our first probe for the northern blot, which extended in the 3' UTR of *RAD23,* shares a common overlapping region of about 90 base pairs with this small mystery transcript. While the equivalent information is unavailable for JEC21, the information from H99 may explain why we always observed two bands with this probe and one band with the full length *RAD23* transcript.

To further solve the remaining mystery of missing domain we used the probe for northern just from the missing domain region, expecting either no band or just one band which should be ideally full length. Our results for this experiment showed just one band, and this was comparable in size to the band we observe with the full length *RAD23* probe. This does not resolve the question of why we were getting missing domain transcripts and we were never able to directly clone a full length *RAD23* transcript. The incorrect clones may have several origins. 1. It could be due to some technical error such as slipping polymerase

activity 2. It is possible that the mystery-splicing event we observe in the clones is not a regular phenomenon and might have to do something to stress induced regulation through *RAD23* as this gene have more than one function. However as we could not achieve enough signals for the KN99α northern blots. The second aspect is more interesting especially in light of the miscellaneous transcript CNAG_12112T0 for which function if any is unknown.

Summary

Conclusions can be drawn from the experiments performed for *RAD23* in *C. neoformans*. 1.) We are successfully able to narrow down to domain IV as the most important for the virulence of *C. neoformans*. 2.) To some extent we are able to uncouple the role of DNA repair (at least Rad4-dependent NER function) versus ubiquitin receptor function in the virulence of *C. neoformans*. The Rad4-dependent NER function of Rad23 seems to have no role to play in the virulence phenotype. This is also supported by evidence that *rad4* and *rad23* mutants do not have identical phenotypes. *Rad4*Δ is more UV-sensitive than *rad23*Δ (**Fig. 18**), and also has no role in virulence (Liu et al. 2008). 3.) We are able to accurately predict the localization of the Rad23 protein, which is mostly nuclear or cytoplasmic but with no evidence of transport to the mitochondria. Hence Rad23 has no function to play in mitochondria, at least based on the resolution acquired with fluorescent tags and confocal microscopy.

CHAPTER 6

CONCLUSIONS AND FUTURE DIRECTIONS

Sensing the presence or absence of light is a trait that is common in many life forms on earth. Perceiving light is primarily associated with vision for motility, but there are other important signals with in the visible and invisible spectrum of light radiations. Sunlight carries the energy that supports the process of photosynthesis in plants, it consists of infrared radiation that signals the presence of heat, and light has ultraviolet wavelengths that have the capability to damage the genome of any organism. UV radiations are a common sterilizing agent used in hospitals, laboratories and even historically in the form of sun drying as a microbiocidal practice to preserve food. The common theme behind all these practices is that UV radiation damages the DNA of microorganisms and hence jeopardizes their survival. Evidence supports the link between DNA repair and virulence potential of pathogenic microorganisms (Alby and Bennett, 2009; Legrand et al., 2007; Liu et al., 2008; McCulloch and Barry, 1999). These studies also stress the importance of diverse DNA repair pathways, which may directly or indirectly influence the virulence potential of the organisms by affecting other virulence related pathways. Also there is research that links the light-sensing machineries with virulence in pathogenic bacteria and fungi (Gourley et al., 2014; Idnurm and Heitman, 2005; Ruiz-Roldan et al., 2008; Swartz et al., 2007). Collectively, this evidence opens the possibility of a three-way connection between light sensing, DNA repair and virulence of microbial pathogens.

The current study explored this link between light sensing, DNA repair and virulence in the human fungal pathogen *C. neoformans*. The work builds from two studies by Idnurm and Heitman (2005) and Liu et al (2008). In *Cryptococcus* a seminal study led to the

discovery of blue light photoreceptor complex Bwc1-Bwc2, and explored the phenotypic consequences of its absence from the fungus (Idnurm and Heitman, 2005). The three phenotypes related to the absence of this photoreceptor complex are mating, UV sensitivity and virulence. Acting through the photoreceptor complex, light repressed the process of mating, conferred resistance to UV radiation and contributed positively to virulence. However, the downstream signaling that regulated these responses was left unexplored. Considering UV to be a component of solar radiation, the virulence defect and UV sensitivity phenotypes observed due to absence of the Bwc1-Bwc2 complex may be governed by the same or related downstream targets, which possibly is a light-regulated DNA repair gene. In the second study (Liu et al., 2008) generated a strain deletion library covering almost one sixth of the *C. neoformans* genes and tested all strains for altered virulence as measured by competitive survival. The study included more than 50 DNA repair genes and about half of them showed some role in the virulence of the fungus. The two gene deletions, which made the fungus hypovirulent, were *RAD23* and *RAD54* and there were at least four other genes whose deletions, surprisingly, made those strains hypervirulent.

The first project was on DNA repair gene *UVE1*, encoding an endonuclease, as a putative downstream target of Bwc1-Bwc2 photoreceptor complex. Major findings of the project uncovered the Bwc1-Bwc2 downstream signaling branch related to the UV sensitivity of *bwc1* or *bwc2* mutants. *UVE1* was established as gene required by *C. neoformans* to survive under UV stress. Transcript levels for *UVE1* under light and dark conditions using northern blots, *UVE1* overexpression in *bwc1*Δ background, and EMSA of Bwc2 binding to the promoter of *UVE1* supported *UVE1* as a direct downstream target of the Bwc1-Bwc2 complex. An important finding is that *UVE1* is a mitochondrial DNA repair enzyme, and this

was confirmed by mitochondrial Uve1-GFP localization and validated by DNA damage assays in which the *uve1*Δ strain lagged in the repair of mitochondrial DNA damage compared to the wild type strain. Bwc1-Bwc2 dependent regulation of *UVE1* occurs in two other fungal species, *N. crassa* and *P. blakesleeanus*. These species are members of the Ascomycota and Mucoromycotina that separated from each other and the Basidiomycota 500-750 million years ago (Taylor and Berbee, 2006). The photoinduction of *UVE1* has been conserved for the same amount of evolutionary time. Though Uve1 is required for the survival of *C. neoformans* under UV stress is established in the study, no role was found in the virulence of the fungus. Wax moth virulence assays for the *uve1*Δ and the mouse data from (Liu et al., 2008) clearly showed that Uve1 is dispensable for virulence. Based on the findings of the study a model is proposed in **Fig. 19b**, that revises the role of the Bwc1-Bwc2 complex in sensing light and subsequent signal transduction.

The second project aimed to uncouple the role of two functions of DNA repair protein Rad23 in the virulence of *C. neoformans*. The two functions are DNA repair by NER and the ubiquitin receptor function with a role in ERAD pathway and unfolded protein response (UPR). Using the domain deletion strategy for the Rad23 protein we were able to define the domain required for the virulence of the fungus. This is domain IV of the protein, known as UBA2 in *S. cerevisiae* with an established role in ubiquitin receptor function. Other domains though with roles in ERAD pathway and UPR did not show any virulence related role. In contrast, the domain III deletion of Rad23, which is a Rad4-binding domain and functions in NER, did not show any virulence defect. Hence the present data exclude the possible DNA repair related role of Rad23 impacting the virulence of the fungus. The virulence assays we performed in wax moth larvae model system, although confirmation in a mouse model is still

needed. Additional data are obtained on the cellular localization of the Rad23 protein, which is mainly nuclear and cytoplasmic. Though the functions of Rad23 in virulence of *C. neoformans* were successfully separated and tested, how exactly the ubiquitin receptor function of Rad23 regulates virulence is yet to be explored in detail. The strains created in this study with different *RAD23* alleles would be particularly helpful for those future studies.

The common finding between these studies on *UVE1* and *RAD23* is that the DNA repair function of the two proteins is dispensable for the virulence of the *C. neoformans*. However, a role of DNA repair in the virulence of *C. neoformans* cannot be completely denied. In the study by Liu et al, 2008 there are other genes with dedicated function in repair of DNA whose mutations reduces the virulence. The *RAD54* gene whose deletion has a hypovirulence phenotype in the mice model and four other genes *MSH201*, *PMS1*, *MLH1* and *OGG1* whose deletions cause hypervirulent phenotype in the mice model are a few candidates needing study. With the exception of *OGG1* the other three are mismatch repair proteins and it is possible that *MSH201*, *PMS1*, *MLH1* and *OGG1* have roles to play in the microevolution of *C. neoformans* by keeping the mutation rate as low as possible. High mutation rate due to reduced fidelity in DNA repair in the absence of these genes may result in the newer strains of the fungus with variable and more virulent strains. A role of DNA mutations in generating host-adapted forms of *C. neoformans* has already been proposed and demonstrated (Magditch et al., 2012). Moreover the genes mentioned here come from the *C. neoformans* gene deletion set that covers only a sixth of the genome. It is probable that in the remaining of the untested *C. neoformans* genome there may be new candidate DNA repair genes required for virulence. Also there is evidence from another fungal pathogen *C. albicans* where a role of DNA mismatch repair genes has been shown in development of

drug resistance strains due to problems like genome instability (Legrand et al., 2007). Inside the host body a pathogen faces many insults, such as oxidative stress, to its genome and thrives to protect and maintain DNA in order to survive and multiply. In such a scenario, intact DNA repair mechanisms must be important for the pathogen.

The light-sensing complex has a clear role in the virulence of *C. neoformans* (Idnurm and Heitman, 2005) and also other pathogens (Canessa et al., 2013; Kim et al., 2011; Ruiz-Roldan et al., 2008). In *C. neoformans* the Bwc1-Bwc2 complex exerts different functions through different branches and downstream targets are being identified. Although *UVE1* is not the DNA repair gene with a role in virulence, the existence of other DNA repair gene regulated through this complex cannot be completely negated. One direction of research can be the investigation of function of Bwc1-Bwc2 complex in the absence of light. Looking at the importance of the environment in survival and mating function of *C. neoformans*, in future more efforts are needed to explore the link between environment sensing, DNA repair and virulence. Such research will help to understand the virulence mechanisms of *C. neoformans* and other fungal human pathogens such as *Histoplasma capsulatum* which shows light and dark based differences in virulence (Campbell and Berliner, 1973) and some plant fungal pathogens.

There are several unanswered questions in the field of *Cryptococcus* or in general fungal photobiology that need to be addressed. Some of these pressing questions are, what type of conformational changes takes place in the white-collar complex on sensing light? Does this protein exist as a complex or does dimerization take place on sensing light? How is the complex targeted to nuclei in order to initiate expression of the downstream targets? Apart from Uve1 what are the other downstream targets especially immediate ones? Uve1 is

a mitochondrial DNA repair protein in *Cryptococcus*, is there any other DNA repair protein that is light-regulated and has a role in nuclear DNA repair? The White-collar complex senses light, can it also sense dark and, if so, what is the mechanism and what are the downstream targets? Finding answers to these questions will advance our understanding of photobiology and is important from the virulence perspective of this fungus as one of the phenotypes of the white-collar mutants is defect in its virulence potential.

APPENDIX

COPYRIGHT CLEARANCE LICENSE

1. Idnurm, A., Y.S. Bahn, K. Nielsen, X. Lin, J.A. Fraser, and J. Heitman. 2005. Deciphering the model pathogenic fungus Cryptococcus neoformans. *Nature reviews. Microbiology*. 3:753-764. (**License No. 3485801079144**, Oct. 11, 2014)
2. Boiteux, S., and S. Jinks-Robertson. 2013. DNA repair mechanisms and the bypass of DNA damage in Saccharomyces cerevisiae. *Genetics*. 193:1025-1064. (**License Id. 3485811053325**, Oct. 11, 2014)
3. Verma, S., and A. Idnurm. 2013. The Uve1 endonuclease is regulated by the white collar complex to protect cryptococcus neoformans from UV damage. *PLoS genetics*. 9:e1003769. **(Open-Access License)** http://www.plosgenetics.org/static/license

REFERENCES

Al-Mehdi, A.B., V.M. Pastukh, B.M. Swiger, D.J. Reed, M.R. Patel, G.C. Bardwell, V.V. Pastukh, M.F. Alexeyev, and M.N. Gillespie. 2012. Perinuclear mitochondrial clustering creates an oxidant-rich nuclear domain required for hypoxia-induced transcription. *Science signaling*. 5:ra47.

Alby, K., and R.J. Bennett. 2009. Stress-induced phenotypic switching in Candida albicans. *Molecular biology of the cell*. 20:3178-3191.

Avery, A.M., B. Kaur, J.S. Taylor, J.A. Mello, J.M. Essigmann, and P.W. Doetsch. 1999. Substrate specificity of ultraviolet DNA endonuclease (UVDE/Uve1p) from Schizosaccharomyces pombe. *Nucleic acids research*. 27:2256-2264.

Basi, G., E. Schmid, and K. Maundrell. 1993. TATA box mutations in the Schizosaccharomyces pombe nmt1 promoter affect transcription efficiency but not the transcription start point or thiamine repressibility. *Gene*. 123:131-136.

Bayram, O., G.H. Braus, R. Fischer, and J. Rodriguez-Romero. 2010. Spotlight on Aspergillus nidulans photosensory systems. *Fungal genetics and biology : FG & B*. 47:900-908.

Bergman, K., A.P. Eslava, and E. Cerda-Olmedo. 1973. Mutants of Phycomyces with abnormal phototropism. *Molecular & general genetics : MGG*. 123:1-16.

Bhatia, P.K., R.A. Verhage, J. Brouwer, and E.C. Friedberg. 1996. Molecular cloning and characterization of Saccharomyces cerevisiae RAD28, the yeast homolog of the human Cockayne syndrome A (CSA) gene. *Journal of bacteriology*. 178:5977-5988.

Boiteux, S., L. Gellon, and N. Guibourt. 2002. Repair of 8-oxoguanine in Saccharomyces cerevisiae: interplay of DNA repair and replication mechanisms. *Free Radic Biol Med*. 32:1244-1253.

Boiteux, S., and S. Jinks-Robertson. 2013. DNA repair mechanisms and the bypass of DNA damage in Saccharomyces cerevisiae. *Genetics*. 193:1025-1064.

Brown, J.C., J. Nelson, B. VanderSluis, R. Deshpande, A. Butts, S. Kagan, I. Polacheck, D.J. Krysan, C.L. Myers, and H.D. Madhani. 2014. Unraveling the biology of a fungal meningitis pathogen using chemical genetics. *Cell*. 159:1168-1187.

Campbell, C.C., and M.D. Berliner. 1973. Virulence differences in mice of type A and B Histoplasma capsulatum yeasts grown in continuous light and total darkness. *Infection and immunity*. 8:677-678.

Canessa, P., J. Schumacher, M.A. Hevia, P. Tudzynski, and L.F. Larrondo. 2013. Assessing the effects of light on differentiation and virulence of the plant pathogen Botrytis cinerea: characterization of the White Collar Complex. *PloS one*. 8:e84223.

Centers for Disease, C., and Prevention. 2010. Emergence of Cryptococcus gattii-- Pacific Northwest, 2004-2010. *MMWR. Morbidity and mortality weekly report*. 59:865-868.

Chauhan, N., T. Ciudad, A. Rodriguez-Alejandre, G. Larriba, R. Calderone, and E. Andaluz. 2005. Virulence and karyotype analyses of rad52 mutants of Candida albicans: regeneration of a truncated chromosome of a reintegrant strain (rad52/RAD52) in the host. *Infection and immunity*. 73:8069-8078.

Chen, C.H., C.S. Ringelberg, R.H. Gross, J.C. Dunlap, and J.J. Loros. 2009. Genome-wide analysis of light-inducible responses reveals hierarchical light signalling in Neurospora. *The EMBO journal*. 28:1029-1042.

Crosthwaite, S.K., J.C. Dunlap, and J.J. Loros. 1997. Neurospora wc-1 and wc-2: transcription, photoresponses, and the origins of circadian rhythmicity. *Science*. 276:763-769.

Dantuma, N.P., C. Heinen, and D. Hoogstraten. 2009. The ubiquitin receptor Rad23: at the crossroads of nucleotide excision repair and proteasomal degradation. *DNA Repair (Amst)*. 8:449-460.

Degli-Innocenti, F., and V.E. Russo. 1984. Isolation of new white collar mutants of Neurospora crassa and studies on their behavior in the blue light-induced formation of protoperithecia. *Journal of bacteriology*. 159:757-761.

Elderfield, R.A., S.J. Watson, A. Godlee, W.E. Adamson, C.I. Thompson, J. Dunning, M. Fernandez-Alonso, D. Blumenkrantz, T. Hussell, M.i. The, M. Zambon, P. Openshaw, P. Kellam, and W.S. Barclay. 2014. Accumulation of human-adapting mutations during circulation of A(H1N1)pdm09 influenza in humans in the UK. *Journal of virology*.

Elsasser, S., R.R. Gali, M. Schwickart, C.N. Larsen, D.S. Leggett, B. Muller, M.T. Feng, F. Tubing, G.A. Dittmar, and D. Finley. 2002. Proteasome subunit Rpn1 binds ubiquitin-like protein domains. *Nat Cell Biol*. 4:725-730.

Estrada, A.F., and J. Avalos. 2008. The White Collar protein WcoA of Fusarium fujikuroi is not essential for photocarotenogenesis, but is involved in the regulation of secondary metabolism and conidiation. *Fungal genetics and biology : FG & B*. 45:705-718.

Evans, E., J.G. Moggs, J.R. Hwang, J.M. Egly, and R.D. Wood. 1997. Mechanism of open complex and dual incision formation by human nucleotide excision repair factors. *The EMBO journal*. 16:6559-6573.

Feaver, W.J., J.Q. Svejstrup, L. Bardwell, A.J. Bardwell, S. Buratowski, K.D. Gulyas, T.F. Donahue, E.C. Friedberg, and R.D. Kornberg. 1993. Dual roles of a multiprotein complex from S. cerevisiae in transcription and DNA repair. *Cell*. 75:1379-1387.

Fishbain, S., S. Prakash, A. Herrig, S. Elsasser, and A. Matouschek. 2011. Rad23 escapes degradation because it lacks a proteasome initiation region. *Nature communications*. 2:192.

Froehlich, A.C., Y. Liu, J.J. Loros, and J.C. Dunlap. 2002. White Collar-1, a circadian blue light photoreceptor, binding to the frequency promoter. *Science*. 297:815-819.

Fuller, K.K., C.S. Ringelberg, J.J. Loros, and J.C. Dunlap. 2013. The fungal pathogen Aspergillus fumigatus regulates growth, metabolism, and stress resistance in response to light. *mBio*. 4.

Gourley, C.R., E. Petersen, J. Harms, and G. Splitter. 2014. Decreased in vivo virulence and altered gene expression by a Brucella melitensis light-sensing histidine kinase mutant. *Pathogens and disease*.

Guzder, S.N., P. Sung, V. Bailly, L. Prakash, and S. Prakash. 1994. RAD25 is a DNA helicase required for DNA repair and RNA polymerase II transcription. *Nature*. 369:578-581.

Guzder, S.N., P. Sung, L. Prakash, and S. Prakash. 1993. Yeast DNA-repair gene RAD14 encodes a zinc metalloprotein with affinity for ultraviolet-damaged DNA. *Proceedings of the National Academy of Sciences of the United States of America*. 90:5433-5437.

Guzder, S.N., P. Sung, L. Prakash, and S. Prakash. 1998a. Affinity of yeast nucleotide excision repair factor 2, consisting of the Rad4 and Rad23 proteins, for ultraviolet damaged DNA. *The Journal of biological chemistry*. 273:31541-31546.

Guzder, S.N., P. Sung, L. Prakash, and S. Prakash. 1998b. The DNA-dependent ATPase activity of yeast nucleotide excision repair factor 4 and its role in DNA damage recognition. *The Journal of biological chemistry*. 273:6292-6296.

Hanawalt, P.C., and G. Spivak. 2008. Transcription-coupled DNA repair: two decades of progress and surprises. *Nat Rev Mol Cell Biol*. 9:958-970.

Heinen, C., K. Acs, D. Hoogstraten, and N.P. Dantuma. 2011. C-terminal UBA domains protect ubiquitin receptors by preventing initiation of protein degradation. *Nature communications*. 2:191.

Heitman, J.K., T. R.; Kwon-chung, K. J.; Perfect, J. R.; Casadevall, A. 2011. Cryptococcus From Human Pathogen To Model Yeast.

Hoeijmakers, J.H. 2001. Genome maintenance mechanisms for preventing cancer. *Nature*. 411:366-374.

Holden, N.S., and C.E. Tacon. 2011. Principles and problems of the electrophoretic mobility shift assay. *J Pharmacol Toxicol Methods*. 63:7-14.

Hull, C.M., M.J. Boily, and J. Heitman. 2005. Sex-specific homeodomain proteins Sxi1alpha and Sxi2a coordinately regulate sexual development in Cryptococcus neoformans. *Eukaryotic cell*. 4:526-535.

Hull, C.M., R.C. Davidson, and J. Heitman. 2002. Cell identity and sexual development in Cryptococcus neoformans are controlled by the mating-type-specific homeodomain protein Sxi1alpha. *Genes & development*. 16:3046-3060.

Hunter, S.E., D. Jung, R.T. Di Giulio, and J.N. Meyer. 2010. The QPCR assay for analysis of mitochondrial DNA damage, repair, and relative copy number. *Methods*. 51:444-451.

Idnurm, A., Y.S. Bahn, K. Nielsen, X. Lin, J.A. Fraser, and J. Heitman. 2005. Deciphering the model pathogenic fungus Cryptococcus neoformans. *Nature reviews. Microbiology*. 3:753-764.

Idnurm, A., S.S. Giles, J.R. Perfect, and J. Heitman. 2007. Peroxisome function regulates growth on glucose in the basidiomycete fungus Cryptococcus neoformans. *Eukaryotic cell*. 6:60-72.

Idnurm, A., and J. Heitman. 2005. Light controls growth and development via a conserved pathway in the fungal kingdom. *PLoS biology*. 3:e95.

Idnurm, A., and J. Heitman. 2010. Ferrochelatase is a conserved downstream target of the blue light-sensing White collar complex in fungi. *Microbiology*. 156:2393-2407.

Idnurm, A., J.L. Reedy, J.C. Nussbaum, and J. Heitman. 2004. Cryptococcus neoformans virulence gene discovery through insertional mutagenesis. *Eukaryotic cell*. 3:420-429.

Idnurm, A., S. Verma, and L.M. Corrochano. 2010. A glimpse into the basis of vision in the kingdom Mycota. *Fungal genetics and biology : FG & B*. 47:881-892.

Idnurm, A., F.J. Walton, A. Floyd, J.L. Reedy, and J. Heitman. 2009. Identification of ENA1 as a virulence gene of the human pathogenic fungus Cryptococcus neoformans through signature-tagged insertional mutagenesis. *Eukaryotic cell*. 8:315-326.

Ishii, T., M. Funakoshi, and H. Kobayashi. 2006. Yeast Pth2 is a UBL domain-binding protein that participates in the ubiquitin-proteasome pathway. *The EMBO journal*. 25:5492-5503.

Ito, H., Y. Fukuda, K. Murata, and A. Kimura. 1983. Transformation of intact yeast cells treated with alkali cations. *Journal of bacteriology*. 153:163-168.

Jackson, S.P., and J. Bartek. 2009. The DNA-damage response in human biology and disease. *Nature*. 461:1071-1078.

Janbon, G., K.L. Ormerod, D. Paulet, E.J. Byrnes, 3rd, V. Yadav, G. Chatterjee, N. Mullapudi, C.C. Hon, R.B. Billmyre, F. Brunel, Y.S. Bahn, W. Chen, Y. Chen, E.W. Chow, J.Y. Coppee, A. Floyd-Averette, C. Gaillardin, K.J. Gerik, J. Goldberg, S. Gonzalez-Hilarion, S. Gujja, J.L. Hamlin, Y.P. Hsueh, G. Ianiri, S. Jones, C.D. Kodira, L. Kozubowski, W. Lam, M. Marra, L.D. Mesner, P.A. Mieczkowski, F. Moyrand, K. Nielsen, C. Proux, T. Rossignol, J.E. Schein, S. Sun, C. Wollschlaeger, I.A. Wood, Q. Zeng, C. Neuveglise, C.S. Newlon, J.R. Perfect, J.K. Lodge, A. Idnurm, J.E. Stajich, J.W. Kronstad, K. Sanyal, J. Heitman, J.A. Fraser, C.A. Cuomo, and F.S. Dietrich. 2014. Analysis of the genome and transcriptome of Cryptococcus neoformans var. grubii reveals complex RNA expression and microevolution leading to virulence attenuation. *PLoS genetics*. 10:e1004261.

Jansen, L.E., R.A. Verhage, and J. Brouwer. 1998. Preferential binding of yeast Rad4.Rad23 complex to damaged DNA. *The Journal of biological chemistry*. 273:33111-33114.

Jung, W.H., A. Sham, T. Lian, A. Singh, D.J. Kosman, and J.W. Kronstad. 2008. Iron source preference and regulation of iron uptake in Cryptococcus neoformans. *PLoS pathogens*. 4:e45.

Kafer, E., and M. Fraser. 1979. Isolation and genetic analysis of nuclease halo (nuh) mutants of Neurospora crassa. *Molecular & general genetics : MGG*. 169:117-127.

Kanno, S., S. Iwai, M. Takao, and A. Yasui. 1999. Repair of apurinic/apyrimidinic sites by UV damage endonuclease; a repair protein for UV and oxidative damage. *Nucleic acids research*. 27:3096-3103.

Kaur, B., J.L. Fraser, G.A. Freyer, S. Davey, and P.W. Doetsch. 1999. A Uve1p-mediated mismatch repair pathway in Schizosaccharomyces pombe. *Mol Cell Biol*. 19:4703-4710.

Kim, H., J.B. Ridenour, L.D. Dunkle, and B.H. Bluhm. 2011. Regulation of stomatal tropism and infection by light in Cercospora zeae-maydis: evidence for coordinated host/pathogen responses to photoperiod? *PLoS pathogens*. 7:e1002113.

Kim, I., K. Mi, and H. Rao. 2004. Multiple interactions of rad23 suggest a mechanism for ubiquitylated substrate delivery important in proteolysis. *Molecular biology of the cell*. 15:3357-3365.

Kwon-Chung, K.J. 1975. A new genus, filobasidiella, the perfect state of Cryptococcus neoformans. *Mycologia*. 67:1197-1200.

Kwon-Chung, K.J., T. Boekhout, J.W. Fell, and M. Diaz. 2002. Proposal to conserve the name Cryptococcus gattii against C. hondurianus and C. bacillisporus (Basidiomycota, Hymenomycetes, Tremellomycetidae). *Taxon*. 51:804-806.

Kwon-Chung, K.J., J.C. Edman, and B.L. Wickes. 1992. Genetic association of mating types and virulence in Cryptococcus neoformans. *Infection and immunity*. 60:602-605.

Lamb, T.M., C.S. Goldsmith, L. Bennett, K.E. Finch, and D. Bell-Pedersen. 2011. Direct transcriptional control of a p38 MAPK pathway by the circadian clock in Neurospora crassa. *PloS one*. 6:e27149.

Lee, J.H., J.M. Choi, C. Lee, K.J. Yi, and Y. Cho. 2005. Structure of a peptide:N-glycanase-Rad23 complex: insight into the deglycosylation for denatured glycoproteins. *Proceedings of the National Academy of Sciences of the United States of America*. 102:9144-9149.

Legrand, M., C.L. Chan, P.A. Jauert, and D.T. Kirkpatrick. 2007. Role of DNA mismatch repair and double-strand break repair in genome stability and antifungal drug resistance in Candida albicans. *Eukaryotic cell*. 6:2194-2205.

Lin, X., C.M. Hull, and J. Heitman. 2005. Sexual reproduction between partners of the same mating type in Cryptococcus neoformans. *Nature*. 434:1017-1021.

Linden, H., P. Ballario, and G. Macino. 1997a. Blue light regulation in Neurospora crassa. *Fungal genetics and biology : FG & B*. 22:141-150.

Linden, H., M. Rodriguez-Franco, and G. Macino. 1997b. Mutants of Neurospora crassa defective in regulation of blue light perception. *Molecular & general genetics : MGG*. 254:111-118.

Lipson, E.D., D.T. Terasaka, and P.S. Silverstein. 1980. Double mutants of Phycomyces with abnormal phototropism. Mol Gen Genet:155-162.

Liu, O.W., C.D. Chun, E.D. Chow, C. Chen, H.D. Madhani, and S.M. Noble. 2008. Systematic genetic analysis of virulence in the human fungal pathogen Cryptococcus neoformans. *Cell*. 135:174-188.

Liu, Y., Q. He, and P. Cheng. 2003. Photoreception in Neurospora: a tale of two White Collar proteins. *Cellular and molecular life sciences : CMLS*. 60:2131-2138.

Liu, Z., and R.A. Butow. 2006. Mitochondrial retrograde signaling. *Annual review of genetics*. 40:159-185.

Lu, Y.K., K.H. Sun, and W.C. Shen. 2005. Blue light negatively regulates the sexual filamentation via the Cwc1 and Cwc2 proteins in Cryptococcus neoformans. *Molecular microbiology*. 56:480-491.

Magditch, D.A., T.B. Liu, C. Xue, and A. Idnurm. 2012. DNA mutations mediate microevolution between host-adapted forms of the pathogenic fungus Cryptococcus neoformans. *PLoS pathogens*. 8:e1002936.

McCulloch, R., and J.D. Barry. 1999. A role for RAD51 and homologous recombination in Trypanosoma brucei antigenic variation. *Genes & development*. 13:2875-2888.

Meadows, K.L., B. Song, and P.W. Doetsch. 2003. Characterization of AP lyase activities of Saccharomyces cerevisiae Ntg1p and Ntg2p: implications for biological function. *Nucleic acids research*. 31:5560-5567.

Medicherla, B., Z. Kostova, A. Schaefer, and D.H. Wolf. 2004. A genomic screen identifies Dsk2p and Rad23p as essential components of ER-associated degradation. *EMBO Rep*. 5:692-697.

Miao, F., M. Bouziane, R. Dammann, C. Masutani, F. Hanaoka, G. Pfeifer, and T.R. O'Connor. 2000. 3-Methyladenine-DNA glycosylase (MPG protein) interacts with human RAD23 proteins. *The Journal of biological chemistry*. 275:28433-28438.

Min, J.H., and N.P. Pavletich. 2007. Recognition of DNA damage by the Rad4 nucleotide excision repair protein. *Nature*. 449:570-575.

Mitra, S., J. Gomez-Raja, G. Larriba, D.D. Dubey, and K. Sanyal. 2014. Rad51-Rad52 mediated maintenance of centromeric chromatin in Candida albicans. *PLoS genetics*. 10:e1004344.

Mocquet, V., J.P. Laine, T. Riedl, Z. Yajin, M.Y. Lee, and J.M. Egly. 2008. Sequential recruitment of the repair factors during NER: the role of XPG in initiating the resynthesis step. *The EMBO journal*. 27:155-167.

Mylonakis, E., R. Moreno, J.B. El Khoury, A. Idnurm, J. Heitman, S.B. Calderwood, F.M. Ausubel, and A. Diener. 2005. *Galleria mellonella* as a model system to study *Cryptococcus neoformans* pathogenesis. *Infect Immun*. 73:3842-3850.

Nielsen, K., G.M. Cox, P. Wang, D.L. Toffaletti, J.R. Perfect, and J. Heitman. 2003. Sexual cycle of Cryptococcus neoformans var. grubii and virulence of congenic a and alpha isolates. *Infection and immunity*. 71:4831-4841.

Park, B.J., K.A. Wannemuehler, B.J. Marston, N. Govender, P.G. Pappas, and T.M. Chiller. 2009. Estimation of the current global burden of cryptococcal meningitis among persons living with HIV/AIDS. *Aids*. 23:525-530.

Pitkin, J.W., D.G. Panaccione, and J.D. Walton. 1996. A putative cyclic peptide efflux pump encoded by the TOXA gene of the plant-pathogenic fungus Cochliobolus carbonum. *Microbiology*. 142 (Pt 6):1557-1565.

Popoff, S.C., A.I. Spira, A.W. Johnson, and B. Demple. 1990. Yeast structural gene (APN1) for the major apurinic endonuclease: homology to Escherichia coli endonuclease IV. *Proceedings of the National Academy of Sciences of the United States of America*. 87:4193-4197.

Ramsey, K.L., J.J. Smith, A. Dasgupta, N. Maqani, P. Grant, and D.T. Auble. 2004. The NEF4 complex regulates Rad4 levels and utilizes Snf2/Swi2-related ATPase activity for nucleotide excision repair. *Mol Cell Biol*. 24:6362-6378.

Resnick, M.A. 1969. A photoreactivationless mutant of Saccharomyces cerevisiae. *Photochemistry and photobiology*. 9:307-312.

Ruff, J.A., J.K. Lodge, and L.G. Baker. 2009. Three galactose inducible promoters for use in *C. neoformans* var. *grubii*. *Fungal genetics and biology : FG & B*. 46:9-16.

Ruiz-Roldan, M.C., V. Garre, J. Guarro, M. Marine, and M.I. Roncero. 2008. Role of the white collar 1 photoreceptor in carotenogenesis, UV resistance, hydrophobicity, and virulence of Fusarium oxysporum. *Eukaryotic cell*. 7:1227-1230.

Sancar, A. 2008. Structure and function of photolyase and in vivo enzymology: 50th anniversary. *The Journal of biological chemistry*. 283:32153-32157.

Sassanfar, M., and L. Samson. 1990. Identification and preliminary characterization of an O6-methylguanine DNA repair methyltransferase in the yeast Saccharomyces cerevisiae. *The Journal of biological chemistry*. 265:20-25.

Swartz, T.E., T.S. Tseng, M.A. Frederickson, G. Paris, D.J. Comerci, G. Rajashekara, J.G. Kim, M.B. Mudgett, G.A. Splitter, R.A. Ugalde, F.A. Goldbaum, W.R. Briggs, and R.A. Bogomolni. 2007. Blue-light-activated histidine kinases: two-component sensors in bacteria. *Science*. 317:1090-1093.

Takao, M., R. Yonemasu, K. Yamamoto, and A. Yasui. 1996. Characterization of a UV endonuclease gene from the fission yeast Schizosaccharomyces pombe and its bacterial homolog. *Nucleic acids research*. 24:1267-1271.

Talora, C., L. Franchi, H. Linden, P. Ballario, and G. Macino. 1999. Role of a white collar-1-white collar-2 complex in blue-light signal transduction. *The EMBO journal*. 18:4961-4968.

Taylor, J.W., and M.L. Berbee. 2006. Dating divergences in the Fungal Tree of Life: review and new analyses. *Mycologia*. 98:838-849.

Teng, Y., H. Liu, H.W. Gill, Y. Yu, R. Waters, and S.H. Reed. 2008. Saccharomyces cerevisiae Rad16 mediates ultraviolet-dependent histone H3 acetylation required for efficient global genome nucleotide-excision repair. *EMBO Rep*. 9:97-102.

Thompson, C.L., and A. Sancar. 2002. Photolyase/cryptochrome blue-light photoreceptors use photon energy to repair DNA and reset the circadian clock. *Oncogene*. 21:9043-9056.

Toffaletti, D.L., T.H. Rude, S.A. Johnston, D.T. Durack, and J.R. Perfect. 1993. Gene transfer in Cryptococcus neoformans by use of biolistic delivery of DNA. *Journal of bacteriology*. 175:1405-1411.

Tomkinson, A.E., N.J. Tappe, and E.C. Friedberg. 1992. DNA ligase I from Saccharomyces cerevisiae: physical and biochemical characterization of the CDC9 gene product. *Biochemistry*. 31:11762-11771.

Troelstra, C., A. van Gool, J. de Wit, W. Vermeulen, D. Bootsma, and J.H. Hoeijmakers. 1992. ERCC6, a member of a subfamily of putative helicases, is involved in Cockayne's syndrome and preferential repair of active genes. *Cell*. 71:939-953.

Unk, I., L. Haracska, R.E. Johnson, S. Prakash, and L. Prakash. 2000. Apurinic endonuclease activity of yeast Apn2 protein. *The Journal of biological chemistry*. 275:22427-22434.

Vance, J.R., and T.E. Wilson. 2001. Repair of DNA strand breaks by the overlapping functions of lesion-specific and non-lesion-specific DNA 3' phosphatases. *Mol Cell Biol*. 21:7191-7198.

Verma, S., and A. Idnurm. 2013. The Uve1 endonuclease is regulated by the white collar complex to protect cryptococcus neoformans from UV damage. *PLoS genetics*. 9:e1003769.

Wade, S.L., and D.T. Auble. 2010. The Rad23 ubiquitin receptor, the proteasome and functional specificity in transcriptional control. *Transcription*. 1:22-26.

Wade, S.L., K. Poorey, S. Bekiranov, and D.T. Auble. 2009. The Snf1 kinase and proteasome-associated Rad23 regulate UV-responsive gene expression. *The EMBO journal*. 28:2919-2931.

Walters, K.J., P.J. Lech, A.M. Goh, Q. Wang, and P.M. Howley. 2003. DNA-repair protein hHR23a alters its protein structure upon binding proteasomal subunit S5a. *Proceedings of the National Academy of Sciences of the United States of America*. 100:12694-12699.

Wang, Z., X. Wu, and E.C. Friedberg. 1993. DNA repair synthesis during base excision repair in vitro is catalyzed by DNA polymerase epsilon and is influenced by DNA polymerases alpha and delta in Saccharomyces cerevisiae. *Mol Cell Biol*. 13:1051-1058.

Wickes, B.L., M.E. Mayorga, U. Edman, and J.C. Edman. 1996. Dimorphism and haploid fruiting in Cryptococcus neoformans: association with the alpha-mating type. *Proceedings of the National Academy of Sciences of the United States of America*. 93:7327-7331.

Withers-Ward, E.S., T.D. Mueller, I.S. Chen, and J. Feigon. 2000. Biochemical and structural analysis of the interaction between the UBA(2) domain of the DNA repair protein HHR23A and HIV-1 Vpr. *Biochemistry*. 39:14103-14112.

Writing Committee of the Second World Health Organization Consultation on Clinical Aspects of Human Infection with Avian Influenza, A.V., A.N. Abdel-Ghafar, T. Chotpitayasunondh, Z. Gao, F.G. Hayden, D.H. Nguyen, M.D. de Jong, A. Naghdaliyev, J.S. Peiris, N. Shindo, S. Soeroso, and T.M. Uyeki. 2008. Update on avian influenza A (H5N1) virus infection in humans. *The New England journal of medicine*. 358:261-273.

Xiao, W., B. Derfler, J. Chen, and L. Samson. 1991. Primary sequence and biological functions of a Saccharomyces cerevisiae O6-methylguanine/O4-methylthymine DNA repair methyltransferase gene. *The EMBO journal*. 10:2179-2186.

Yajima, H., M. Takao, S. Yasuhira, J.H. Zhao, C. Ishii, H. Inoue, and A. Yasui. 1995. A eukaryotic gene encoding an endonuclease that specifically repairs DNA damaged by ultraviolet light. *The EMBO journal*. 14:2393-2399.

Yasuhira, S., and A. Yasui. 2000. Alternative excision repair pathway of UV-damaged DNA in Schizosaccharomyces pombe operates both in nucleus and in mitochondria. *The Journal of biological chemistry*. 275:11824-11828.

Yu, S., T. Owen-Hughes, E.C. Friedberg, R. Waters, and S.H. Reed. 2004. The yeast Rad7/Rad16/Abf1 complex generates superhelical torsion in DNA that is required for nucleotide excision repair. *DNA Repair (Amst)*. 3:277-287.

VITA

Surbhi Verma was born on October 21, 1982 in Ghaziabad, U.P., India. In May 2004 Surbhi graduated from University of Delhi, Delhi, India. She received degree in B. Sc. Microbiology (Honors). She received Masters degree in June 2006 from Devi Ahilya University, Indore, India. From 2007 to 2008 she worked at Department of Genetics, University of Delhi South Campus, India. In August 2008 she moved to Kansas City, Missouri, U.S.A. where she joined graduate school at University of Missouri-Kansas City (UMKC). At UMKC she received Master's degree in Cell and Molecular Biology in May 2010.